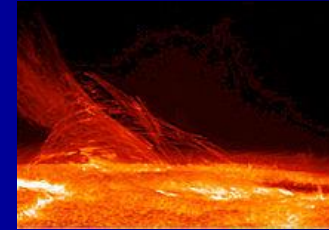
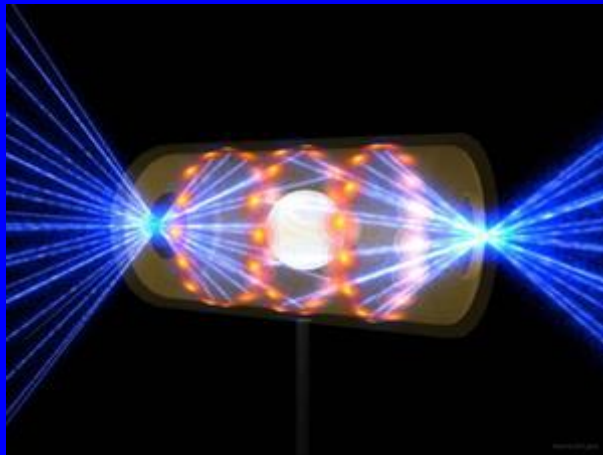


Prof. J. Glosík
KFPP MFF UK

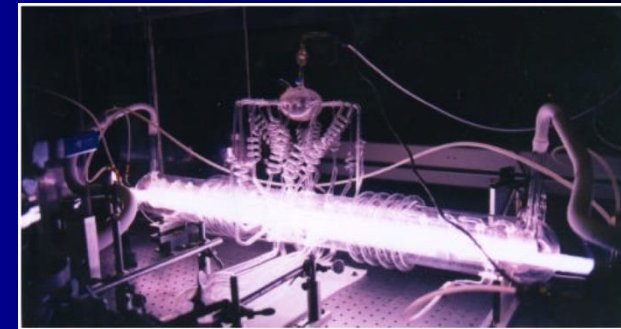
jazyk - česky, slovensky, anglicky, rusky ... v aproximaci



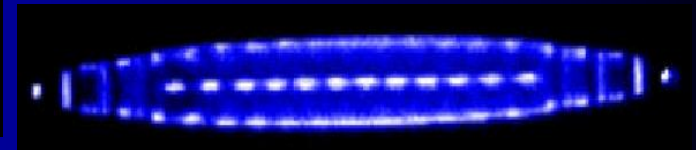
Slunce - vlákna plazmatu



Fusion in a flash. At the National Ignition Facility (NIF) at Lawrence Livermore National Lab, 192 powerful lasers blast a BB-sized fuel pellet inside a metallic cylinder to generate nuclear fusion.



Ultra cold Plasma
Experiment: $T \sim 6$ mK



This presentation is only for students attending the lecture PLASMA PHYSICS at MFF UK,

Not for public use, Preliminary version without references

**This presentation is only for students attending
the lecture PLASMA PHYSICS at MFF UK,**

**Not for public use,
Preliminary version without references**

Recommended literature :

Úvod do fyziky plazmatu

(Introduction to Plasma Physics)

Francis F. Chen

Academia Praha 1984 (Plenum press 1974)

Základy fyziky plazmy

Viktor Martišovič

Bratislava 2004

Učebný text pre 3. ročník magisterského štúdia

Fundamentals of plasma physics

J. A. Bittencourt

Springer,

Third Edition 2004

Physics of Ionized Gases

Boris M. Smirnov

John Wiley&Sons 2001

Základy klasické a kvantové fyziky plazmatu

J.Kracík, B. Šesták a L. Aubrecht

Academia Praha 1974

„Velký Kracík“

Fyzika plazmatu

J.Kracík, J. Tobiáš

Academia, Praha 1966

„Malý Kracík“

ASTRONOMIE A FYZIKA NA PŘELOMU TISÍCILETÍ

Pod vedením Petra Kulhánka

Aldebaran Group for Astrophysics, 2004

Vybrané kapitoly z fyziky plazmatu

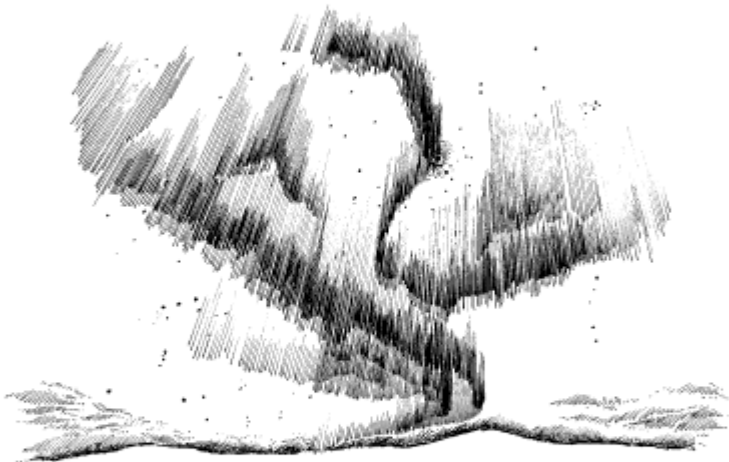
Petr Kulhánek

AGA, Praha 2017

Aldebaran ...

Etc.

Úvod do teorie plazmatu

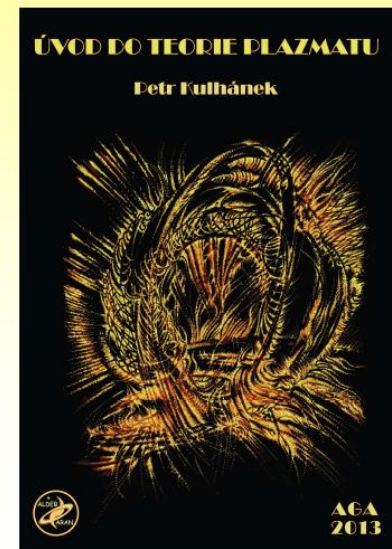


Petr Kulhánek

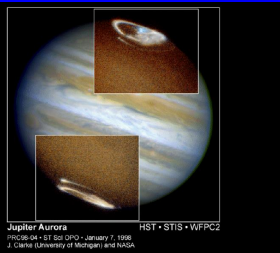
AGA 2020

- V textu byly použity některé obrázky a text z knihy:

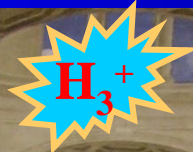
P. Kulhánek, Úvod do teorie plazmatu, AGA 2011, Praha.



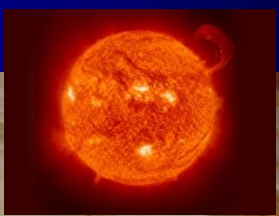
Plasma is everywhere, but where is truth



Jupiter Auroras
HST • STIS • WFC3
2004-04-01 00:00 - January 7, 1999
J. Clarke University of Michigan and NASA



Scio me nihil scire



Πλασμα



Socrates

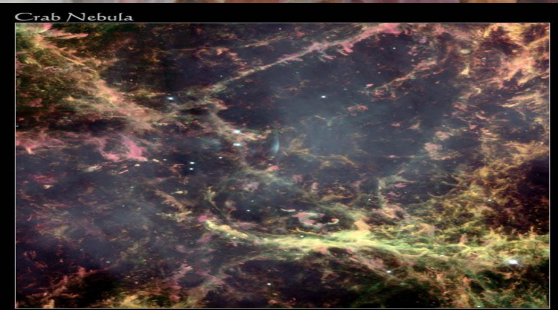
Platon Aristoteles

Archimedes

Pythagoras

Michelangelo

Diogenes

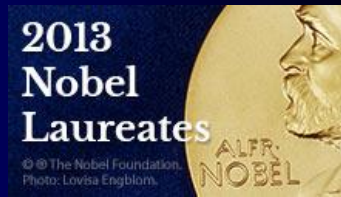


Crab Nebula

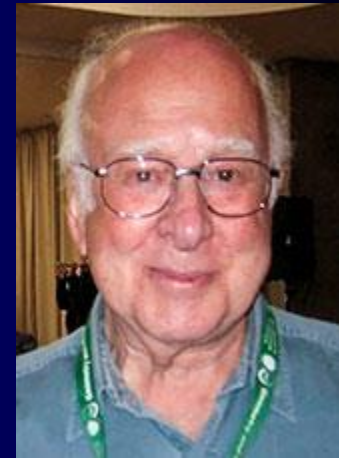
Hubble
Space Telescope

Okomentovaná prednáška pro KFPP MFF UK

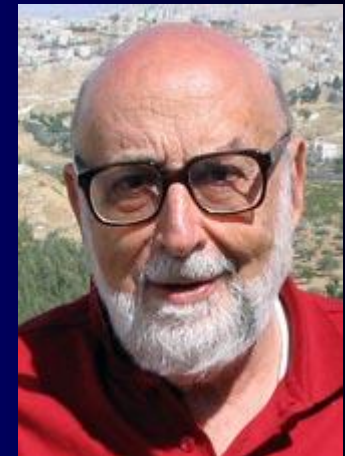
“School of Athens” Rafael, Vatican



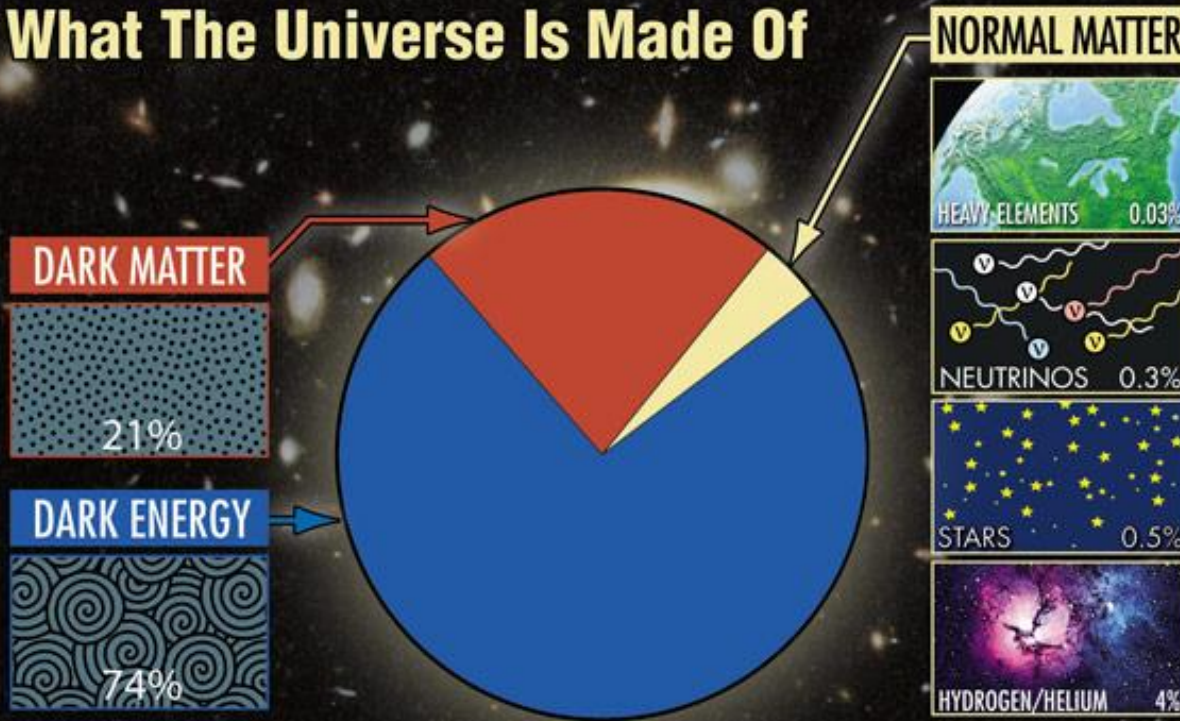
Peter W. Higgs



François Englert



What The Universe Is Made Of



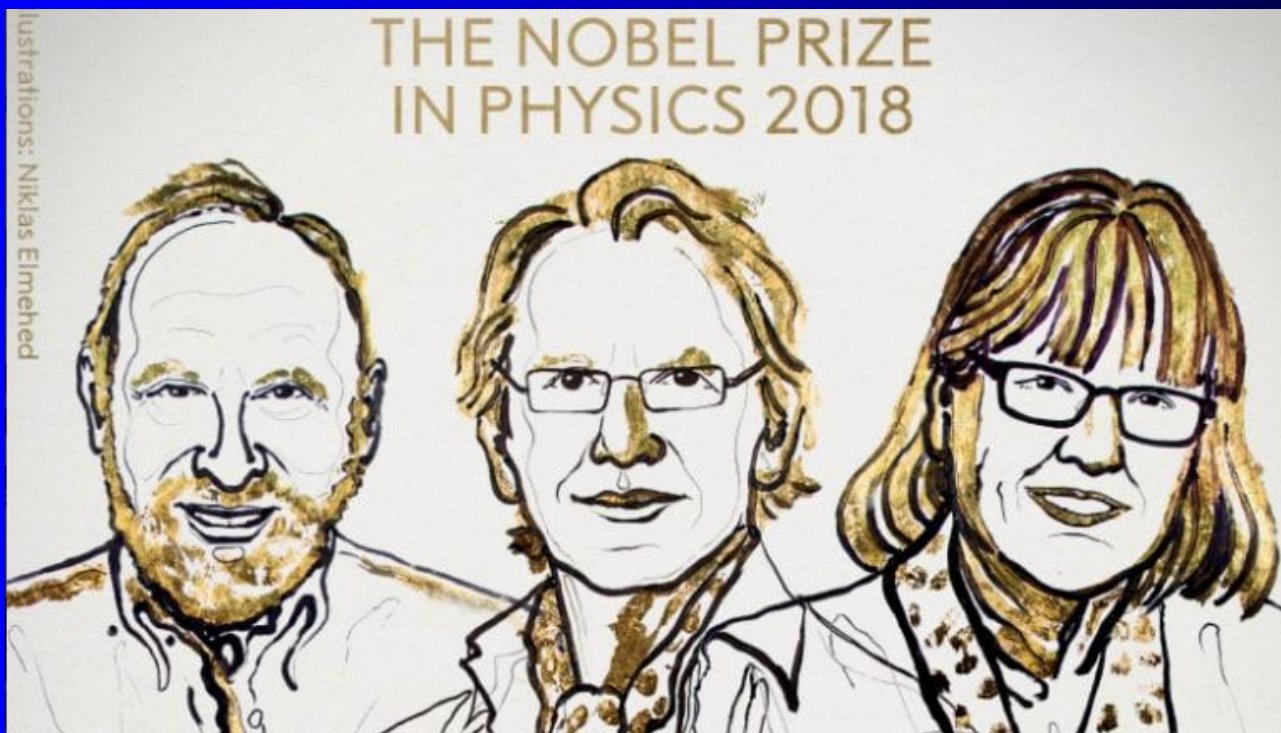
The Nobel Prize in Physics 2013

François Englert and Peter W. Higgs “for the theoretical discovery of a mechanism that contributes to our understanding of the origin of mass of subatomic particles, and which recently was confirmed through the discovery of the predicted fundamental particle, by the ATLAS and CMS experiments at CERN’s Large Hadron Collider”

Normal matter ...4.83%

... and now it is clear

02. 10. 2018



The 2018 Nobel Prize in Physics on October 2, 2018, was awarded to Arthur Ashkin of the US, Gerard Mourou of France and Donna Strickland of Canada.

Arthuru Ashkinovi za vynález tzv. optické pinzety a její aplikaci v biologických systémech. druhou polovinu se podělí Francouz Gérard Mourou a Kanadanka Donna Stricklandová, autoři metody generování velmi krátkých optických pulzů s vysokou intenzitou.

Nobelova cena za fyziku (3)

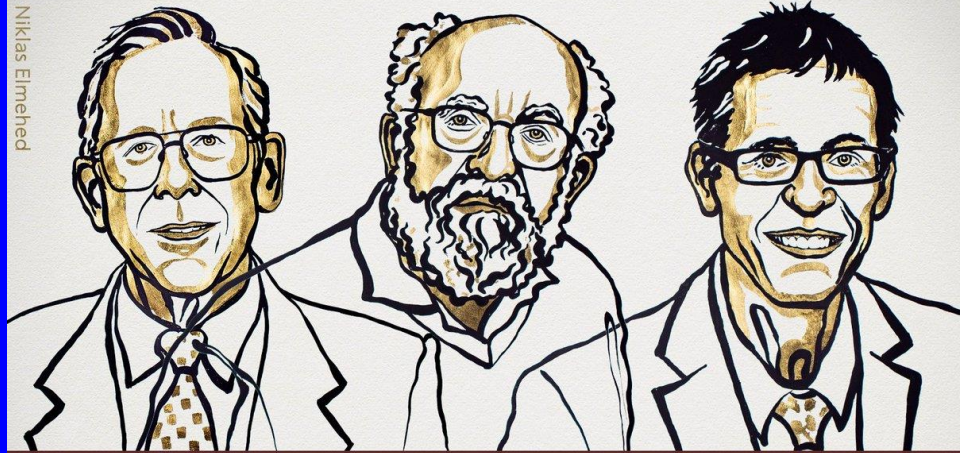
1903 - [Marie Curie-Sklodovská](#)

1963 - Maria Goeppert-Mayer

2018 - Donna Strickland

THE NOBEL PRIZE IN PHYSICS 2019

Illustrations: Niklas Elmehed



James
Peebles

“for theoretical
discoveries
in physical
cosmology”

Michel
Mayor

“for the discovery of an exoplanet
orbiting a solar-type star”

Didier
Queloz

THE ROYAL SWEDISH ACADEMY OF SCIENCES

The Nobel Prize in Physics 2019

“for contributions to our understanding of the evolution of the universe and Earth’s place in the cosmos”

The Nobel Prize in Physics 2020 (6. 10.)



Roger Penrose, born 1931 in Colchester, UK. Ph.D. 1957 from University of Cambridge, UK. Professor at University of Oxford, UK.

Reinhard Genzel, born 1952 in Bad Homburg vor der Höhe, Germany. Ph.D. 1978 from University of Bonn, Germany. Director at Max Planck Institute for Extraterrestrial Physics, Garching, Germany and Professor at University of California, Berkeley, USA.

Andrea Ghez, born 1965 in City of New York, USA. Ph.D. 1992 from California Institute of Technology, Pasadena, USA. Professor at University of California, Los Angeles, USA.

The Nobel Prize in Physics 2020 was divided, one half awarded to Roger Penrose "for the discovery that black hole formation is a robust prediction of the general theory of relativity", the other half jointly to Reinhard Genzel and Andrea Ghez "for the discovery of a supermassive compact object at the centre of our galaxy."

Nobelova cena za fyziku ženy (4x)

1903 - Marie Curie-Sklodovská

1963 - Maria Goeppert-Mayer

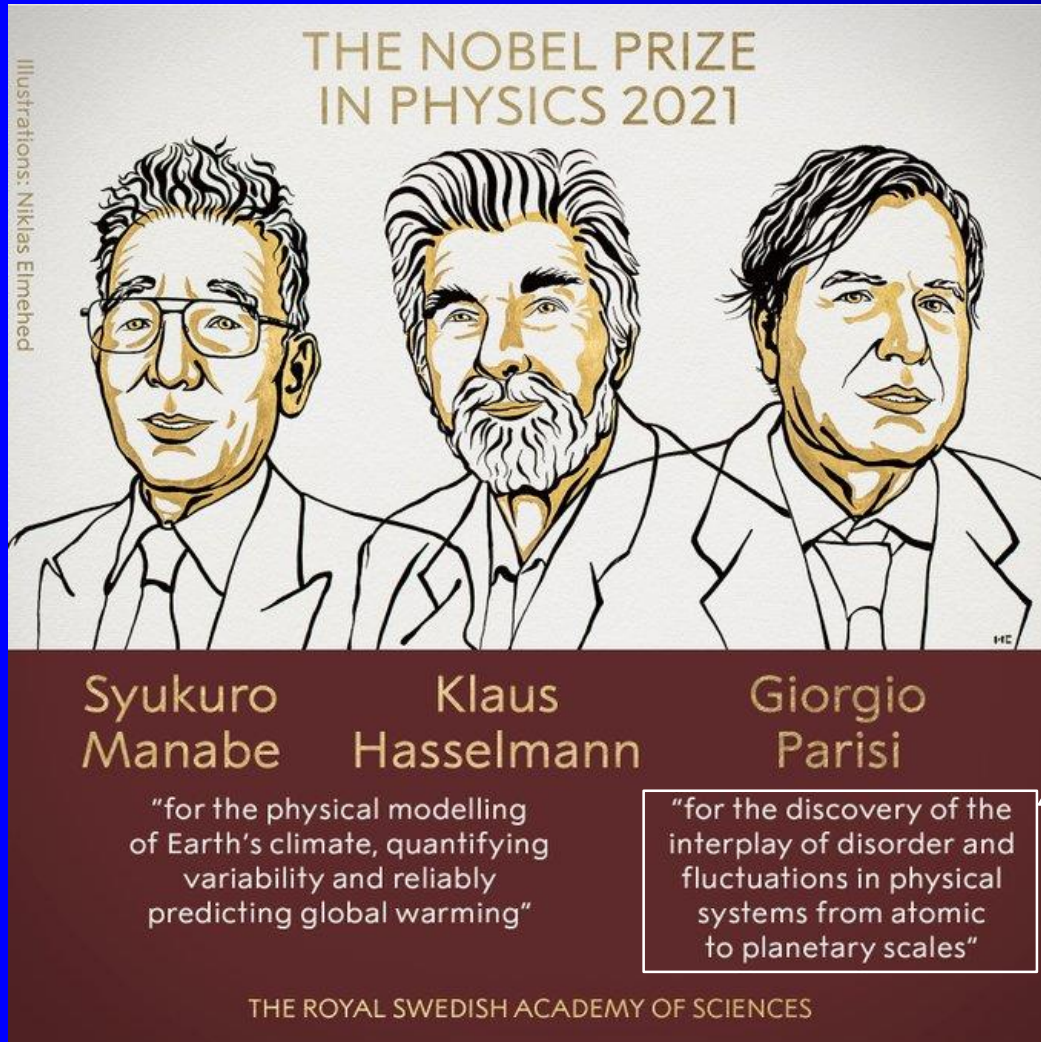
2018 - Donna Strickland

2020 - **Andrea Ghez**

Cenu za fyziku doteraz udelili 212 vedcom.

Doteraz (do 2018) cenu získali tri ženy, Marie Curiová v roku 1903, Maria Goeppert-Mayerová v roku 1963 a Donna Stricklandová roku 2018.

BREAKING NEWS: The Royal Swedish Academy of Sciences has decided to award the 2021 Nobel Prize in Physics to Syukuro Manabe, Klaus Hasselmann and Giorgio Parisi “for groundbreaking contributions to our understanding of complex physical systems.”



05. 10. 2021

“It’s clear that for the future generation, we have to act now in a very fast way.” - 2021 physics laureate Giorgio Parisi speaks about the current climate situation at this morning's Nobel Prize press conference.

For discovery of the interplay of disorder and fluctuations in physical systems from atomic to planetary scales.

2021 Nobelova cena za fyziku byla udělena z jedné poloviny společně Syukuro Manabemu a Klausu Hasselmannovi „za fyzikální modelování zemského klimatu, kvantifikaci jeho proměnlivosti a spolehlivou předpověď globálního oteplování“ a z druhé poloviny Giorgiu Parisimu „za objev vzájemného působení neuspořádanosti a fluktuací ve fyzikálních systémech od atomárních po planetární měřítko“.



04. 10. 2022

The Nobel Prize in Physics 2022



Ill. Niklas Elmehed © Nobel Prize Outreach

Alain Aspect

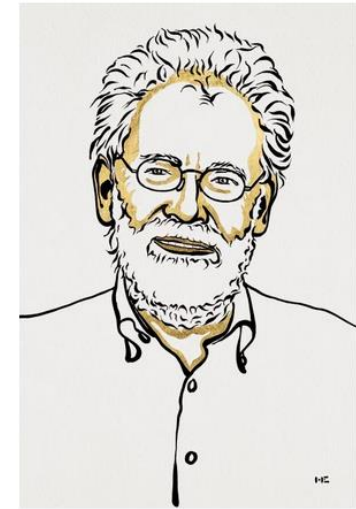
Prize share: 1/3



Ill. Niklas Elmehed © Nobel Prize Outreach

John F. Clauser

Prize share: 1/3



Ill. Niklas Elmehed © Nobel Prize Outreach

Anton Zeilinger

Prize share: 1/3

The Nobel Prize in Physics 2022 was awarded to Alain Aspect, John F. Clauser and Anton Zeilinger "for experiments with entangled photons, establishing the violation of Bell inequalities and pioneering quantum information science"

03. October 2023

The Nobel Prize in Physics 2023



III. Niklas Elmehed © Nobel Prize Outreach

Pierre Agostini

Prize share: 1/3



III. Niklas Elmehed © Nobel Prize Outreach

Ferenc Krausz

Prize share: 1/3



III. Niklas Elmehed © Nobel Prize Outreach

Anne L'Huillier

Prize share: 1/3

The Nobel Prize in Physics 2023 was awarded to Pierre Agostini, Ferenc Krausz and Anne L'Huillier "for experimental methods that generate attosecond pulses of light for the study of electron dynamics in matter"

Pierre Agostini The Ohio State University, Columbus, USA

Ferenc Krausz Max Planck Institute of Quantum Optics, Garching and Ludwig-Maximilians-Universität München, Germany

Anne L'Huillier Lund University, Sweden

Nobelova cena za fyziku ženy (5x)

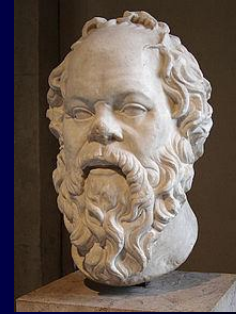
1903 - **Marie Curie-Sklodovská**

1963 - **Maria Goeppert-Mayer**

2018 - **Donna Strickland**

2020 - **Andrea Ghez**

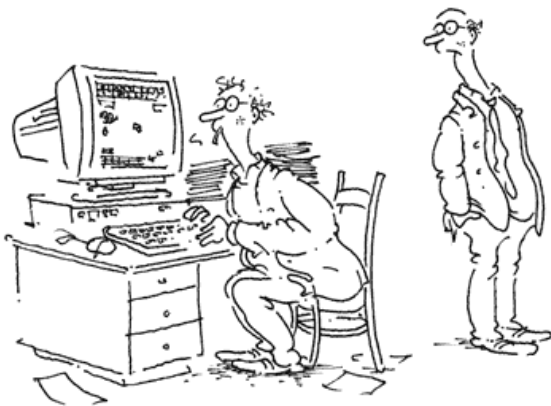
2023 – **Anne L'Huillier**



Information

Scio me nihil scire

(„Vím, že nic nevím.“ I know that I know nothing)



SPRÁVNĚ, CO MOŽNO NEJVÍC INFORMACÍ! ALE NEPŘEKROČIT HRANICI, ZA KTEROU SE Z PŘEMÍRY INFORMACÍ ZAČNE BLBNOUT.



THE EXPERTS SPEAK[†]

- “There is not the slightest indication that [nuclear] energy will ever be obtained” — *Albert Einstein, 1932*
- “Anyone who expects a source of power from the transformation of these atoms is talking moonshine.” — *Ernest Rutherford, 1933*
- “A few decades hence, [when controlled fusion is achieved], energy will be free — just like the unmeted air.” — *John von Neumann, 1956*
- “Radio has no future.” — *Lord Kelvin, 1897*
- “I think there is a world market for about five computers.” — *Thomas J. Watson, 1943*
- Where a calculator like ENIAC is equipped with 18,000 vacuum tubes and weighs 30 tons, computers in the future may have only 1,000 vacuum tubes and perhaps only weigh 1½ tons.” — *Popular Mechanics, March 1949*
- “640k ought to be enough for anybody.” — *Bill Gates, 1981*

[†] C. Cerf and V. Navasky, Villard, New York, 1998

e^- , H^+ , H , H^- , H_2^+ , H_2 , $\dots H_3^+$

The Orion molecular clouds

© Royal Observatory, Edinburgh / Anglo-Australian Observatory

92.1% of nucleons in the universe are protons
7.8% are helium nuclei!

H

He

▪ ▪ ▪ ▪
C N O Ne
▪ ▪ ▪ ▪
Si S Ar
▪
Fe

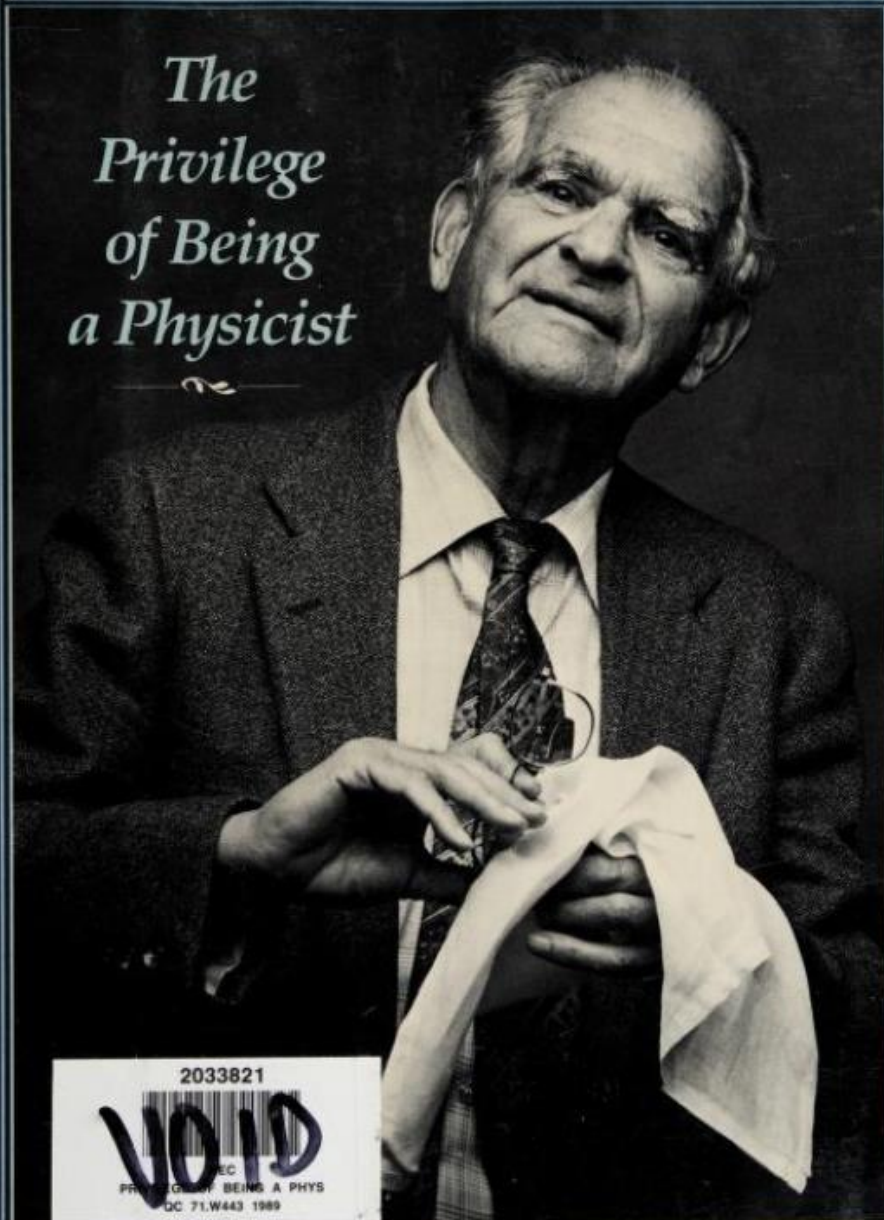
Mg

*Cosmic Abundance
of some elements*

Element	Abundance
hydrogen (H)	1.000.000
helium	80.147
oxygen	739
carbon	445
neon	138
nitrogen	91
magnesium	40
Silcon	37
Sulfur	19

Victor F. Weisskopf

*The
Privilege
of Being
a Physicist*



2033821

VOID
EC
PRIVILEGE OF BEING A PHYS
DC 71.W443 1989

Motivation:



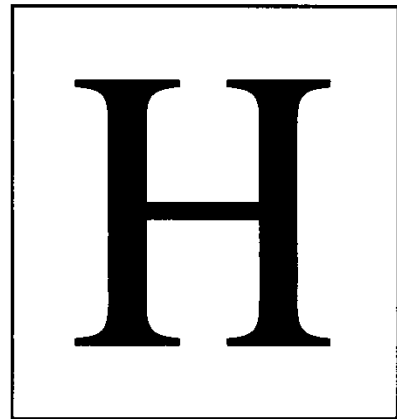
Just for pleasure.

$$\psi(x) \propto \sum_n A_n e^{ip_n x / \hbar}$$

The Orion molecular clouds

© Royal Observatory, Edinburgh / Anglo-Australian Observatory

92.1% of nucleons in the universe are protons
7.8% are helium nuclei !



Mg

Fe

▪ ▪ ▪ ▪
C N O Ne
▪ ▪ ▪ ▪
Si S Ar

The Privilege of Being a Physicist

Victor F. Weisskopf

There are certain obvious privileges that a physicist enjoys in our society. He is reasonably paid; he is given instruments, laboratories, complicated and expensive machines, and he is asked not to make money with these tools, like most other people, but to spend money. Furthermore, he is supposed to do what he himself finds most interesting, and he accounts for what he spends to the money givers in the form of progress reports and scientific papers that are much too specialized to be understood or evaluated by those who give the money—the federal authorities and, in the last analysis, the taxpayer. Still, we believe that the pursuit of science by the



“Intelligent play with simple, natural phenomena, the joys of discovery of unexpected experiences, are much better ways of learning to think than any teaching by rote.”

Cosmic Abundance of some elements

Element	Abundance
hydrogen (H)	1,000,000
helium	80,147
oxygen	739
carbon	445
neon	138
nitrogen	91
magnesium	40
Silicon	37
Sulfur	19

Plasma

History of the term “plasma” In the mid-19th century the Czech physiologist Jan Evangelista Purkyně introduced use of the Greek word plasma (meaning “formed or molded”) to denote the clear fluid which remains after removal of all the corpuscular material in blood.

Half a century later, the American scientist Irving Langmuir proposed in 1922 that the electrons, ions and neutrals in an ionized gas could similarly be considered as corpuscular material entrained in some kind of fluid medium and called this entraining medium plasma. However it turned out that unlike blood where there really is a fluid medium carrying the corpuscular material, there actually is no “fluid medium” entraining the electrons, ions, and neutrals in an ionized gas. Ever since, plasma scientists have had to explain to friends and acquaintances that they were not studying blood!

Jan Evangelista Purkyně was a Czech anatomist and physiologist. In 1839, he coined the term protoplasm for the fluid substance of a cell. He was one of the best known scientists of his time. [Wikipedia](#)

Purkyně also introduced the scientific terms plasma (for the component of blood left when the suspended cells have been removed) and protoplasm (the substance found inside cells.)

Plasma

- Velmi často se o plazmatu mluví jako o čtvrtém skupenství hmoty
- Název plazma pro ionizovaný plyn poprvé použil Irwing Langmuir (1881–1957) v roce 1928, protože mu chováním tento stav látky připomínal krevní plazmu
- Za své objevy, které byly na pomezí fyziky a chemie (např. Využití atomárního vodíku – svařování atomárním vodíkem), získal v roce 1932 Nobelovu cenu právě za chemii



Langmuir

Plazma 1922 or 1928 ????

- Definic plazmatu je v literatuře celá řada
 - *Plazma je kvazineutrální plyn složený z nabitých a neutrálních částic, vykazující kolektivní chování*
 - *Fyzikální plynné plazma se skládá z různých druhů částic, elektricky nabitých či neutrálních v rozličných kvantových stavech*
- Co je **kvazineutralita**? $\mathbf{n}_i = \mathbf{n}_e (= \mathbf{n}_g)$
- Co je **kolektivní chování**? – rozumí se jím pohyby, které závisí nejen na lokálních podmínkách, ale také na stavu plazmatu ve vzdálených oblastech

Definition of a plasma

Although a plasma is loosely described as an electrically neutral medium of positive and negative particles, a more rigorous definition requires three criteria to be satisfied:

The plasma approximation:

Charged particles must be close enough together that each particle influences many nearby charged particles, rather than just the interacting with the closest particle (these collective effects are a distinguishing feature of a plasma). The plasma approximation is valid when the number of electrons within the sphere of influence (called the *Debye sphere* whose radius is the Debye (screening) length) of a particular particle is **large**. The average number of particles in the Debye sphere is given by the plasma parameter, Λ .

Bulk interactions:

The Debye screening length (defined above) is short compared to the physical size of the plasma. This criterion means that interactions in the bulk of the plasma are more important than those at its edges, where boundary effects may take place.

Plasma frequency:

The electron plasma frequency (measuring plasma oscillations of the electrons) is large compared to the electron-neutral collision frequency (measuring frequency of collisions between electrons and neutral particles). When this condition is valid, plasmas act to shield charges very rapidly (quasineutrality is another defining property of plasmas).

Charged Particle Trajectories Are Different In Plasmas

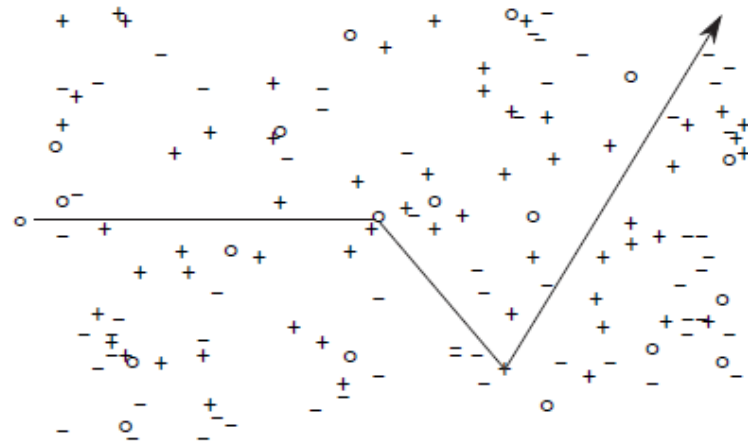


Figure 3: The trajectory of a neutral particle in a partially ionized gas exhibits “straight-line” motion between abrupt atomic collisions. The typical distance between neutral particle collisions is called the collision “**mean free path.**” Symbols: neutrals (circles), electrons (minus signs) and ions (plus signs).

Plasma

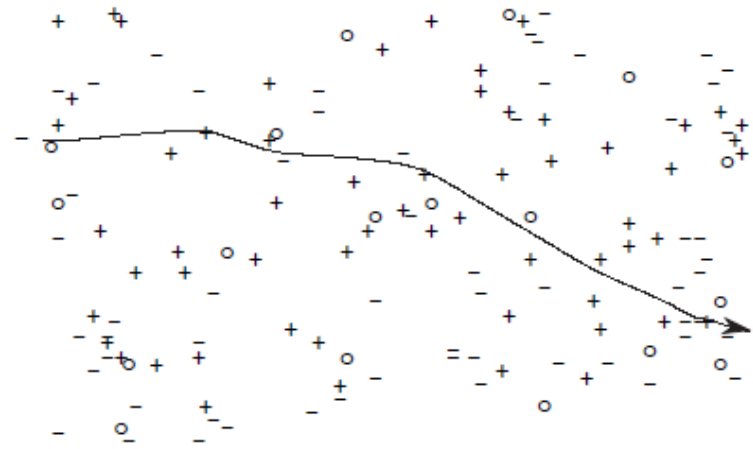
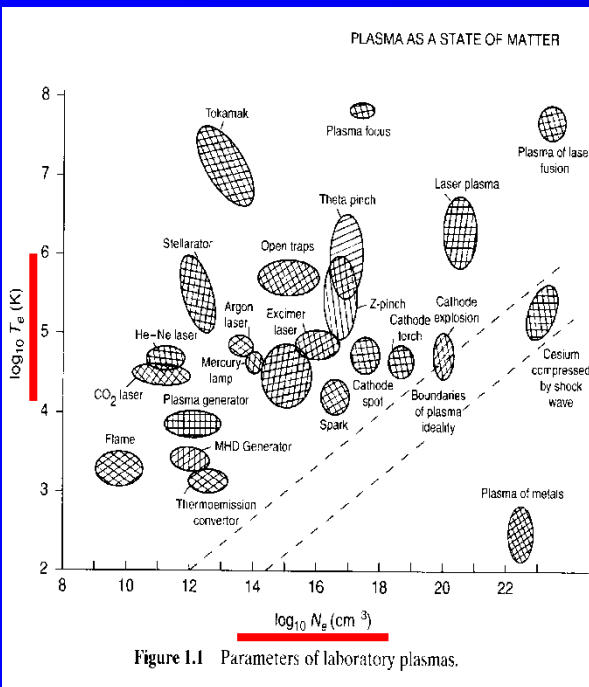
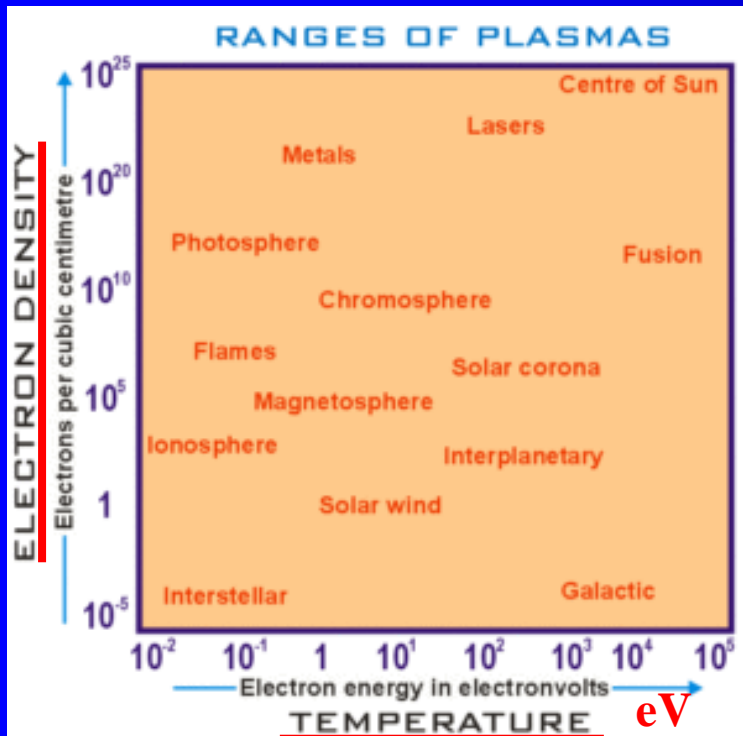


Figure 4: The trajectory of a “test” electron in a plasma exhibits continuous small-angle Coulomb collisional scatterings of its direction of motion. The “**collision length**” is the exponential decay length over which an average charged particle in a plasma loses its initially directed momentum.



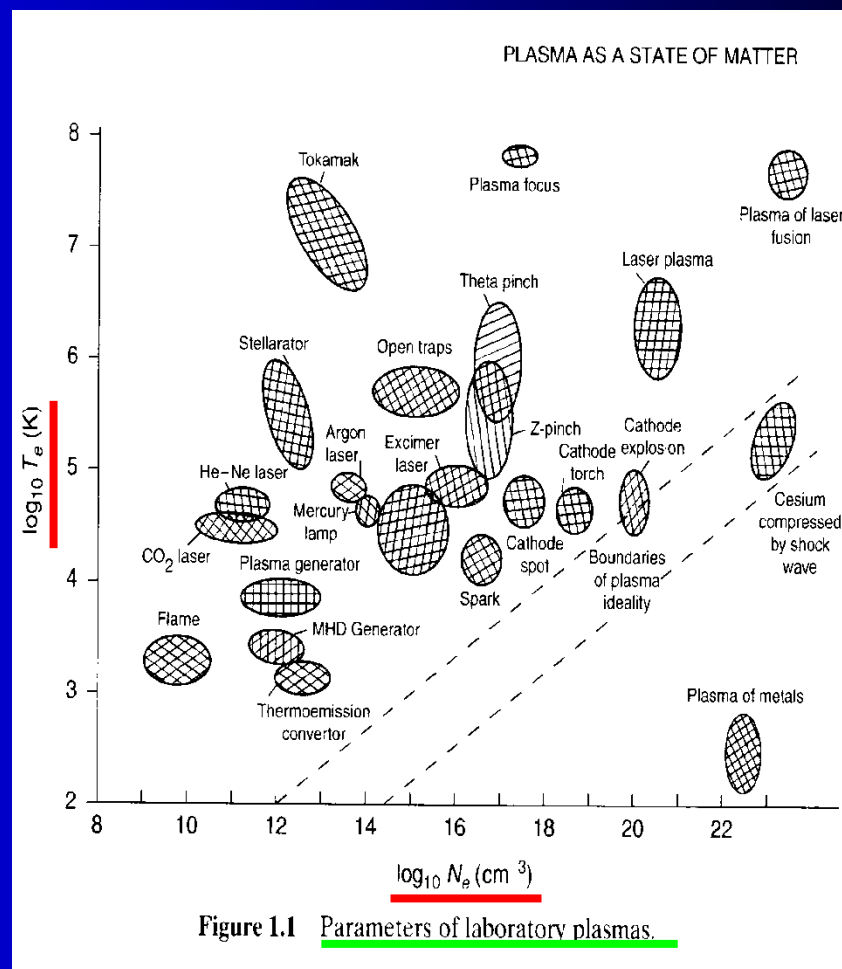
Typical ranges of plasma parameters

Characteristic	Terrestrial plasmas	Cosmic plasmas
Size in metres	10^{-6} m (lab plasmas) to 10^2 m (lightning)	10^{-6} m (spacecraft sheath) to 10^{25} m (intergalactic nebula)
Lifetime in seconds	10^{-12} s (laser-produced plasma) to 10^7 s (fluorescent lights)	10^1 s (solar flares) to 10^{17} s (intergalactic plasma)
Density in particles per cubic metre	10^7 m ⁻³ to 10^{32} m ⁻³ (inertial confinement plasma)	10^0 (i.e., 1) m ⁻³ (intergalactic medium) to 10^{30} m ⁻³ (stellar core)
Temperature in kelvins	~ 0 K (crystalline non-neutral plasma) to 10^8 K (magnetic fusion plasma)	10^2 K (aurora) to 10^7 K (solar core)
Magnetic fields in teslas	10^{-4} T (lab plasma) to 10^3 T (pulsed-power plasma)	10^{-12} T (intergalactic medium) to 10^{11} T (near neutron stars)



Ranges of plasma parameters

Density increases upwards, temperature increases towards the right. The free electrons in a metal may be considered an electron plasma [1]. Plasma parameters can take on values varying by many orders of magnitude, but the properties of plasmas with apparently disparate parameters may be very similar (see plasma scaling). The following chart considers only conventional atomic plasmas and not exotic phenomena like quark gluon plasmas:



05. 10. 2021

04. 10. 2022

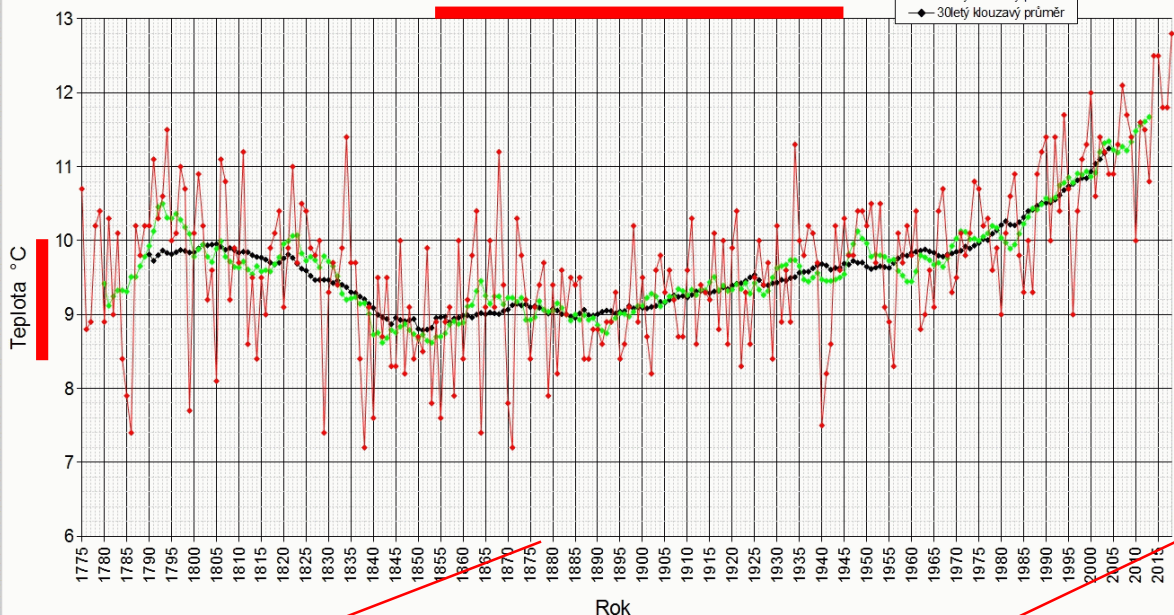
26. 10. 2023

Energie

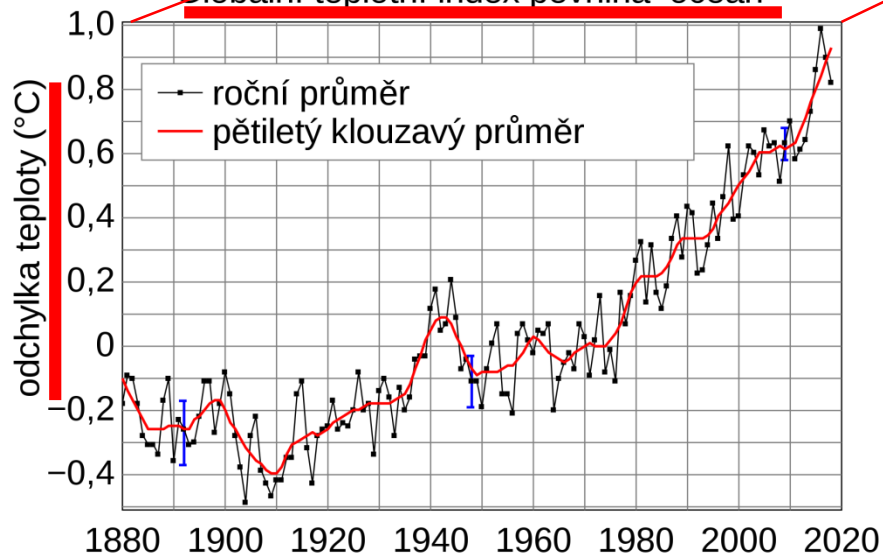
220 054 686	Energie spotřebovaná dnes (MWh), z toho:
187 322 974	- z neobnovitelných zdrojů
33 138 316	- z obnovitelných zdrojů
1 378 873 597 221	Solární energie dopadající na Zemi dnes (MWh)

Information

Průměrné roční teploty v Praze-Klementinu 1775-2018



Globální teplotní index pevnina-oceán



“Kdo z vás je bez hříchu, první hod’ na ni kamenem”

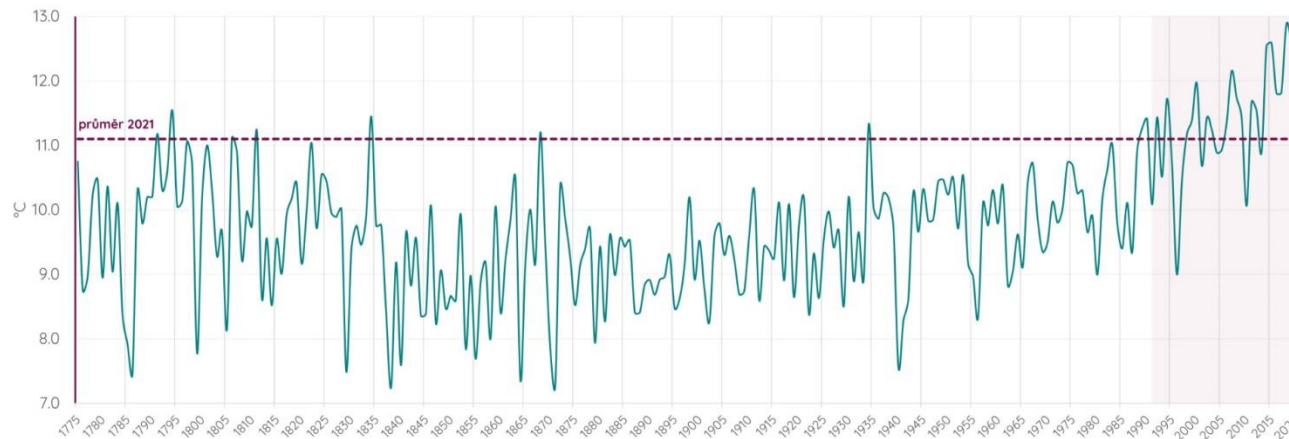
(see ref.: **Nový zákon**, ... Ježíš ... hora Olivetská ...)

Jesus

He that is without sin among you, let him be the first to cast a stone at her.



Průměrná roční teplota 1775–2021, Praha-Klementinum



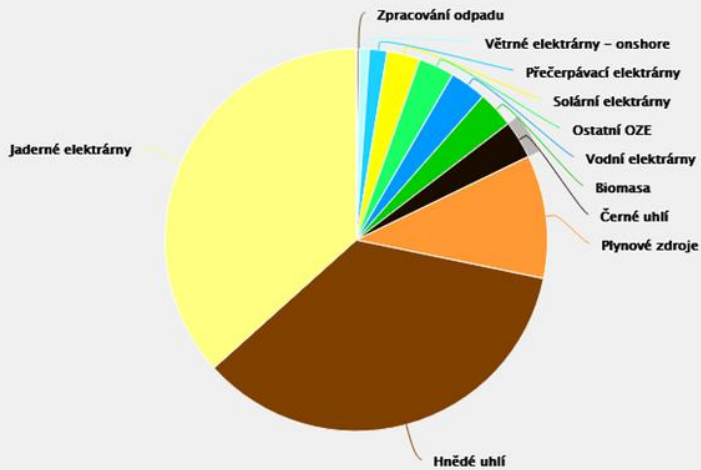
Graf výše ukazuje průměrné roční teploty na stanici Praha-Klementinum za období 1775 až 2020. V grafu je vyznačena přerušovanou čarou hladina průměrné roční teploty za rok 2021 a vyšrafovaná je období 1991 až 2020.

Jak ukazuje výše uvedená infografika, v kontextu posledních 30 let (období 1991 až 2020) a zejména pak poslední dekády (2011 až 2020) opravdu byl rok 2021 chladnější. Při hodnocení klimatu však nejsou podstatné krátkodobé výkyvy, ale dlouhodobý trend. Z grafu výše je jasné patrné, že v dlouhodobém hledisku byl i rok 2021 velmi teplý a do roku 1990 bychom za více než 200 let našly jen 9 roků, které byly v průměru teplejší. Oproti předchozímu třicetiletí 1961–1990 to byl rovněž rok silně nadnormální (+1,1 °C). Trend je zcela zřejmý, a to **dlouhodobé zvyšování teploty**, které se v posledních letech velmi akcelerovalo. To však **neznamená, že se nemůže vyskytnout chladnější rok** (a stejně tak globální oteplování neznamená, že se v zimě nemohou vyskytnout velmi chladné dny, dlouhodobě jich ale ubývá). Ještě lepším příkladem než rok 2021 je v tomto směru rok 1996 a 2010. Ani tyto dva roky ale nelze považovat za velmi chladné z dlouhodobého hlediska. Při pohledu na celkový průběh je patrné, že rok 1996 byl blízko průměru 1775–1990 a rok 2010 byl z dlouhodobého pohledu teplotně nadprůměrný.



Česká republika: Podíl zdrojů na výrobě elektřiny

Data od: 1. 1. 2021 do: 31. 12. 2021



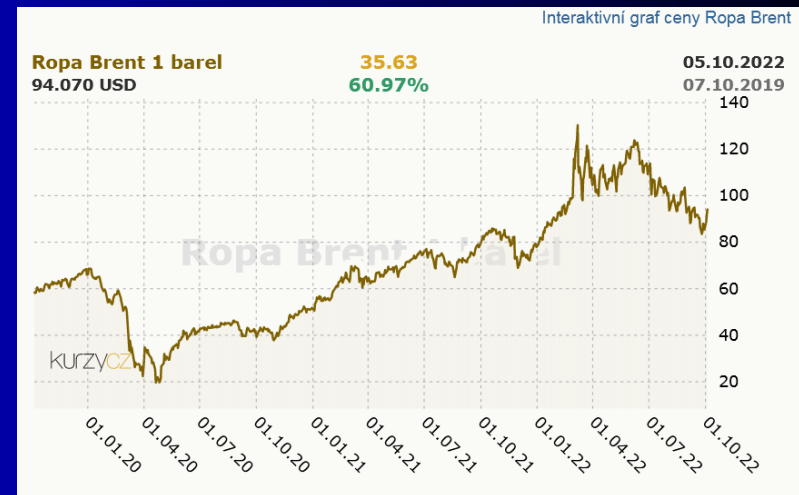
Podíl zdrojů na výrobě elektřiny v roce 2021

(v %)

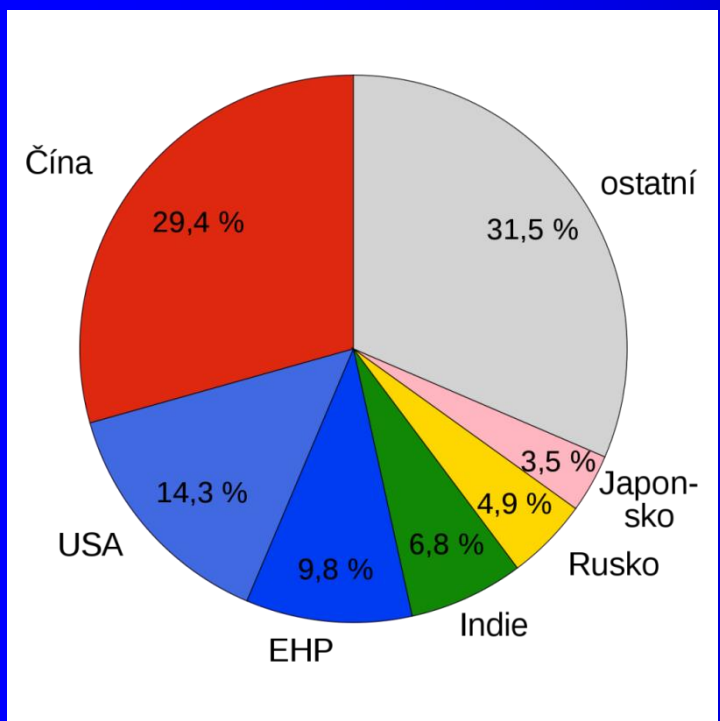
	Česko	Slovensko	Maďarsko	Rakousko	Německo	Polsko	Francie
Jaderné elektrárny	36.6	54.3	51.2	0	13	0	70.4
Hnědé uhlí	35.1	3.5	10.3	0	19.5	26.1	0
Plynové zdroje	10.4	13.7	29.2	16.1	10.4	8	6.4
Černé uhlí	3.2	1.3	0	0	10.3	50.4	0.8
Biomasa	3.1	3.1	3.8	2.6	7.8	1.2	0.6
Vodní elektrárny	4.7	15.5	0.6	65.2	4.7	1.8	11.9
Fotovoltaické elektrárny	2.9	2.1	0	1.6	9.4	2.9	2.7
Větrné elektrárny	0.9	0	2.1	12.6	22.8	9.6	6.9
Ostatní obnovitelné zdroje	3	1.8	0.8	1.6	1.5	0	0.3
Ostatní	0.1	4.7	2	0.3	0.6	0	0
Celkem OZE	14.6	22.5	7.3	83.6	46.2	15.5	22.4

Cui bono?

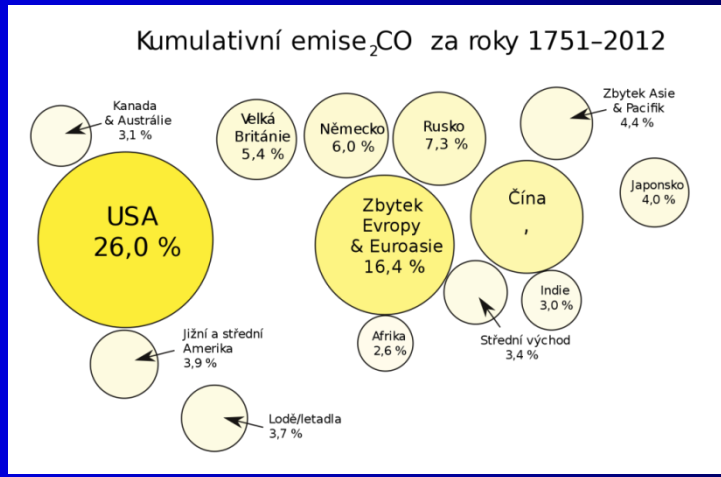
Qui Bonum



Not actualized, approximation



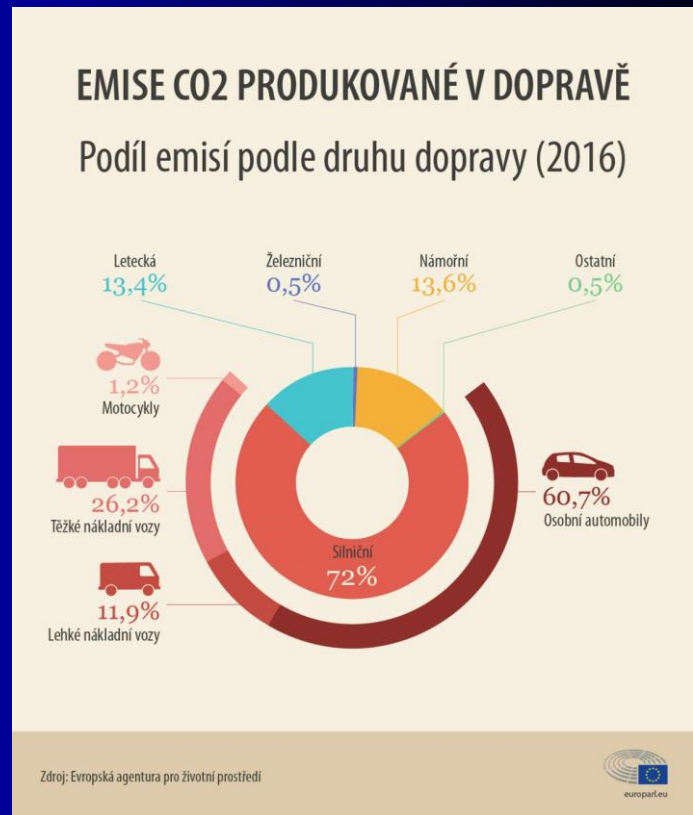
Největší producenti CO2 na světě



Podíl na globálních emisích CO2 mezi roky 1751–2012 podle různých regionů

Jesus
He that is without sin among you, let him be the first to cast a stone at her.

~2019

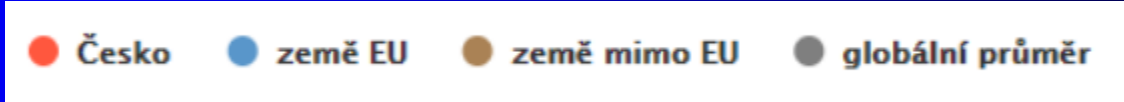
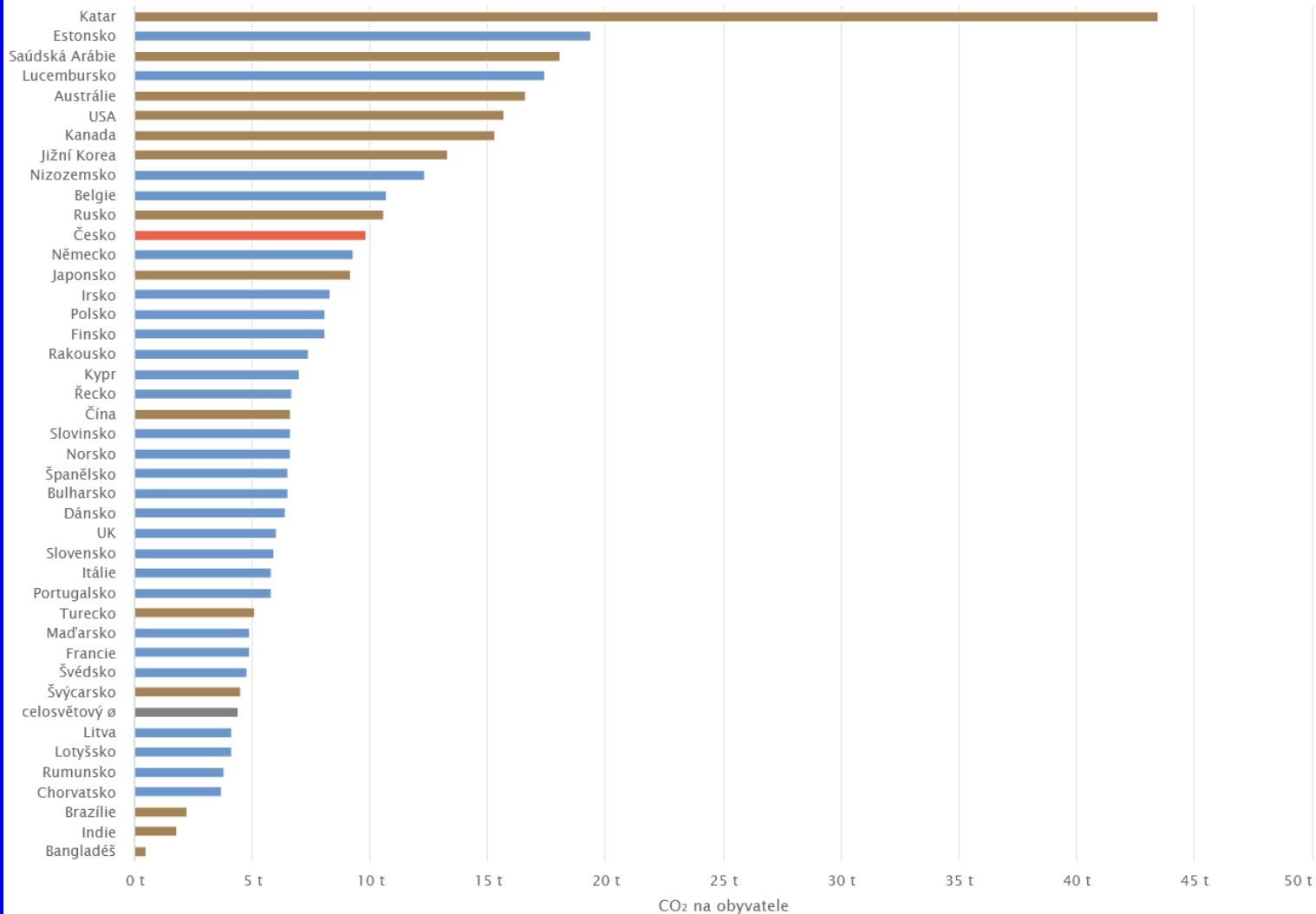


Zdroj: Evropská agentura pro životní prostředí



Emise CO₂ na hlavu

vybrané země, 2017



“Kdo z vás je bez hříchu, první hod’ na ni kamenem”

(see ref.: **Nový zákon**, Jan 8 ... hora Olivetska ...)

Jesus

He that is without sin among you, let him be the first to cast a stone at her.

05. 10. 2021

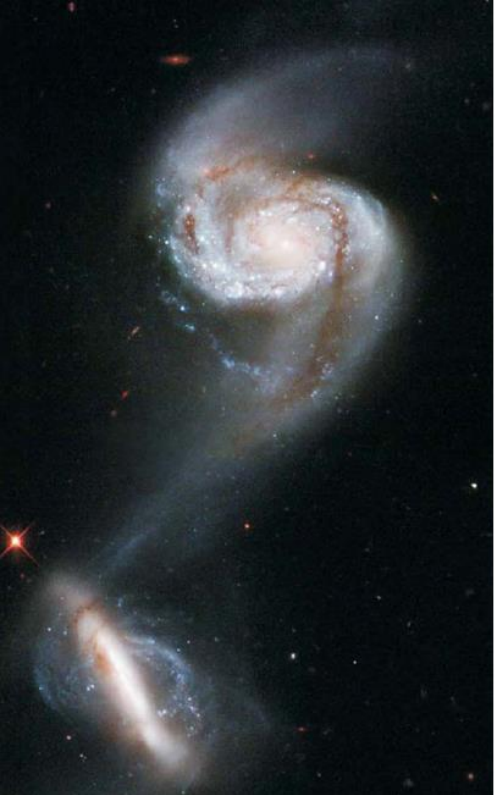
04. 10. 2022

26. 10. 2023

Energie

26. 10. 2023

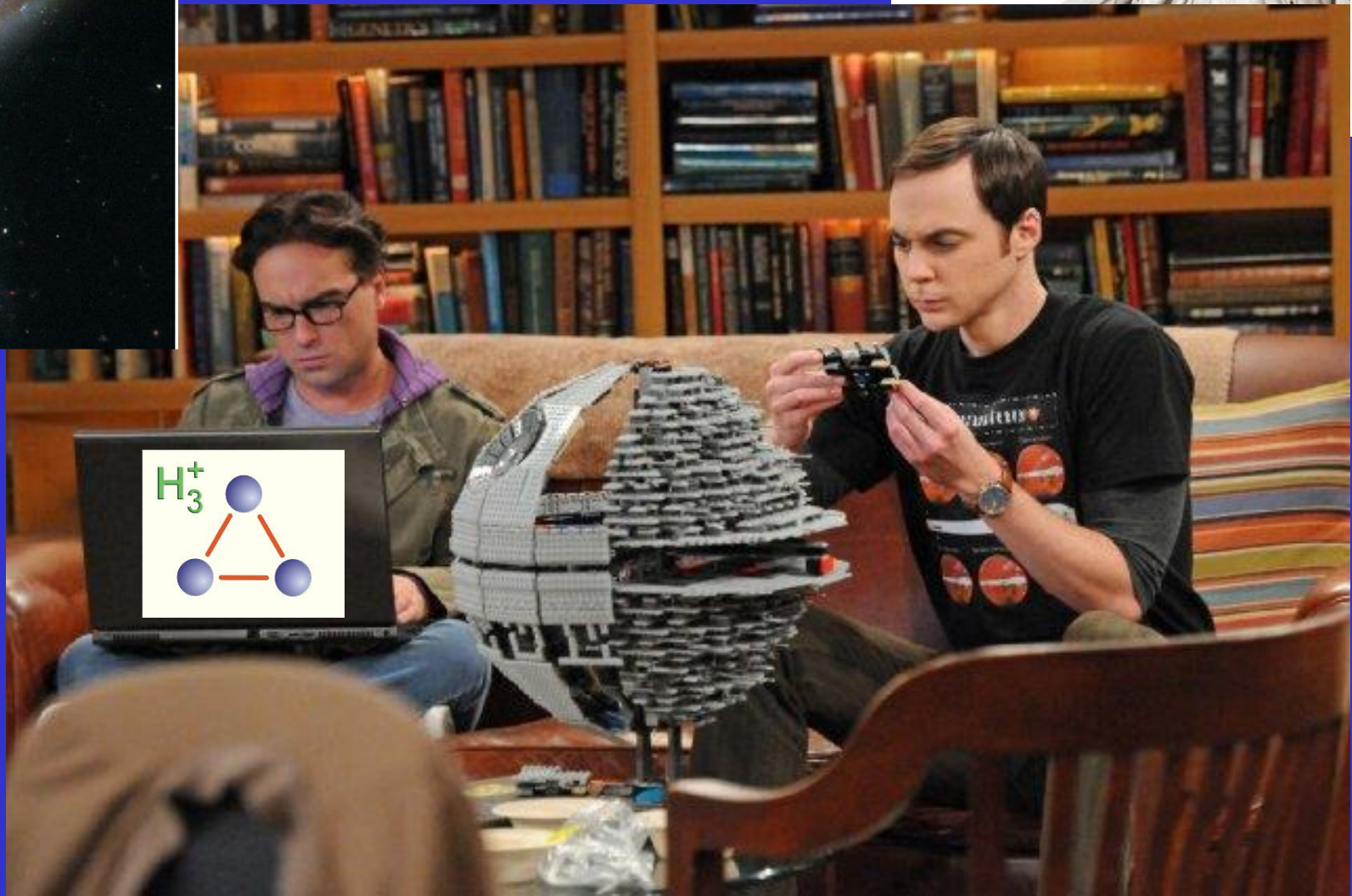
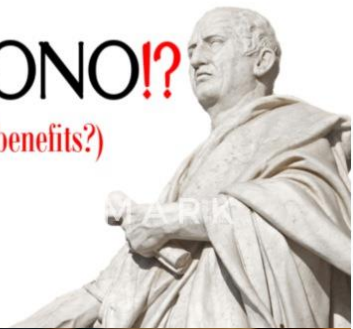
220 054 686	Energie spotřebovaná dnes (MWh), z toho:
187 322 974	- z neobnovitelných zdrojů
33 138 316	- z obnovitelných zdrojů
1 378 873 597 221	Solární energie dopadající na Zemi dnes (MWh)



CUI BONO!?

(Who benefits?)

Cicero

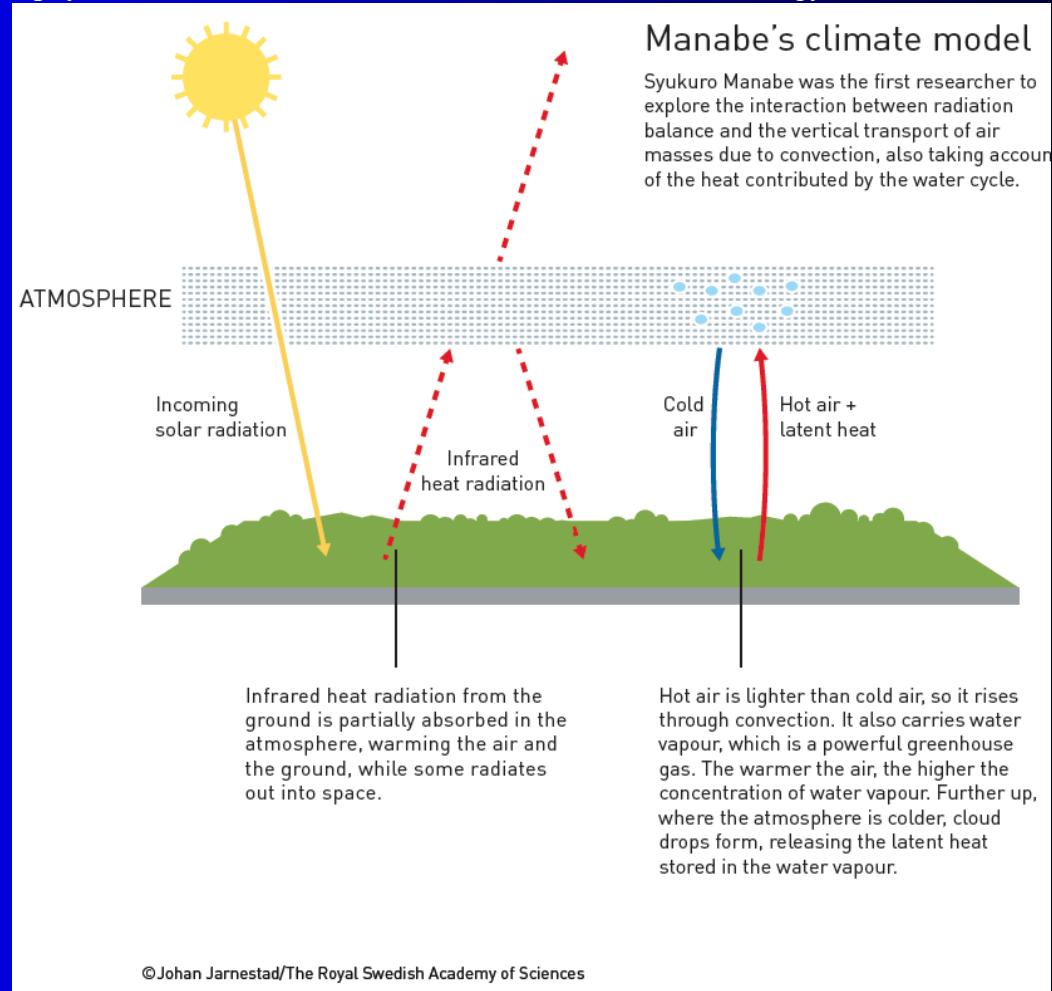
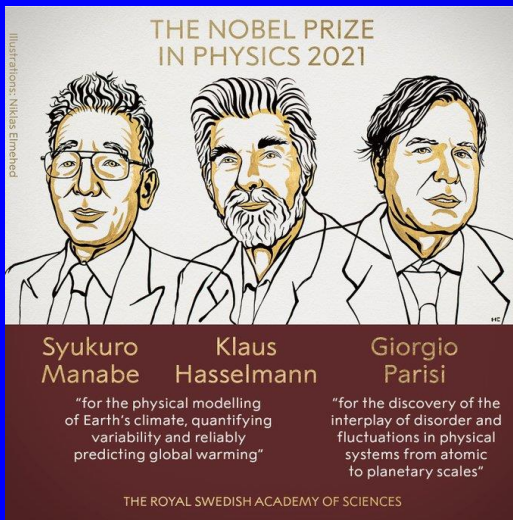


Manabe's work in the 1960s demonstrated how increased levels of carbon dioxide in the atmosphere caused the Earth's temperature to rise. In doing so, he "laid the foundation for the development of current climate models," the Royal Swedish Academy of Sciences said in a statement.

A decade later, Hasselmann "created a model that links together weather and climate."

Parisi's discoveries, meanwhile, "make it possible to understand and describe many different and apparently entirely random complex materials and phenomena." This is not only true for physics but also for other areas, such as mathematics, biology, neuroscience and machine learning, the academy added.

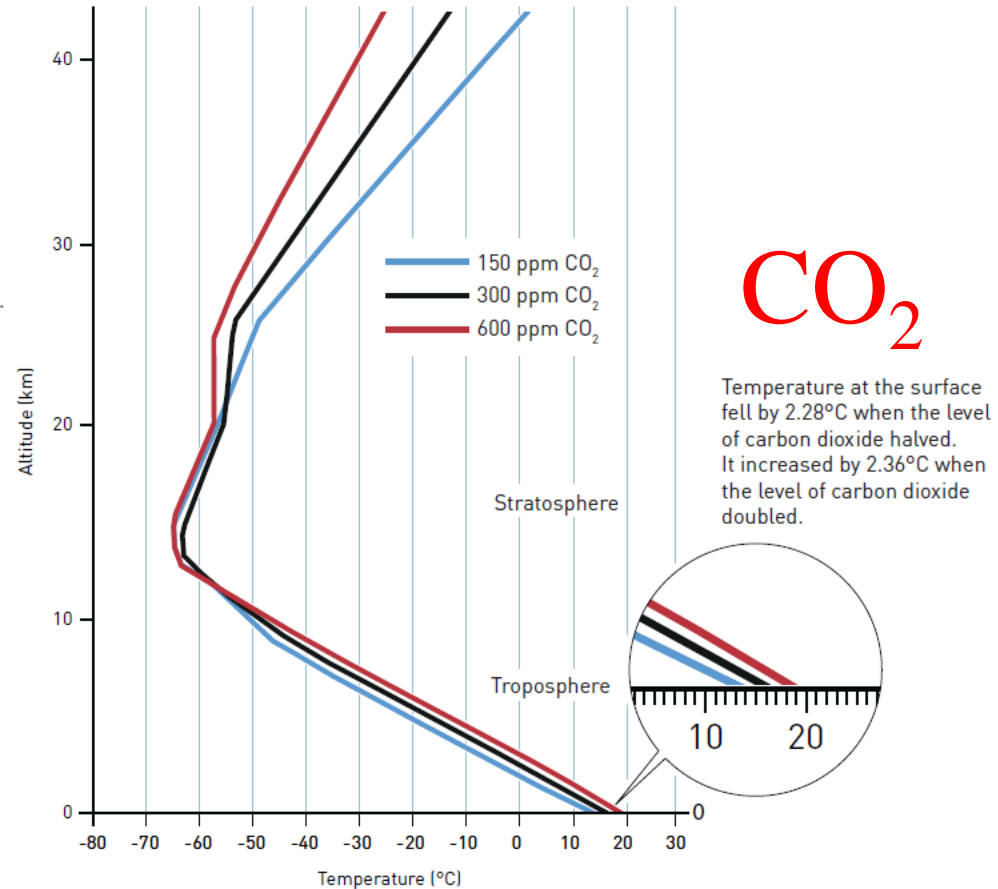
05. 10. 2021



The committee's decision to recognize pioneering work on climate change comes weeks before the world's leaders meet at COP26, [a crucial summit in the United Kingdom.](#)

Carbon dioxide heats the atmosphere

Increased levels of carbon dioxide lead to higher temperatures in the lower atmosphere, while the upper atmosphere gets colder. Manabe thus confirmed that the variation in temperature is due to increased levels of carbon dioxide; if it was caused by increased solar radiation, the entire atmosphere should have warmed up.



Source: Manabe and Wetherald (1967) Thermal equilibrium of the atmosphere with a given distribution of relative humidity, *Journal of the atmospheric sciences*, Vol. 24, Nr 3, May.

©Johan Jarnestad/The Royal Swedish Academy of Sciences

NOBELPRISET I FYSIK 2021
THE NOBEL PRIZE IN PHYSICS 2021

KUNGL. VETENSKAPS-AKADEMIEN
THE ROYAL SWEDISH ACADEMY OF SCIENCES

"för banbrytande bidrag till vår förståelse av komplexa fysikaliska system"
"for groundbreaking contributions to our understanding of complex physical systems"




Photo: Markus Menzies

Syukuro Manabe,
USA

"för fysikalisk modellering av jordens klimat, kvantitativ analys av variationer och tillförlitlig förutsägelse av global uppvärmning"
"for the physical modelling of Earth's climate, quantifying variability and reliably predicting global warming"




Photo: Venice International University

Klaus Hasselmann,
Germany





Photo: Barbara Sobott, Press Office, Scienza

Giorgio Parisi,
Italy

"för upptäckten av hur ordning och fluktuationer samverkar i fysikaliska system från atomära till planetära skalor"
"for the discovery of the interplay of disorder and fluctuations in physical systems from atomic to planetary scales"

THE NOBEL PRIZE
IN PHYSICS 2021



Syukuro
Manabe

"for the physical modelling of Earth's climate, quantifying variability and reliably predicting global warming"

Klaus
Hasselmann

Giorgio
Parisi

"for the discovery of the interplay of disorder and fluctuations in physical systems from atomic to planetary scales"

THE ROYAL SWEDISH ACADEMY OF SCIENCES



Member of the Nobel Committee for Physics Thors Hans Hansson, Secretary General of the Royal Swedish Academy of Sciences Goran K. Hansson, and member of the Nobel Committee for Physics John Wettlaufer announce the winners of the 2021 Nobel Prize in Physics at the Royal Swedish



The committee's decision to recognize pioneering work on climate change comes weeks before the world's leaders meet at COP26, [a crucial summit in the United Kingdom.](#)

For discovery of the interplay of disorder and fluctuations in physical systems from atomic to planetary scales.

24. 09. 2021

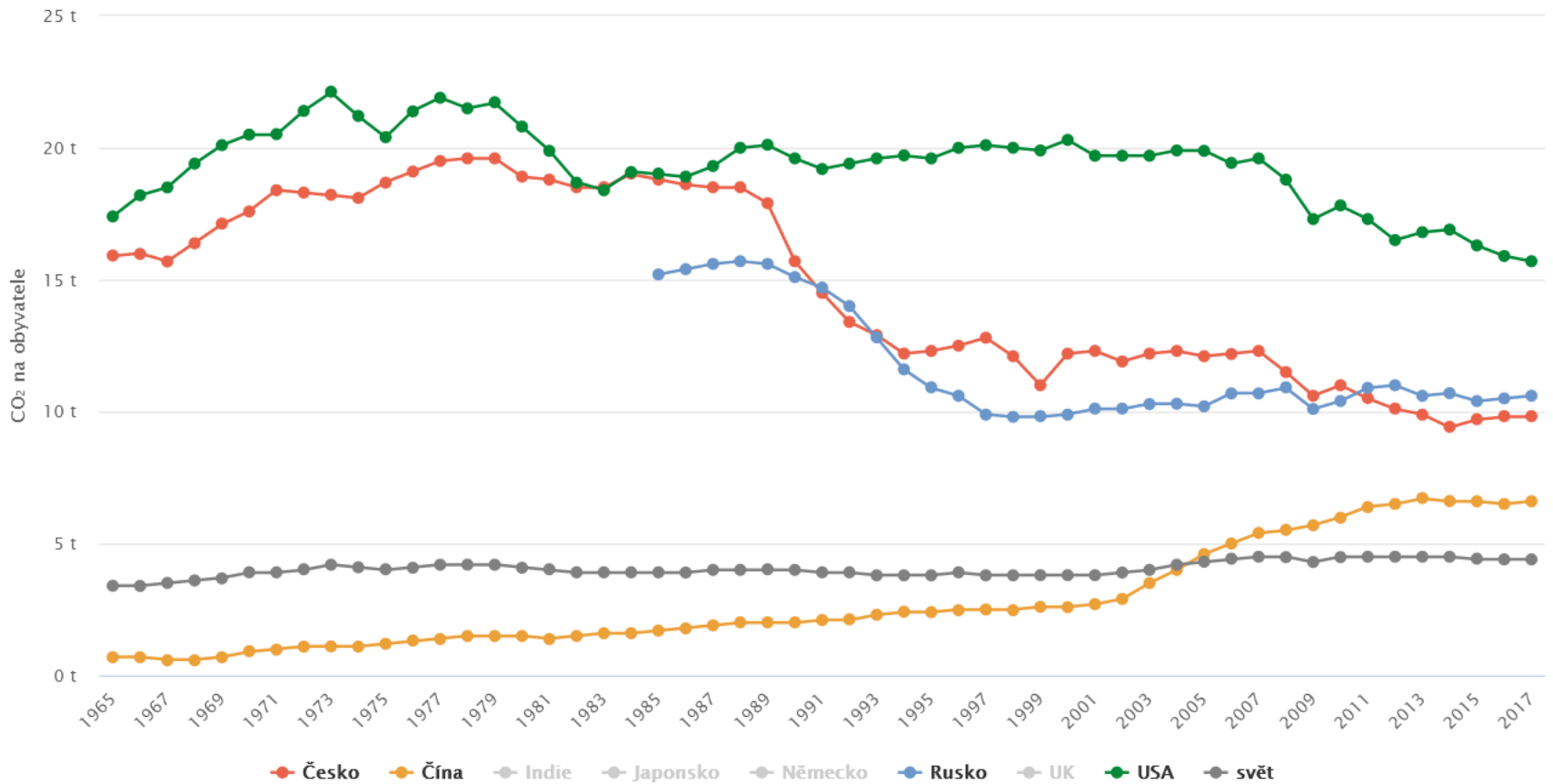
Průzkum: Teenageři se změn klimatu bojí. Protestům fandí, ale nechodí na ně

V Praze se na Malostranském náměstí sešlo kolem 500 lidí, uvedla pro server iROZHLAS na místě policie. Šlo o první studentskou stávku za klima svolanou iniciativou Fridays for Future od loňského září.



Emise CO₂ na hlavu, časová řada

vybrané země, 1965 až 2017



Not actualized, approximation

<https://www.worldometers.info/cz/>

~7 815 369 848

Současná světová populace (8.10. 2019)

~7 897 522 492

Současná světová populace (4. 10. 2021)

~8 068 951 824

Současná světová populace (10:48, 26. 10. 2023)

8.10.2019 do 13:00

in 1 594 603 663 589

Solární energie dopadající na Zemi dnes (MWh)

out 216 185 179

Energie spotřebovaná dnes (MWh)

out/in ~ 0.00013 negligible

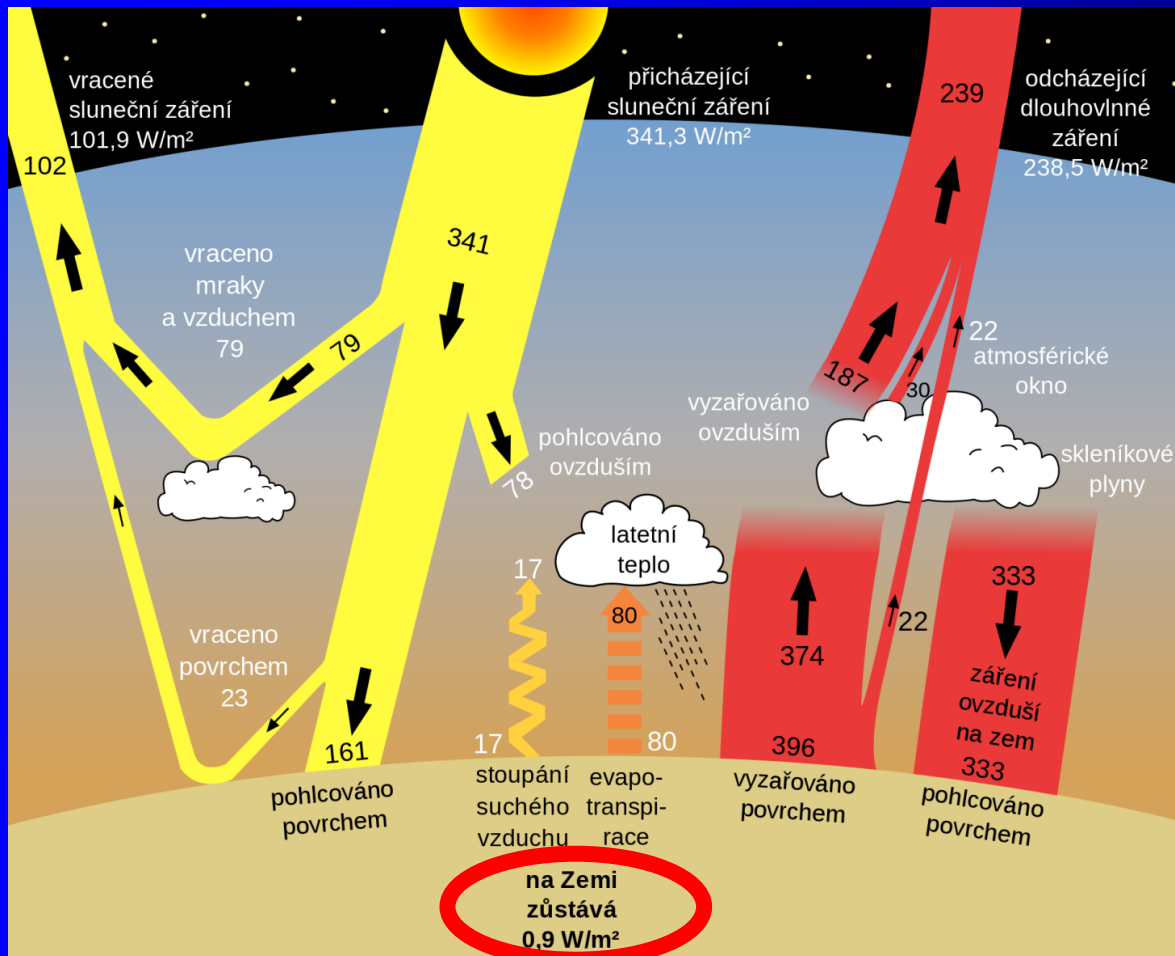
>191 109 298 413

Odeslaných e-mailových zpráv dnes ...

“Kdo z vás je bez hříchu, první hod’ na ni kamenem”

Not actualized, approximation

[wikipedia.org/wiki/Terestriální_záření](https://cs.wikipedia.org/wiki/Terestriální_záření)



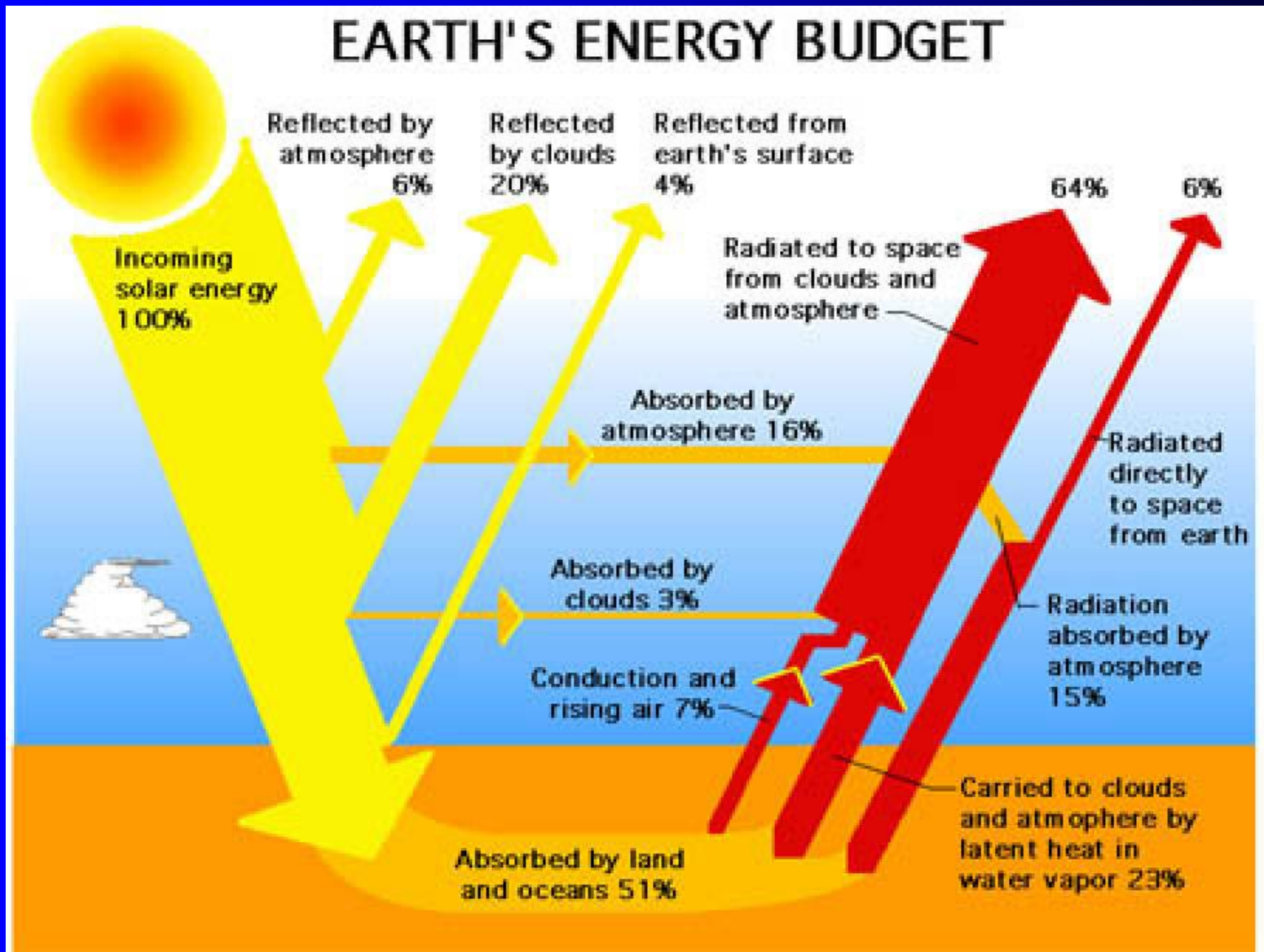
Krátkovlnné záření ze Slunce dopadající na zemský povrch a atmosféru. Dlouhovlnná část záření je emitována z povrchu a téměř zcela absorbována do atmosféry.

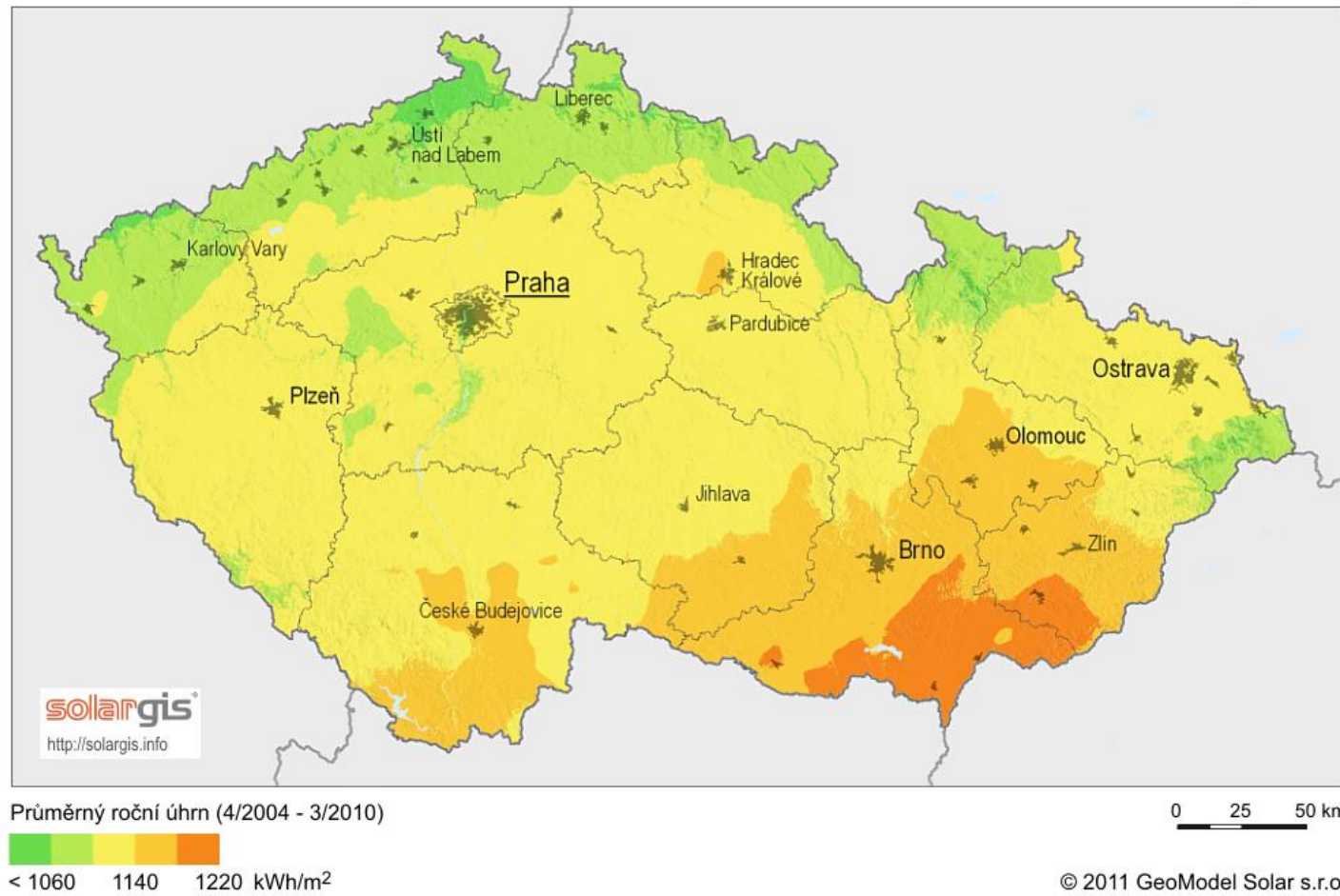
V tepelné rovnováze je absorbovaná energie z atmosféry ~ stejná jako ta vydávaná do vesmíru.

Čísla ukazují výkon záření ve wattch na metr čtvereční v období let 2000–2004

Průměrná hustota toku energie ze zemského povrchu vzhůru činí asi 400 W/m^2 , což odpovídá teplotě $16 \text{ }^\circ\text{C}$; hustota toku, který Země vyzařuje do vesmíru, činí ale jen asi 240 W/m^2 a odpovídá to teplotě zhruba 255 K . Terestriální (též terestrické, pozemské) záření je v naprosté většině dlouhovlnné infračervené záření.

EARTH'S ENERGY BUDGET



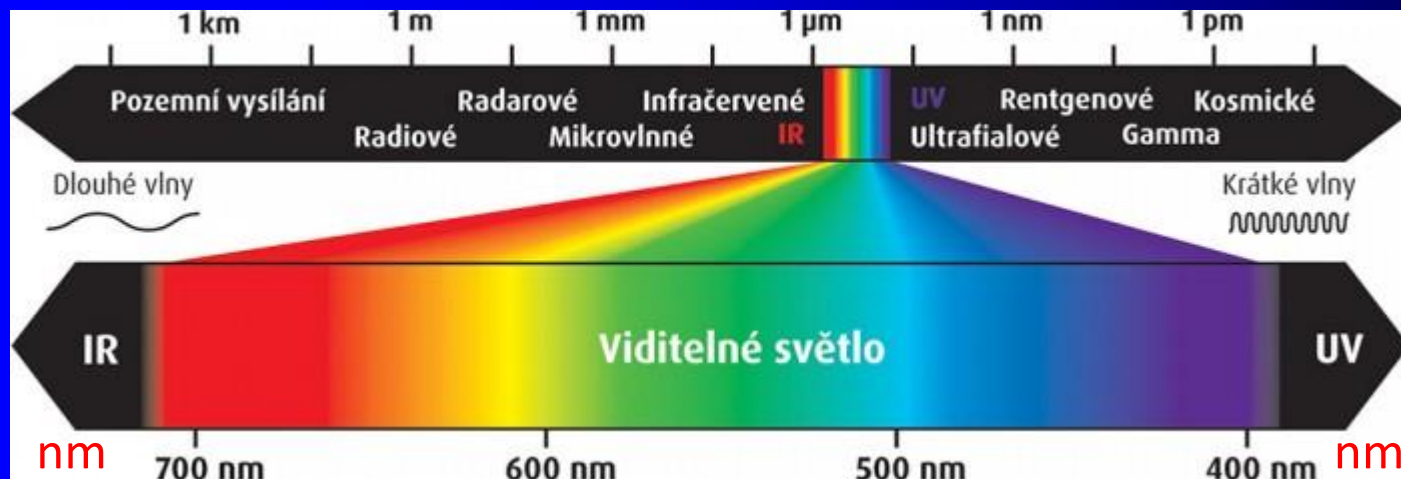


.... elektřiny stanoven na 6 Kč/kWh s DPH

.... plynu na 3 Kč/kWh s DPH.

Spektrum elektromagnetického záření

Information



Viditelné světlo - elektromagnetické záření v rozmezí vlnových délek 380–760 nm.

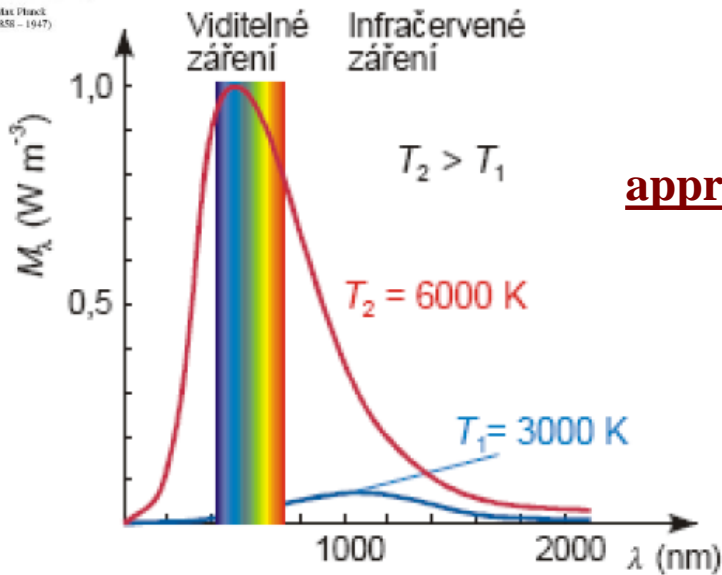
eV



Záření černého tělesa



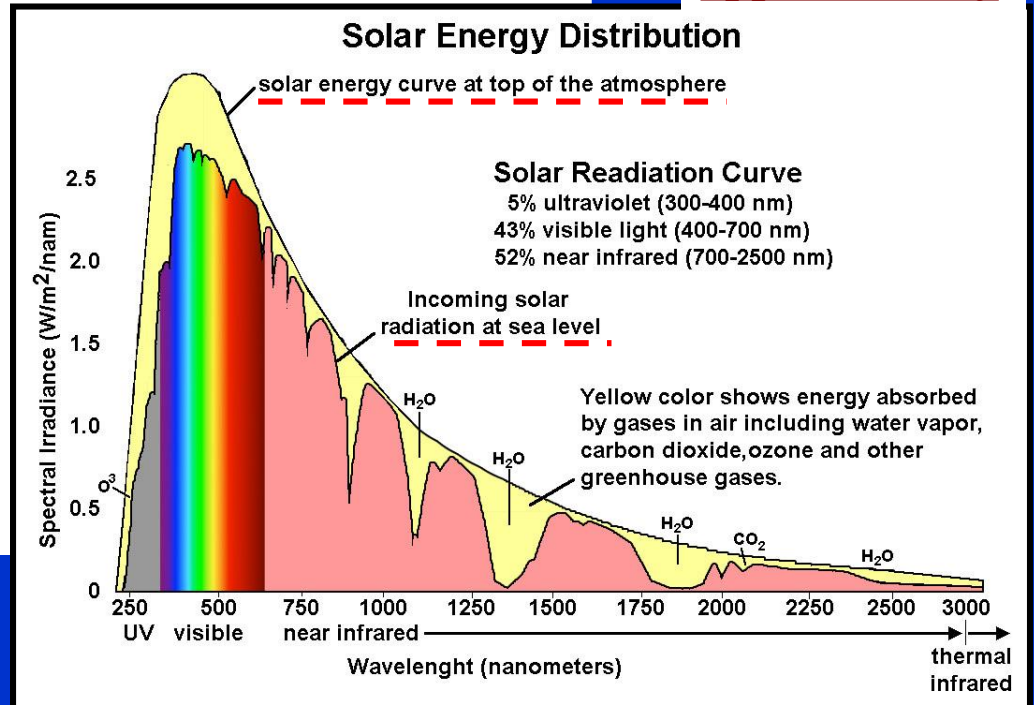
Max Planck
(1858 - 1947)



approximately

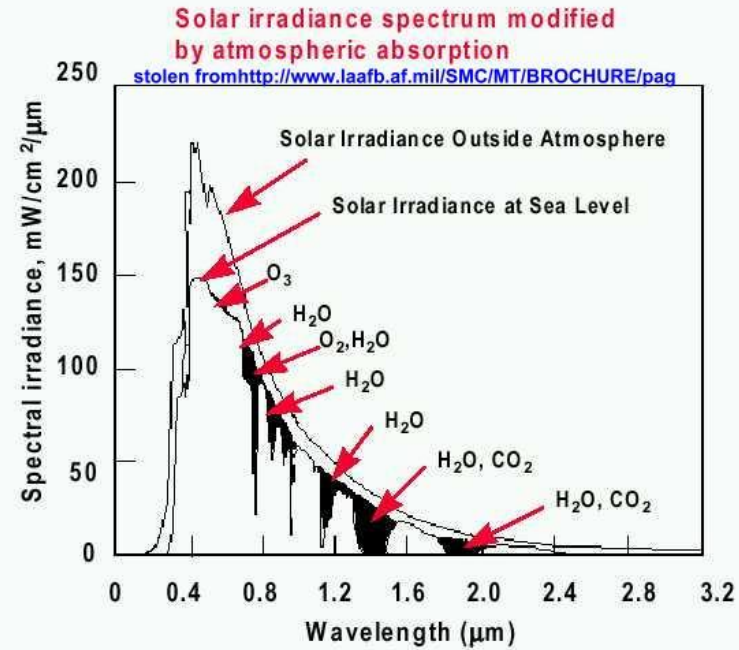
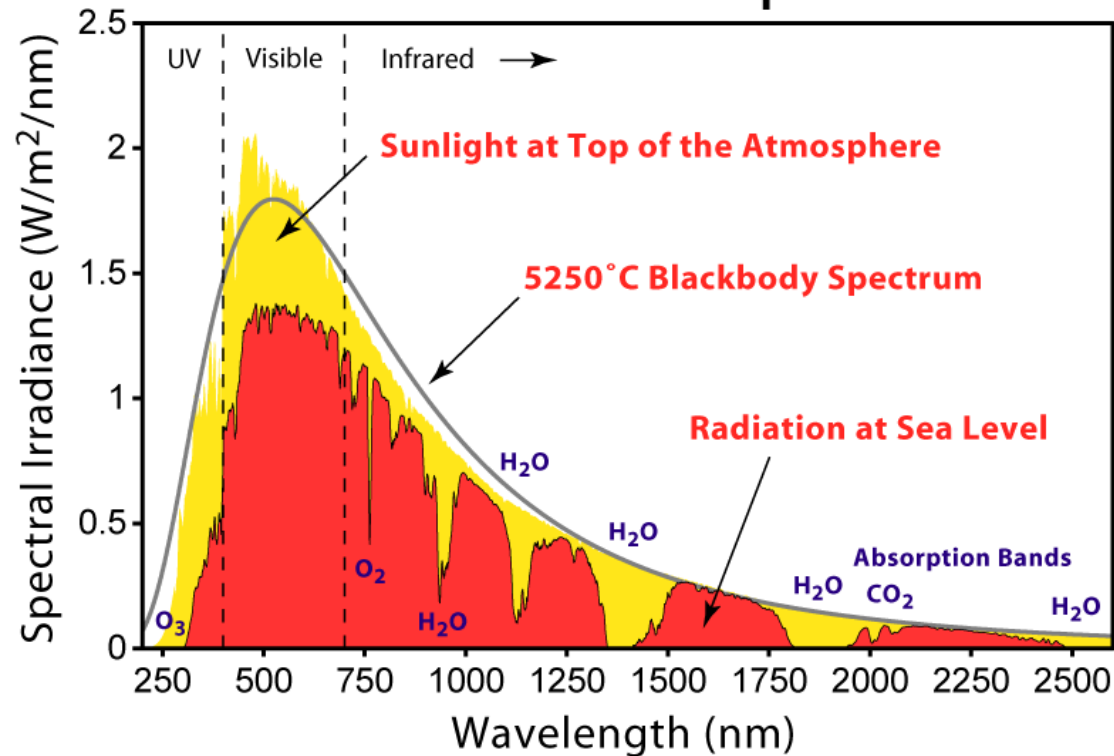
Průběh **spektrální intenzity vyzařování** v závislosti na vlnové délce a teplotě. S rostoucí termodynamickou teplotou tělesa se zvyšuje maximum spektrální intenzity vyzařování a posouvá se směrem k nižší vlnové délce

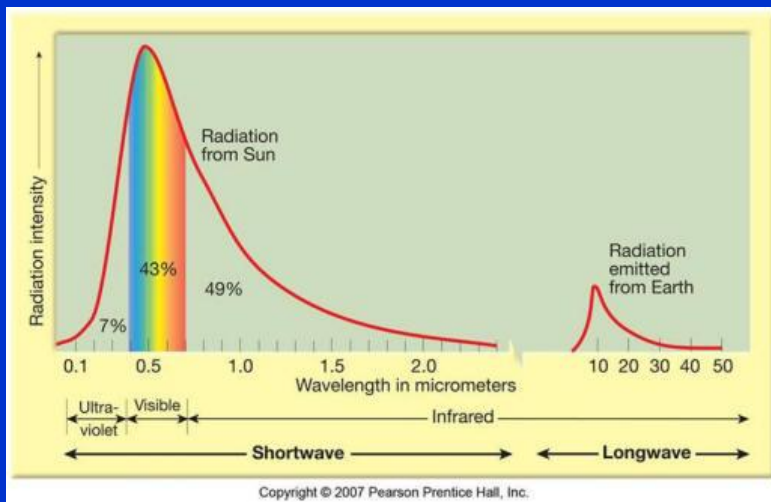
approximately



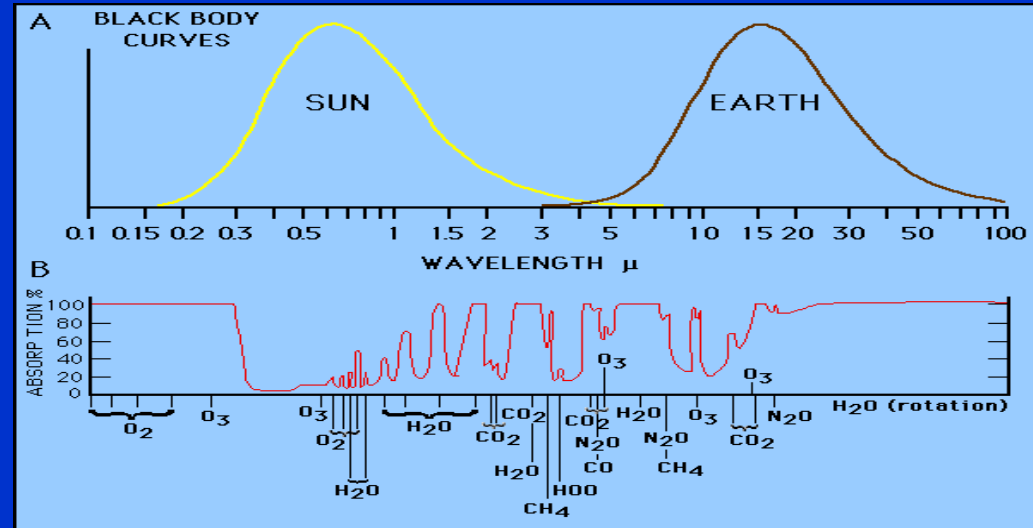
Spectrum of solar radiation modified by atmospheric absorption

Solar Radiation Spectrum





Detail 0.1-100 μm



Absorption

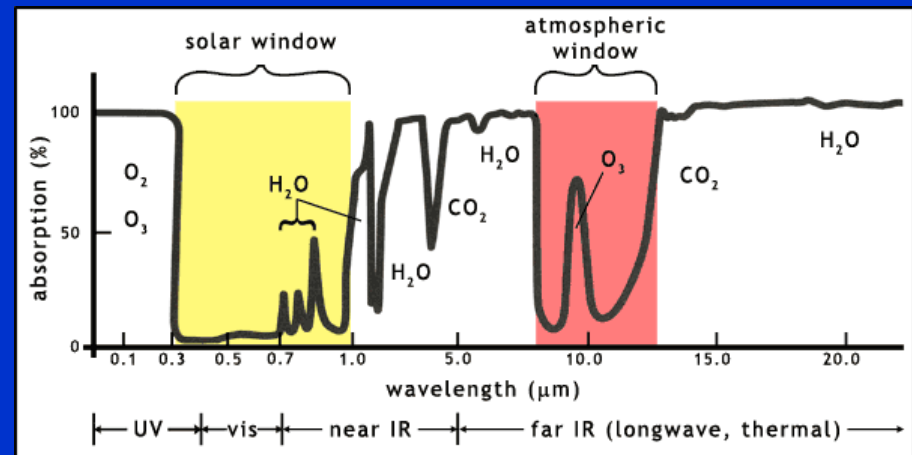
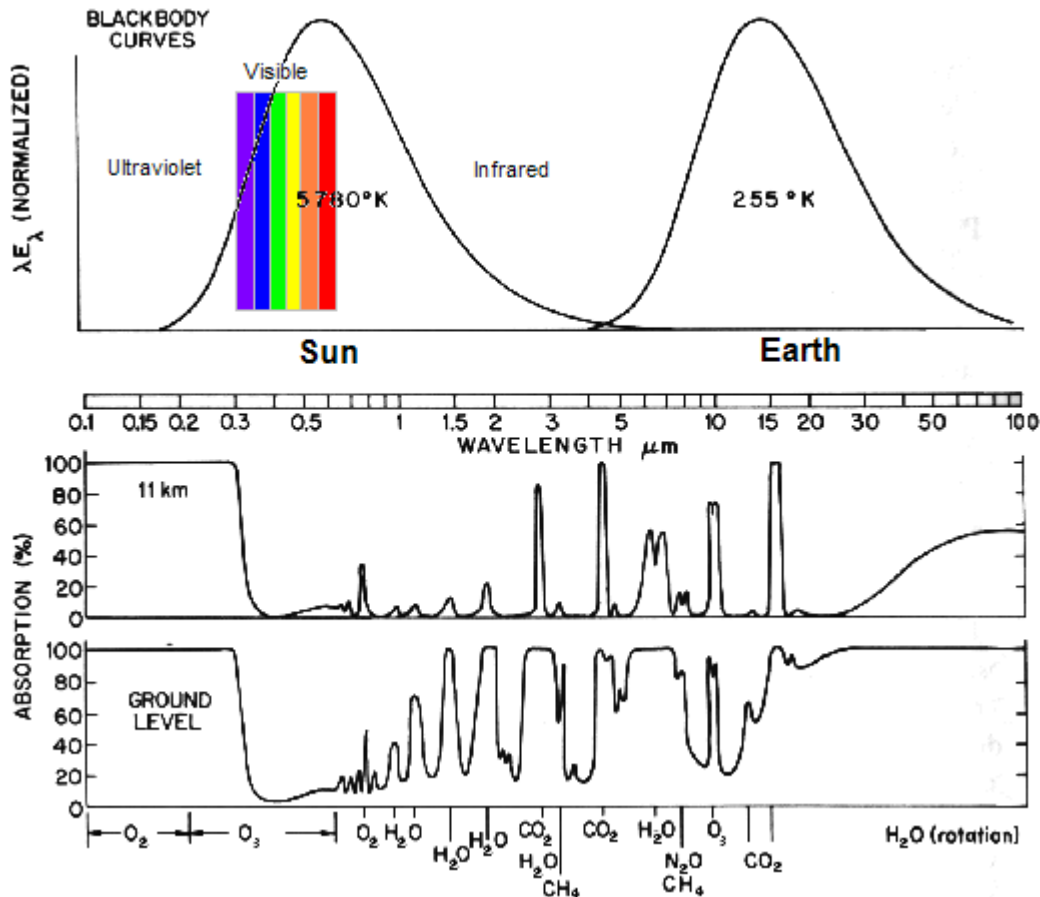
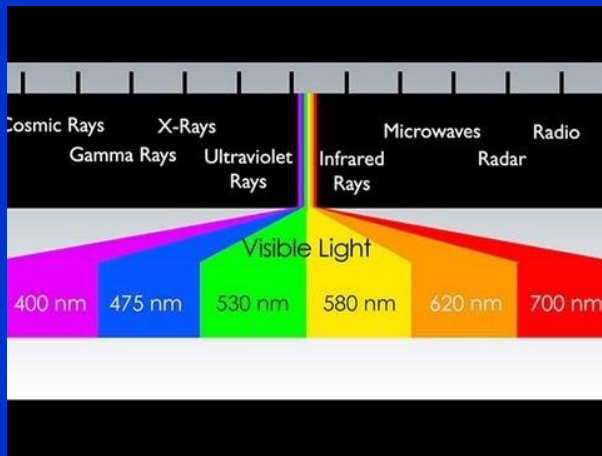
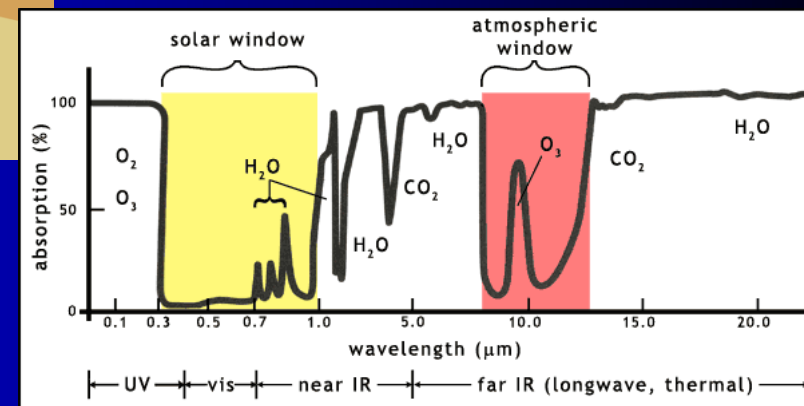
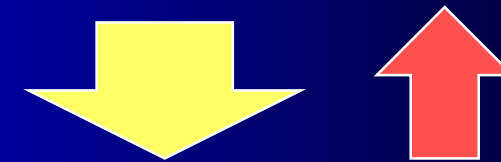
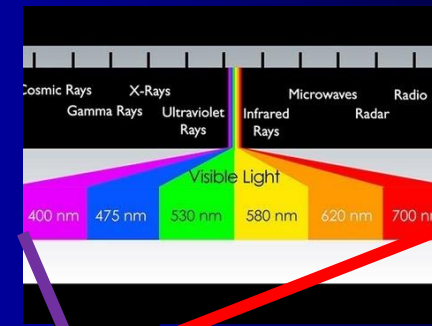
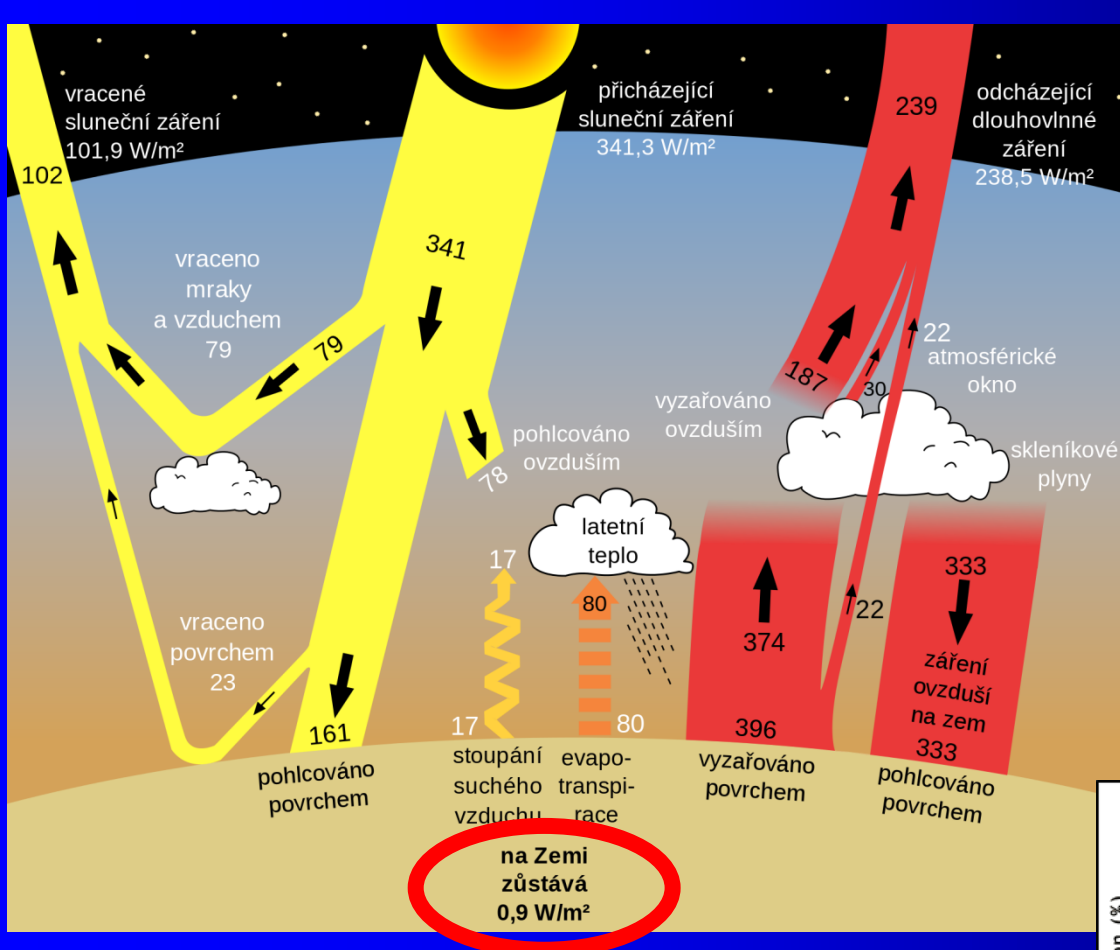


Figure 3. The wavelengths of incoming solar radiation and emitted radiation absorbed by the Earth's atmosphere, showing the solar window and atmospheric (thermal) window. The graph shows the regions of the electromagnetic spectrum (light) that are absorbed by specific molecules. Key: CO₂, carbon dioxide; H₂O, water; IR, infrared light; O₂, oxygen; O₃, ozone; UV, ultraviolet light; vis, visible light (adapted from a figure in Turco 2002, p334)

Absorption



approximation

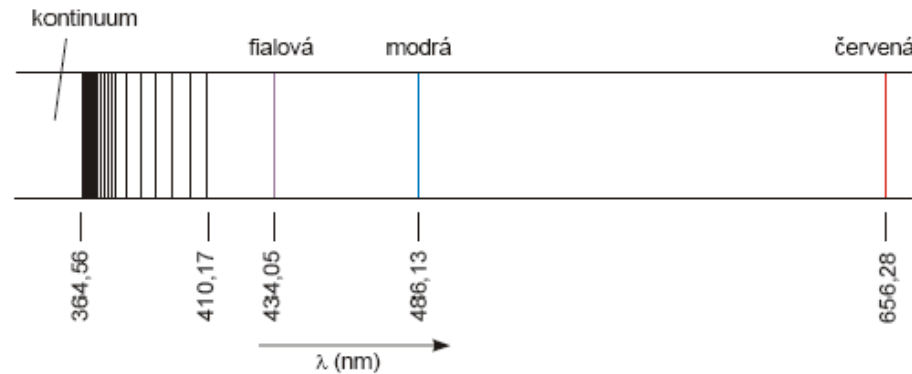
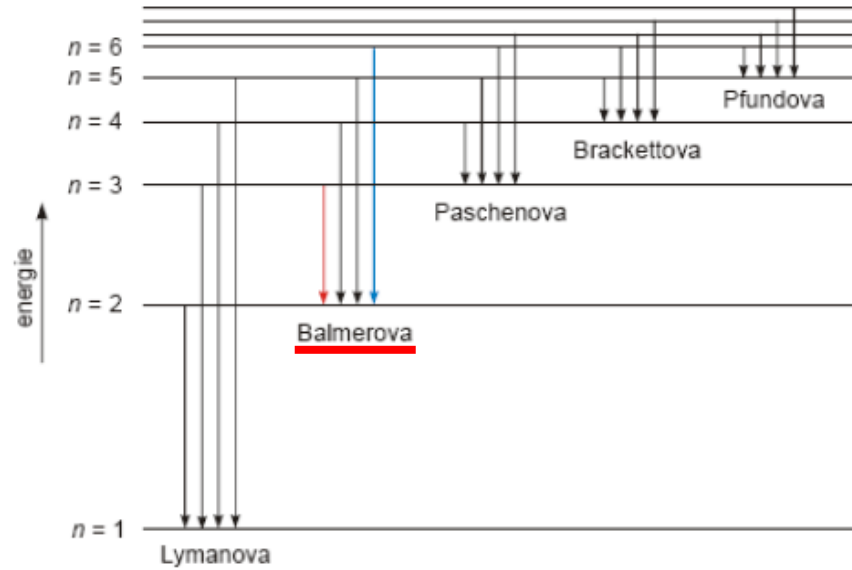
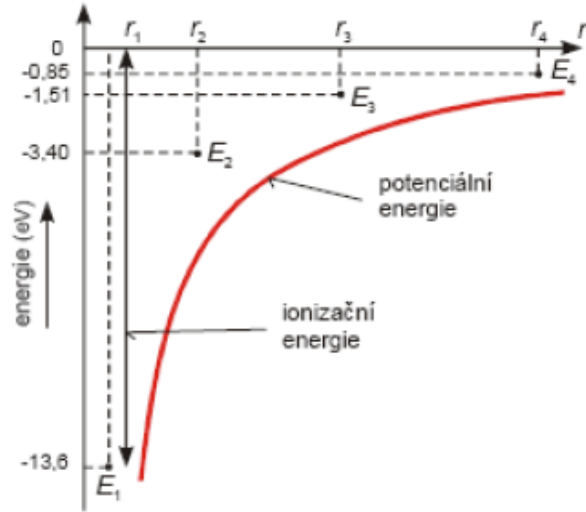


Krátkovlnné záření ze Slunce dopadající na zemský povrch a atmosféru. Dlouhovlnná část záření je emitována z povrchu a téměř zcela absorbována do atmosféry. V tepelné rovnováze je absorbovaná energie z atmosféry stejná jako ta vydávaná do vesmíru. Čísla ukazují výkon záření ve watech na metr čtvereční v období let 2000–2004



Niels Bohr

Spektrum atomu vodíku



$$h\nu = 13.6 \left(\frac{1}{n_f^2} - \frac{1}{n_i^2} \right) [eV]$$

Energy levels H

Selection rule

$$\Delta l = \pm 1; \quad \Delta m_l = 0, \pm 1$$

Grotrian diagram H

Angular momentum of photon is s=1

5.2 Atomic structure and atomic spectra

13.6eV

Fig. 15.12. A Grotrian diagram which summarizes the appearance and analysis of the spectrum of atomic hydrogen. The thicker the line, the more intense the transition.

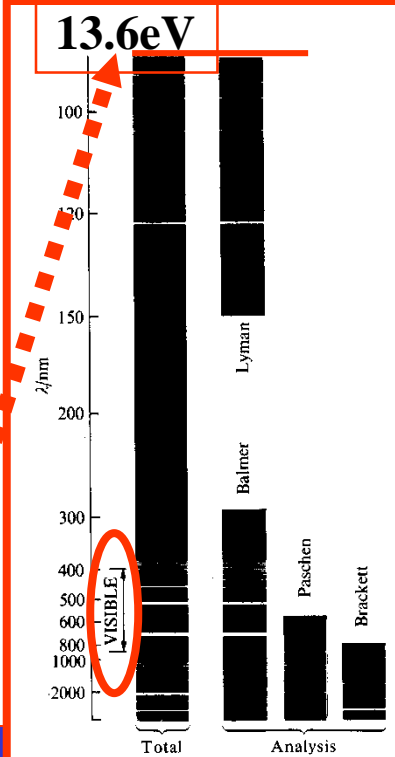
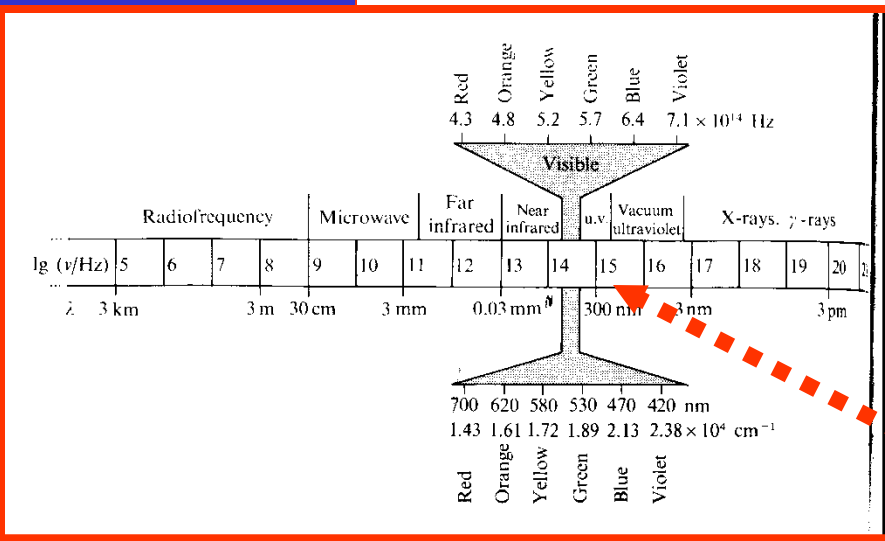
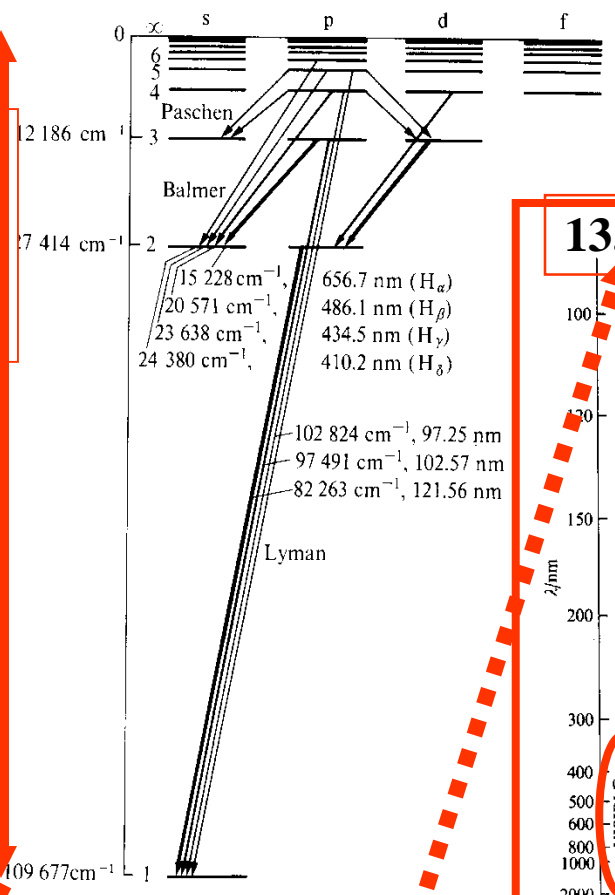


Fig. 15.1. The spectrum of atomic hydrogen. The spectrum is shown on the left, and is analysed into its overlapping series on the right. Note that the Balmer series lies in the visible region.

$$E_n = -\frac{Z^2 \mu e^4}{32\pi^2 \epsilon_0^2 \hbar^2} \times \frac{1}{n^2}$$



$$h\nu = 13.6 \left(\frac{1}{n_f^2} - \frac{1}{n_i^2} \right) [eV]$$

13.6eV x 8065,5 cm⁻¹ → 109000 cm⁻¹ → 91nm

Classical or quantum approach?

Electron:

$$\begin{aligned} 1\text{eV} &\rightarrow v = 5.9 \times 10^7 \text{ cm s}^{-1} \\ &\tau \sim a_0/v \sim 10^{-8} / 5.9 \times 10^7 = 2 \times 10^{-16} \text{ s} \\ &\lambda \sim 2A = 2 \times 10^{-8} \text{ cm de Broglie} \\ &\text{za } 1\mu\text{s} \dots\dots\dots 1\mu\text{s} \times 5.9 \times 10^7 \text{ cm s}^{-1} = 59 \text{ cm} \end{aligned}$$

Ar+:

$$\begin{aligned} 1\text{eV} &\rightarrow v = 2 \times 10^5 \text{ cm s}^{-1} \\ &\tau \sim a_0/v \sim 10^{-8} / 2 \times 10^5 \sim 6 \times 10^{-14} \text{ s} \\ &\lambda \sim 9 \times 10^{-11} \text{ cm de Broglie} \end{aligned}$$

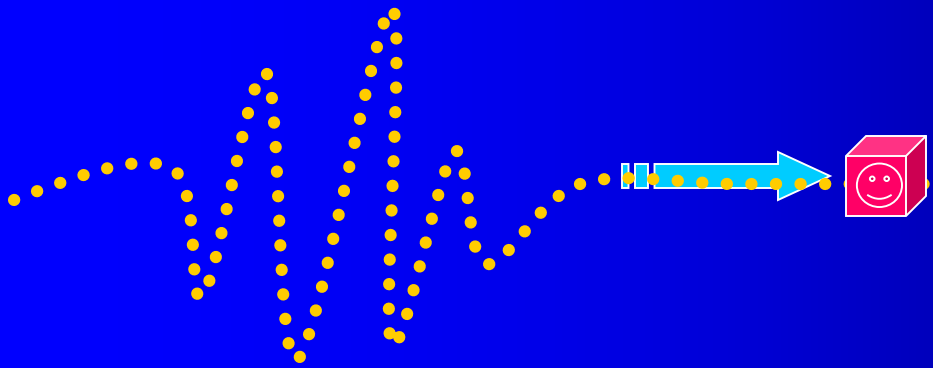
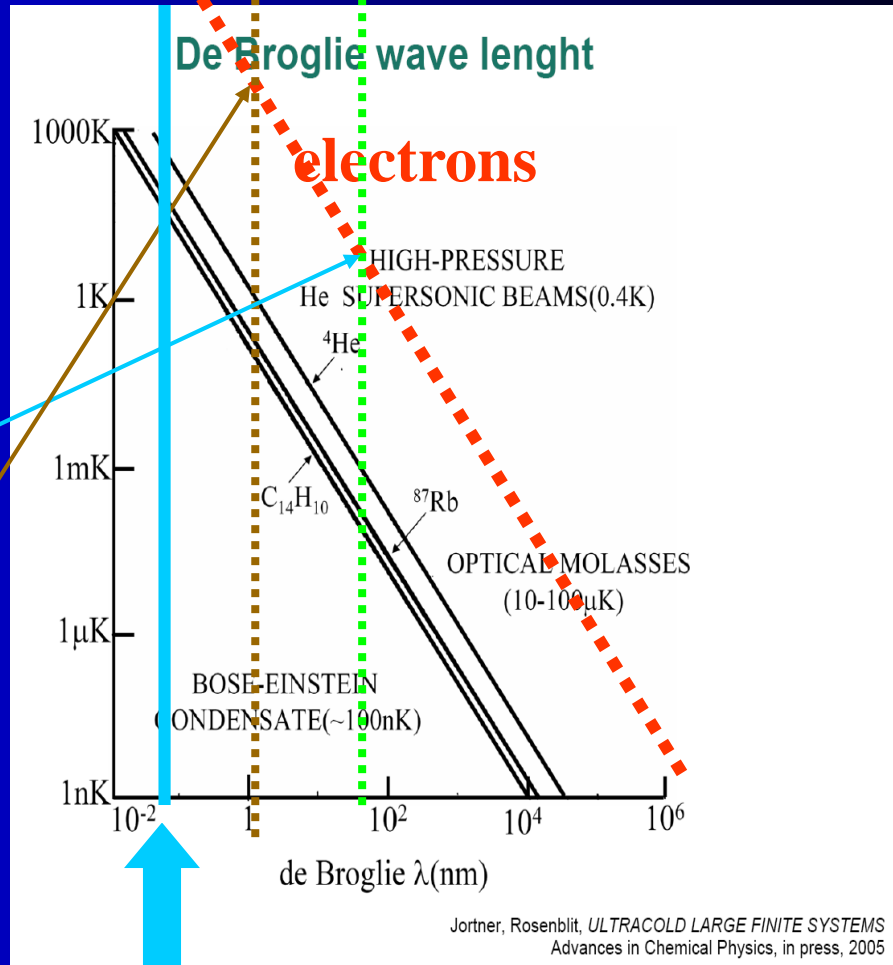
$$40 \times 1800 = 72\,000$$

De Broglie wave length

$$\lambda = \frac{h}{p} = \frac{h}{mv} \sqrt{1 - \frac{v^2}{c^2}}$$

$$\lambda_e (4K) \sim 540 \text{ \AA} \sim 54 \times 10^{-9} \text{ m}$$

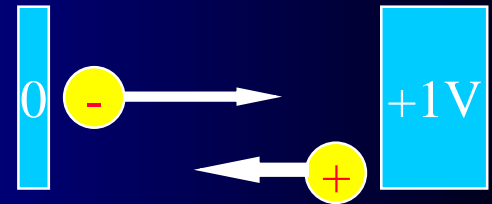
$$\lambda_e (1eV) \sim 11.6 \text{ \AA} \sim 1.16 \times 10^{-9} \text{ m}$$



a_0

Electronvolt

$$E \leftrightarrow kT$$
$$1\text{eV} \sim 11\,604.5\text{ K}$$
$$1\text{K} \sim 9 \times 10^{-5}\text{eV}$$



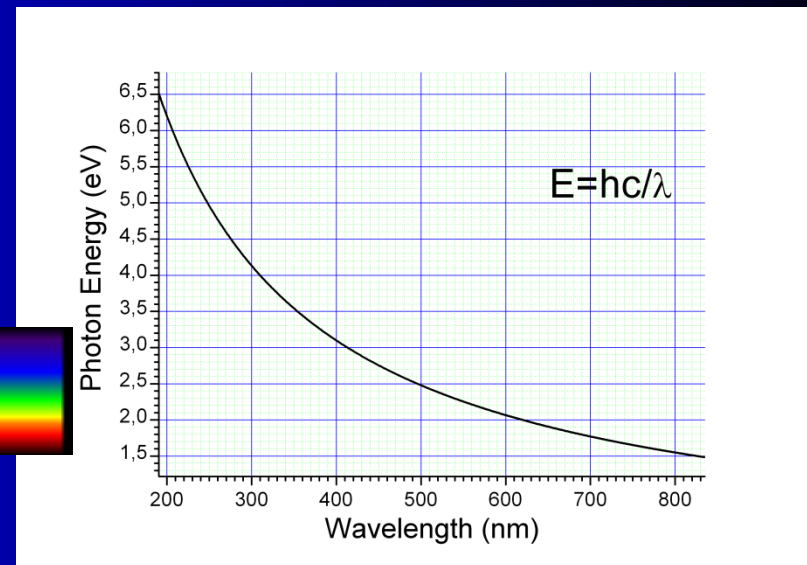
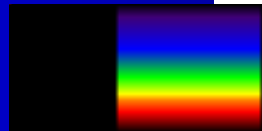
By definition, it is equal to the amount of kinetic energy gained by a single unbound electron when it accelerates through an electric potential difference of one volt

Conversion factors:

1 eV = $1.6021765(40) \times 10^{-19}\text{J}$ (the conversion factor is numerically equal to the elementary charge expressed in coulombs).

1 eV (per atom) is 96.485 kJ/mol.

1.65 to 3.27 eV: the photon energy of visible light.



13.6 eV: The energy required to ionize atomic hydrogen.
Molecular bond energies are on the order of one eV per molecule

1 TeV: A trillion electronvolts, or $1.602 \times 10^{-7}\text{ J}$, about the kinetic energy of a flying mosquito

14 TeV: the design proton collision energy at the Large Hadron Collider (which has operated at half of the energy since March 30, 2010).

Mol (značka mol) je základní fyzikální jednotka látkového množství.

Jeden mol libovolné látky obsahuje stejný počet částic, jaký je obsažen atomů v 12 g nuklidu uhlíku.

Tento počet udává Avogadrova konstanta, jejíž hodnota je přibližně $6,022 \times 10^{23}\text{ mol}^{-1}$.

Conversion factors

$E \leftrightarrow kT$

$1 \text{ eV} \sim 11\,604.5 \text{ K}$

$1 \text{ K} \sim 9 \times 10^{-5} \text{ eV}$

$$1 \text{ eV}/k = \frac{1 \text{ eV}}{8,617\,333\,262 \times 10^{-5} \text{ eV/K}} = 11\,604,518\,12 \dots \text{ K}$$

$$R\mathcal{F} = 2.4789 \text{ kJ mol}^{-1}$$

$$R\mathcal{F}/F = 25.693 \text{ mV}$$

$$2.3026R\mathcal{F}/F = 59.159 \text{ mV}$$

$$k\mathcal{F}/hc = 207.223 \text{ cm}^{-1}$$

$$V_m^\ominus = R\mathcal{F}/p^\ominus = 2.4465 \times 10^{-2} \text{ m}^3 \text{ mol}^{-1} = 24.465 \text{ dm}^3 \text{ mol}^{-1}$$

T/K	100.00	298.15	500.00	1000.0	1500.0	2000.0
$(kT/kc)/\text{cm}^{-1}$	69.50	207.22	347.51	659.03	1042.5	1390.1

$$p^\ominus = 100 \text{ kPa} = 1 \times 10^5 \text{ N m}^{-2}$$

$$1 \text{ atm} = 101.325 \text{ kPa} = 1.013\,25 \times 10^5 \text{ N m}^{-2} = 1.013\,25 \times 10^5 \text{ J m}^{-3}$$

$$1 \text{ atm} = 760 \text{ Torr (exactly)}$$

$$1 \text{ Torr} = 133.322 \text{ Pa (exactly)}$$

$$1 \text{ mmHg} = 133.3224 \text{ Pa}$$

$$1 \text{ eV} = 1.602\,19 \times 10^{-19} \text{ J} \triangleq 96.485 \text{ kJ mol}^{-1} \triangleq 8065.5 \text{ cm}^{-1}$$

$$1 \text{ cm}^{-1} \triangleq 1.986 \times 10^{-23} \text{ J} \triangleq 11.96 \text{ J mol}^{-1} \triangleq 0.1240 \text{ meV}$$

1 eV ~ 23.06 hc

$$hc = 1.986\,48 \times 10^{-23} \text{ J cm}$$

$$hc/k = 1.438\,79 \text{ cm K}$$

$$g/\text{m s}^{-2} = 9.8064 - 0.0259 \cos \{2(\text{latitude})\} = 9.811 \text{ at } 50^\circ$$

$$1 \text{ cal} = 4.184 \text{ J}$$

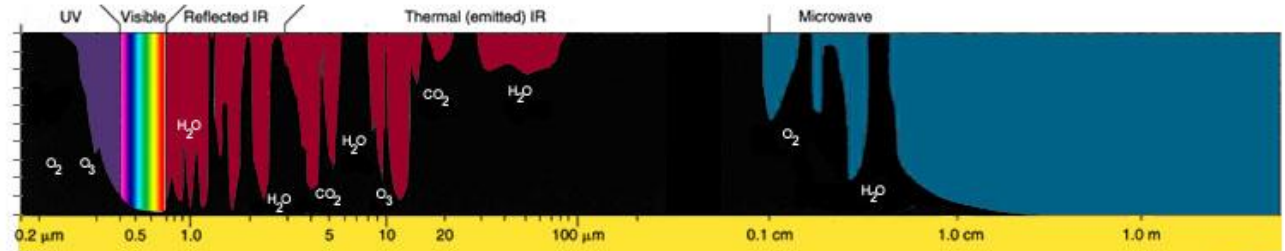
$$1 \text{ D (debye)} = 3.335\,64 \times 10^{-30} \text{ C m}$$

$$1 \text{ N} = 1 \text{ J m}^{-1} = 10^5 \text{ dyne} \quad 1 \text{ W} = 1 \text{ J s}^{-1} \quad 1 \text{ T} = 1 \text{ J C}^{-1} \text{ s m}^{-2}$$

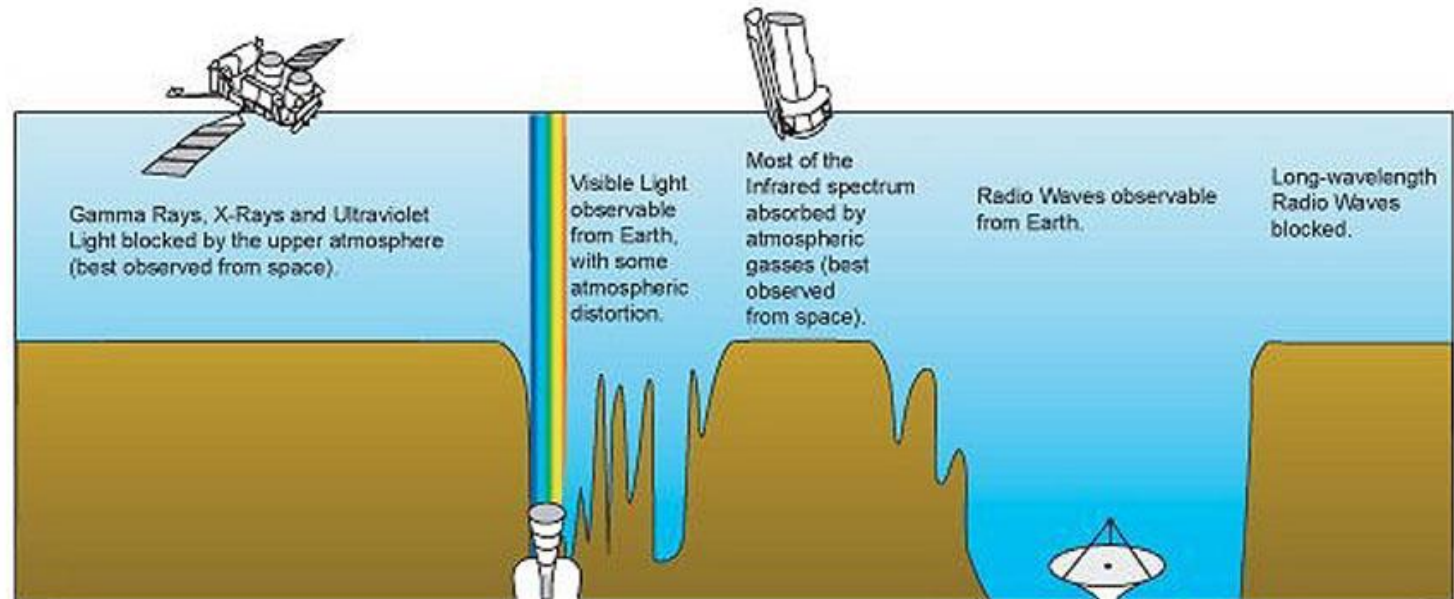
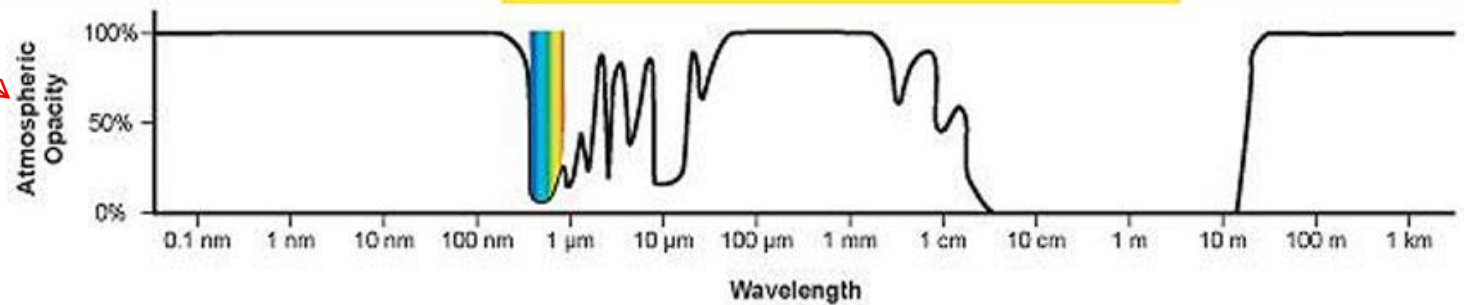
$$1 \text{ J} = 10^7 \text{ erg} \quad 1 \text{ A} = 1 \text{ C s}^{-1} \quad 1 \text{ J} = 1 \text{ A V s}$$



Detail 0.1nm-1 km

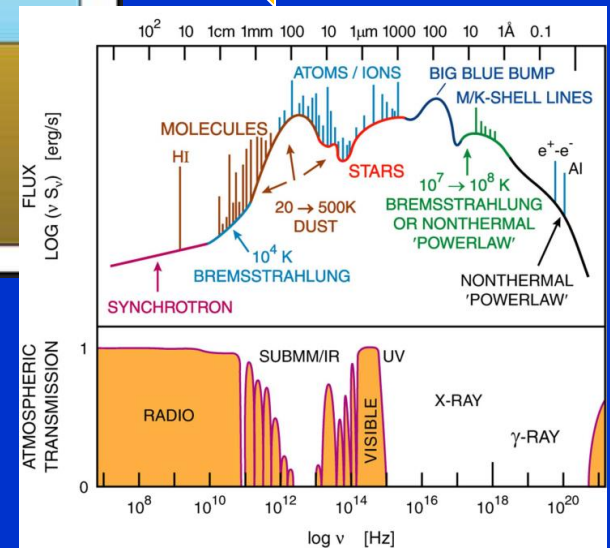
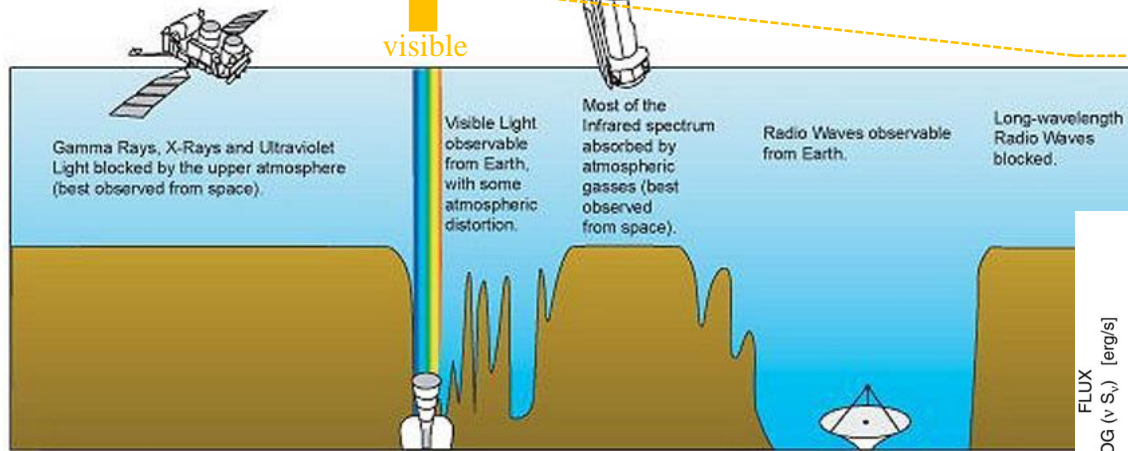
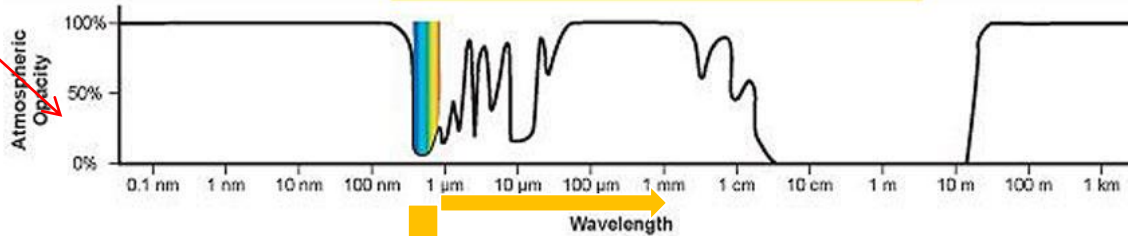
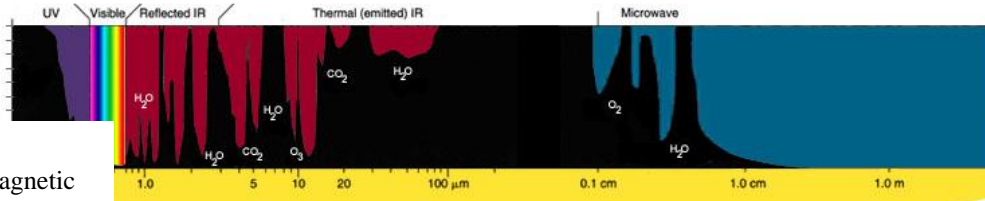


Opacity is the measure of impenetrability to electromagnetic or other kinds of radiation, especially visible light.



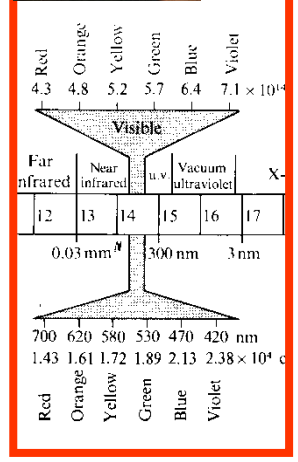
Detail 0.1nm-1 km

Opacity is the measure of impenetrability to electromagnetic or other kinds of radiation, especially visible light.



Before

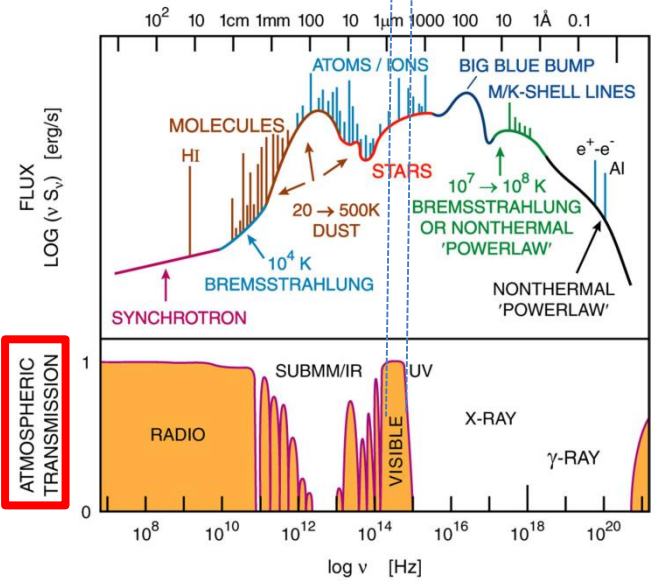
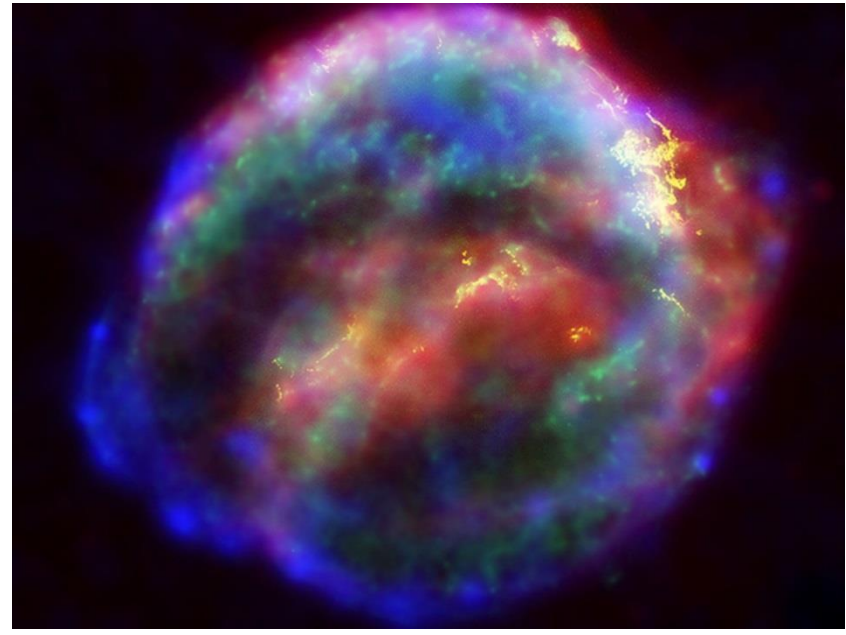
The Supernova of 1604



visible



The Supernova of 1604



ATMOSPHERIC TRANSMISSION

The first recorded observation was in northern Italy on October 9, 1604. [\[2\]](#) [Johannes Kepler](#) began observing the luminous display while working at the imperial court in [Prague](#) for [Emperor Rudolf II](#) on October 17. [\[3\]](#) It was subsequently named after him because his observations tracked the object for an entire year and because of his book on the subject, entitled *De Stella nova in pede Serpentarii* ("On the new star in Ophiuchus's foot", Prague 1606).

It was the second supernova to be observed in a generation (after [SN 1572](#) seen by [Tycho Brahe](#) in [Cassiopeia](#)). No further supernovae have since been observed with certainty in the Milky Way, though many others outside our galaxy have been seen since [S Andromedae](#) and [SN 1987A](#) in the [Large Magellanic Cloud](#) was visible to the naked eye.

1722



socha Atlanta

Astronomická věž

1722



Věž byla dokončena v roce 1722. Na vrcholu věže stojí socha Atlanta (olověná socha s železnou vnitřní konstrukcí, váha asi 600 kg, výška 2,4 m). Atlas nese nebeskou sféru (průměr asi 1,6 m, váha asi 150 kg) s korouhví.

(Pravděpodobně

Matyáš Braun)

1722



Klementinum and astronomy.

Astronomická věž

socha Atlanta



1722



Věž byla dokončena v roce 1722. Na vrcholu věže stojí socha Atlanta (olověná socha s železnou vnitřní konstrukcí, váha asi 600 kg, výška 2,4 m). Atlas nese nebeskou sféru (průměr asi 1,6 m, váha asi 150 kg) s korouhví.

(Pravděpodobně

Matyáš Braun)

Golden Age of Astrochemistry



Спутник

4. října 1957

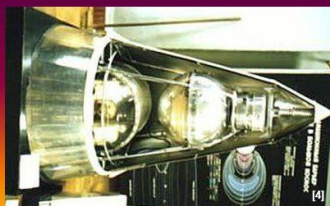
Byla zkonstruována koncem 50. let 20. století Sergejem Koroljovem v Sovětském svazu. Byla vynesena 4. října 1957 19:28 UTC upravenou dvoustupňovou nosnou raketou R-7, která byla z vojenské verze pro kosmonautiku upravena a přejmenována na raketu Sputnik. Odstartovala z kosmodromu Bajkonur na území Kazašské SSR. Vypuštěna byla v rámci Mezinárodního geofyzikálního roku.^[2] Patří do kategorie vědeckých družic.

Družice měla sférický tvar o průměru 58 cm a hmotnost 83,6 kg.

1957 - PES LAJKA



- 3. listopadu 1957 vyslal Sovětský svaz na palubě družice Sputnik 2 na oběžnou dráhu prvního pozemského živého tvora – fenku Lajku.
- Zpátky na Zem se však nevrátila, protože to tehdejší technika ještě neuměla.



Sputnik 2

Hmotnost

508 kg

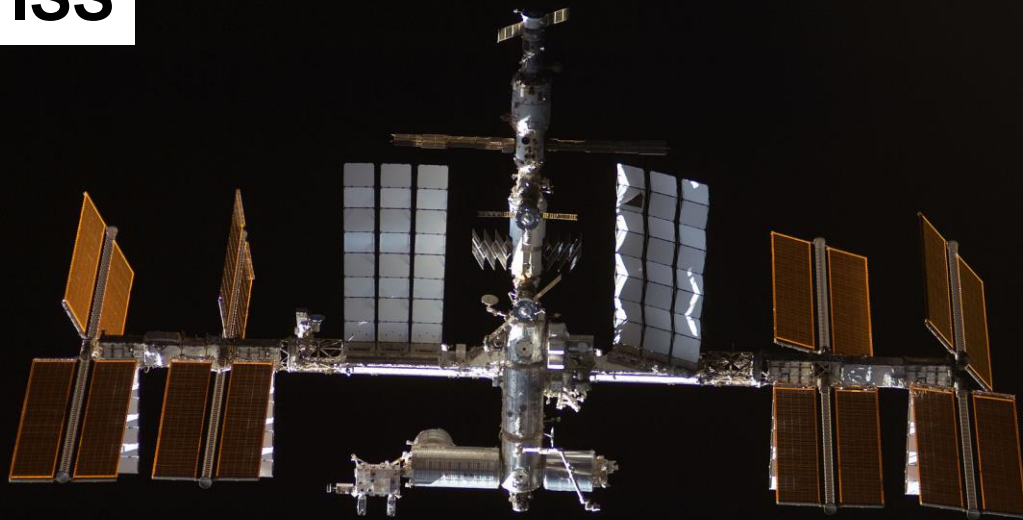
Lajka

3. listopadu 1957 z kosmodromu Bajkonur.

2020

~ 63 roků

ISS

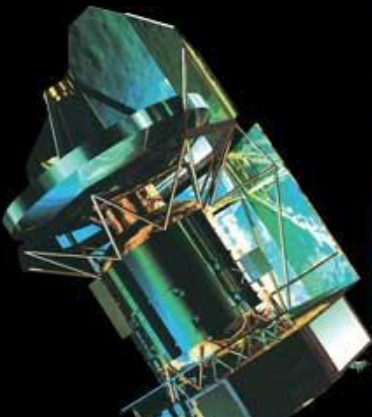


[Magion 1](#), the first Czechoslovak satellite launched into orbit on October 24, 1978
Charles University Prague

Golden Age of Astrochemistry



Herschel



United Kingdom Infrared Telescope
Mauna Kea, Hawaii

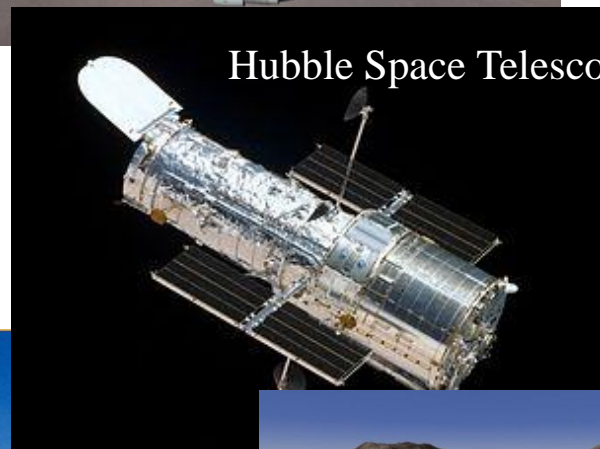
Five-hundred-meter Aperture Spherical radio
Telescope (China: Tianyan, 2016)



SOFIA



The Arecibo Observatory
RT in [Puerto Rico](#) (~1960)

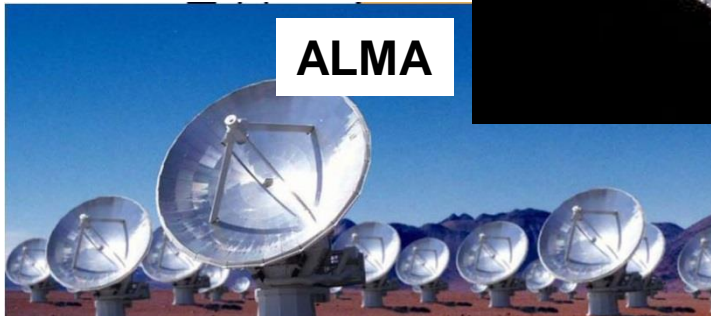


Hubble Space Telescope



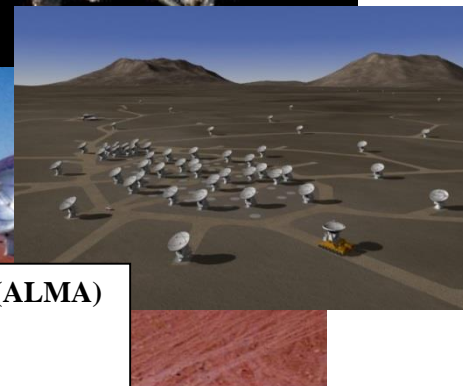
[Třetí nebeský palác](#)

Tiangong, officially the Tiangong space station



ALMA

The Atacama Large Millimeter/sub-millimeter Array (ALMA)
astronomical interferometer of radio telescopes
Atacama desert of northern Chile



Hubble Space Telescope



From April 24, 1990

The Hubble Space Telescope is a space telescope that was launched into low Earth orbit in 1990 and remains in operation

The telescope is operating as of 2019, and could last until 2030–2040.

Hubble is the only telescope designed to be maintained in space by astronauts. Five Space Shuttle missions have repaired, upgraded, and replaced systems on the telescope, including all five of the main instruments. The fifth mission was canceled on safety grounds following the [Columbia disaster](#) (2003), but NASA administrator [Michael D. Griffin](#) approved the [fifth servicing mission](#) which was completed in 2009. The telescope was still operating as of April 24, 2020, its 30th anniversary,^[1] and could last until 2030–2040.^[2] One successor to the Hubble telescope is the [James Webb Space Telescope](#) (JWST) which is scheduled to be launched in late 2021.^[1]

Not actualized, approximation

Hubble má potíže, přestal fungovat čtvrtý gyroskop, který pomáhá s orientací teleskopu

08. 10. 2018

[Hubble Teleskopy](#)

V pátek se vesmírný teleskop Hubble přepnul do tzv. safe módu poté, co přestal fungovat jeden z gyroskopů, které teleskopu pomáhají udržet správnou orientaci při pozorování vzdálených cílů ve vesmíru. Hubble měl celkem 6 těchto gyroskopů a potřebuje nejméně tři pro optimální operace. Dva však už delší dobu nefungují a další nefunguje optimálně. Po odchodu čtvrtého tak zbývají pouze dva funkční gyroskopy. Operátoři mise nyní zkoumají možnosti, kterými uvést teleskop zpátky do plného provozu.

Pokud se nepodaří na dálku opravit porouchaný gyroskop, hodlají operátoři vyzkoušet onen třetí, který nefunguje optimálně. Aktuálně tak hledají cesty, jak teleskop na dálku opravit, pokud se to nepodaří, teleskop může pracovat dál se dvěma, nebo dokonce jedním gyroskopem. Je dokonce pravděpodobné, že pokud se oprava nepodaří, mise bude dále pokračovat pouze s jedním gyroskopem a druhý bude ponechán jako rezerva.

Všech šest gyroskopů teleskopu Hubble bylo vyměněno při poslední misi astronautů k teleskopu v roce 2009. Po dosloužení raketoplánů však teleskop nebyl astronauty navštíven a zatím se neplánuje žádná podobná mise s novými vesmírnými loděmi, které by NASA měla mít v následujících letech k dispozici. Hubble je ve vesmíru od roku 1990.

Vesmírný teleskop Hubble - teleskop Hubble obíhá Zemi od roku 1990 ve výšce asi 540 kilometrů.

ACTUAL October 6. 2021: The telescope completed 30 years in operation in April 2020 and could last until 2030–2040.

Hubble Space Telescope



From April 24, 1990

Not actualized, approximation

Hubble má potíže, přestal fungovat čtvrtý gyroskop, který pomáhá s orientací teleskopu

08. 10. 2018

[Hubble Teleskopy](#)

V pátek se vesmírný teleskop Hubble přepnul do tzv. safe módu poté, co přestal fungovat jeden z gyroskopů, které teleskopu pomáhají udržet správnou orientaci při pozorování vzdálených cílů ve vesmíru. Hubble měl celkem 6 těchto gyroskopů a potřebuje nejméně tři pro optimální operace. Dva však už delší dobu nefungují a další nefunguje optimálně. Po odchodu čtvrtého tak zbývají pouze dva funkční gyroskopy. Operátoři mise nyní zkoumají možnosti, kterými uvést teleskop zpátky do plného provozu.

Pokud se nepodaří na dálku opravit porouchaný gyroskop, hodlají operátoři vyzkoušet onen třetí, který nefunguje optimálně. Aktuálně tak hledají cesty, jak teleskop na dálku opravit, pokud se to

Recent News

Oct. 19, 2023, 2:36 AM ET (Yahoo News)

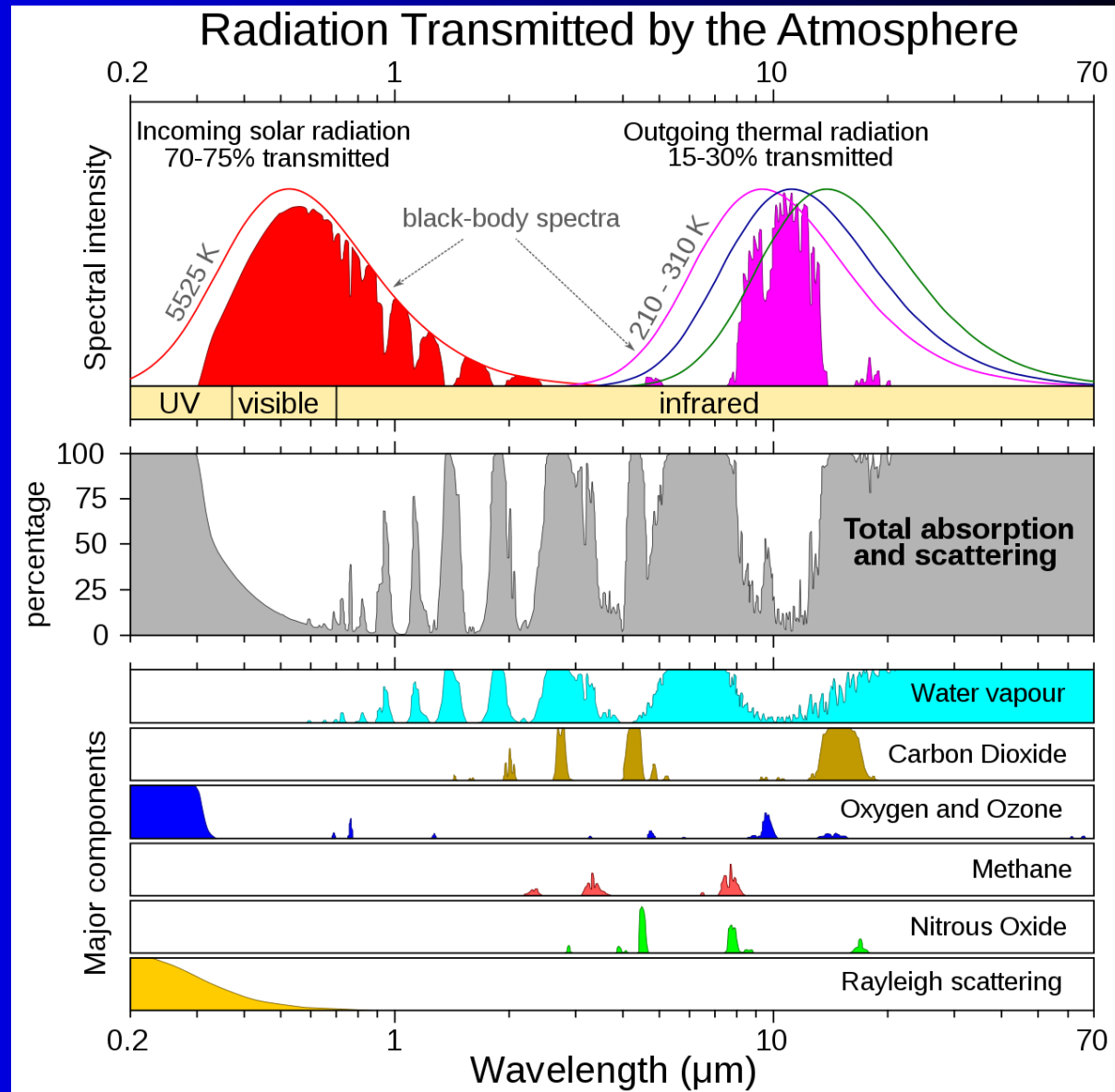
Hubble Telescope captures the bright core of a loosely wound

Oct. 17, 2023, 3:33 AM ET (Space.com)

NASA's Hubble, Chandra space telescopes face possible ...

ACTUAL October 6, 2021: The telescope completed 30 years in operation in April 2020 and could last until 2030–2040.

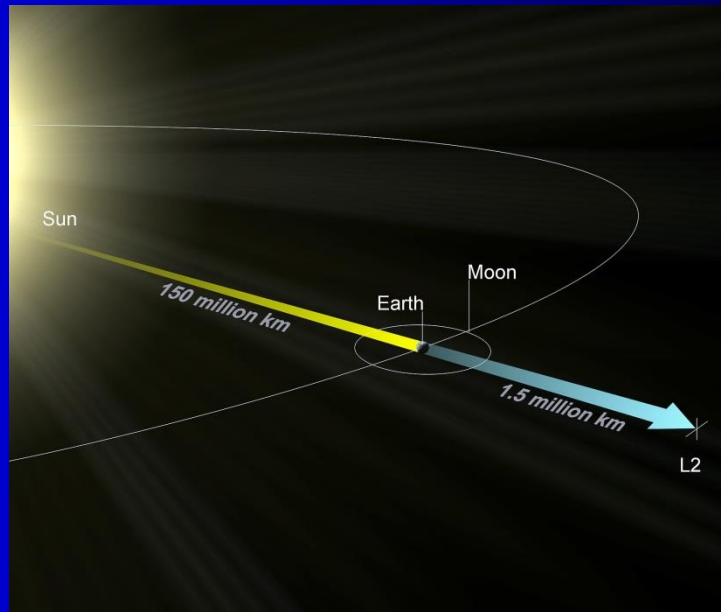
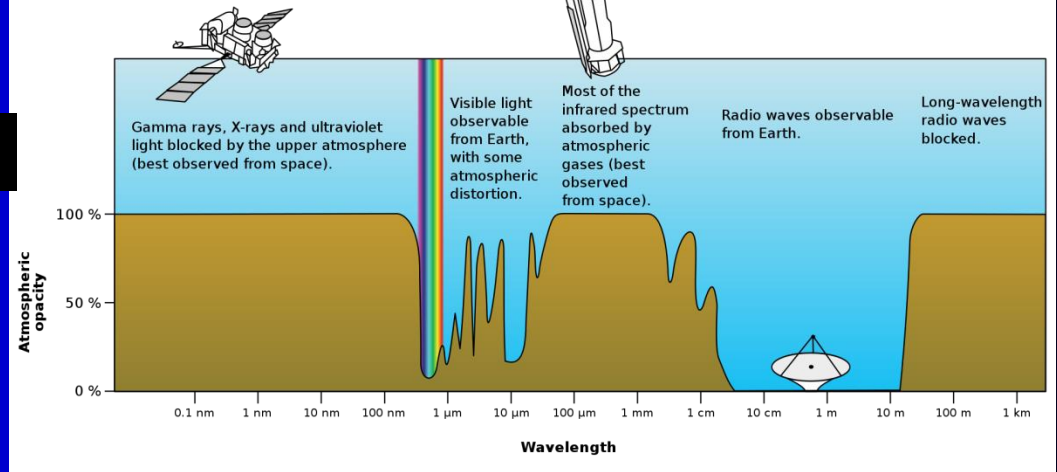
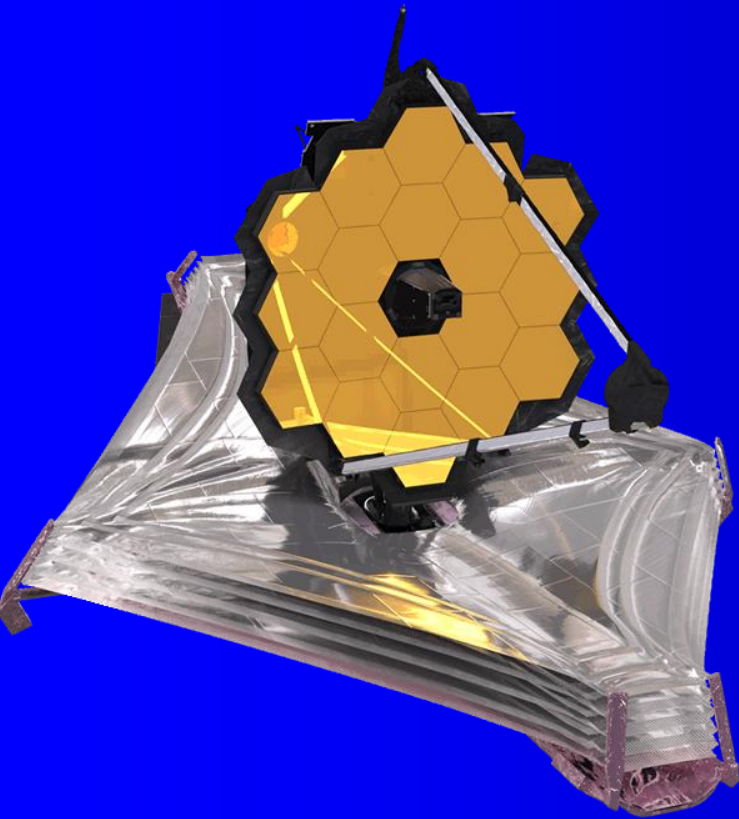
en.wikipedia.org/wiki/Hubble_Space_Telescope



Atmospheric windows in the infrared: Much of this type of light is blocked when viewed from the Earth's surface. It would be like looking at a rainbow but only seeing one colour.

infrared astronomy

James Webb Space Telescope (JWST)



The **James Webb Space Telescope (JWST)** is a space telescope which conducts infrared astronomy. As the largest optical telescope in space, its high resolution and sensitivity allow it to view objects too old, distant, or faint for the Hubble Space Telescope. This will enable investigations across many fields of astronomy and cosmology, such as observation of the first stars, the formation of the first galaxies, and detailed atmospheric characterization of potentially habitable exoplanets.

~1/6 of mass is interstellar

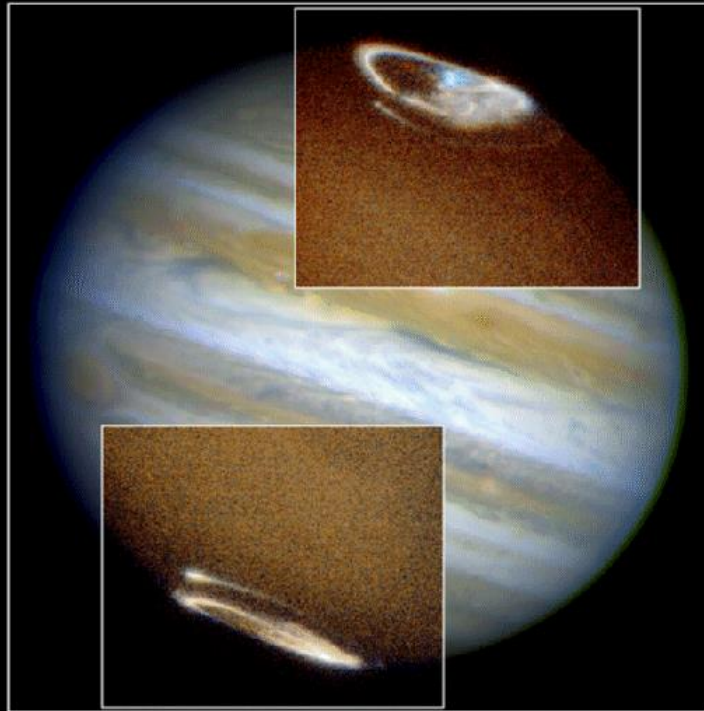
~1/2 of interstellar matter is molecular!



Milky Way has $\sim 10^{66}$ molecules!
Earth has only $\sim 10^{50}$ molecules

Different views of the Milky Way (different wavelengths)

Hydrogen dominated plasma

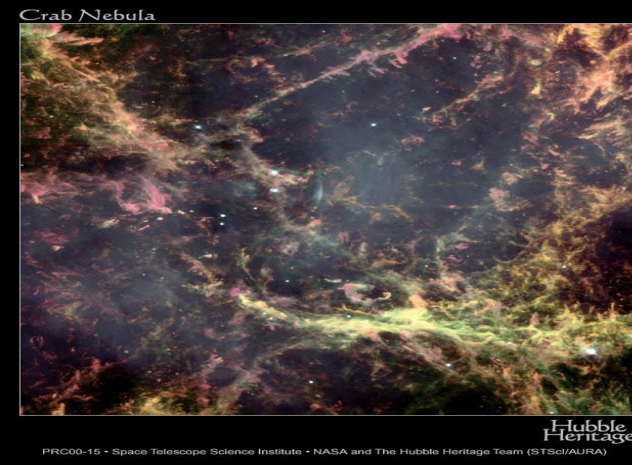


Jupiter Aurora

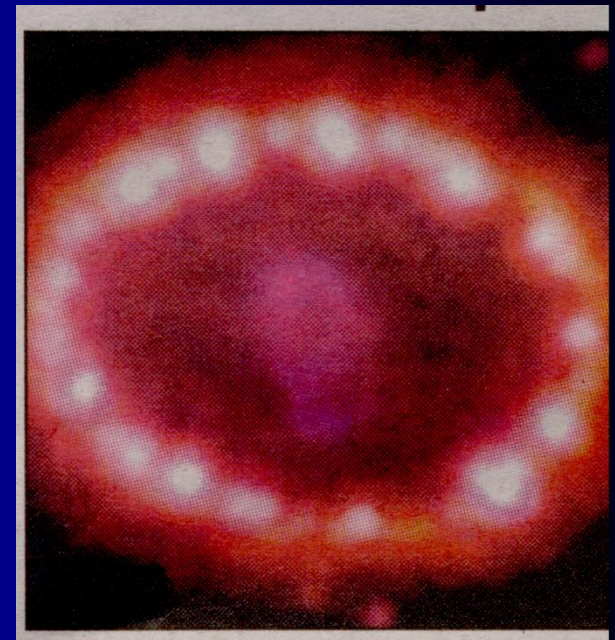
HST • STIS • WFPC2

PRC98-04 • ST Sci OPO • January 7, 1998
J. Clarke (University of Michigan) and NASA

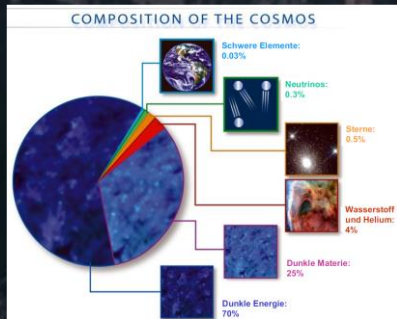
Hydrogen plasma in Jupiter Aurora



Crab Nebula



1994 -Supernova 1987A



The Herschel Space Observatory was a space observatory built and operated by the European Space Agency. **It was active from 2009 to 2013**, and was the largest infrared telescope ever launched, carrying a 3.5-metre mirror and instruments sensitive to the far infrared and submillimetre wavebands.



Herschel



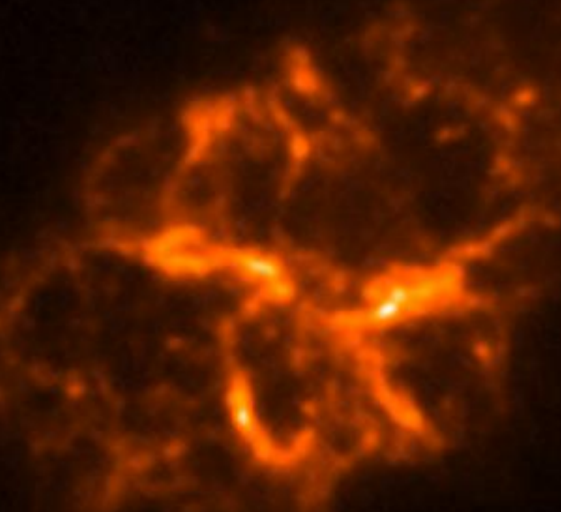
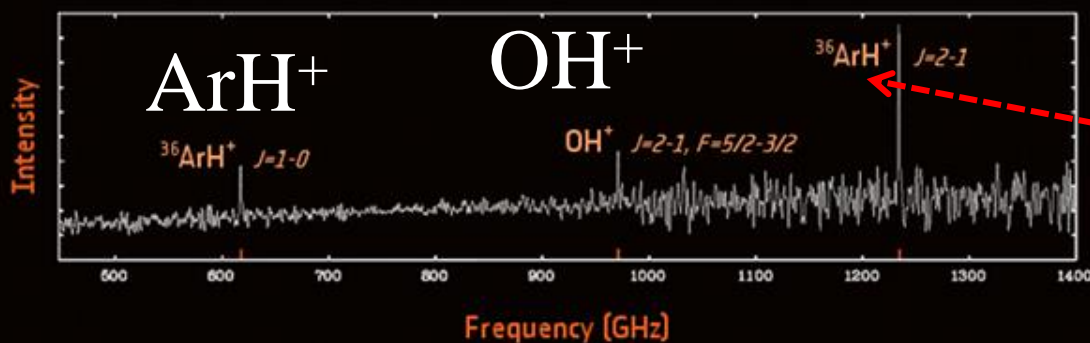
Herschel (red) and Hubble (blue) composite image of the Crab Nebula. *Credit: ESA/Herschel/PACS/MESS Key Programme Supernova Remnant Team; NASA, ESA and Allison Loll/Jeff Hester (Arizona State Uni)*

The **Crab Nebula** is the remnant of a supernova explosion that was observed by Chinese astronomers in the year 1054.



Hubble Space Telescope

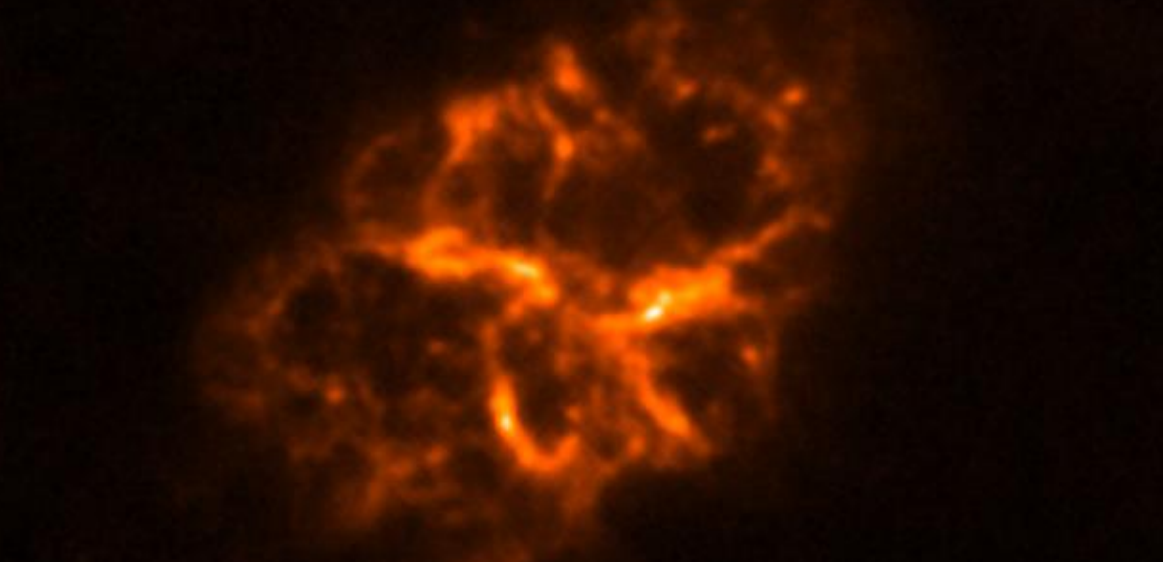
12 December 2013

ArH⁺***³⁶ArH⁺***

Using ESA's Herschel Space Observatory, a team of astronomers has found first evidence of a noble-gas based molecule in space. A compound of argon, the molecule was detected in the gaseous filaments of the Crab Nebula, one of the most famous supernova remnants in our Galaxy. While argon is a product of supernova explosions, the formation and survival of argon-based molecules in the harsh environment of a supernova remnant is an unforeseen surprise.

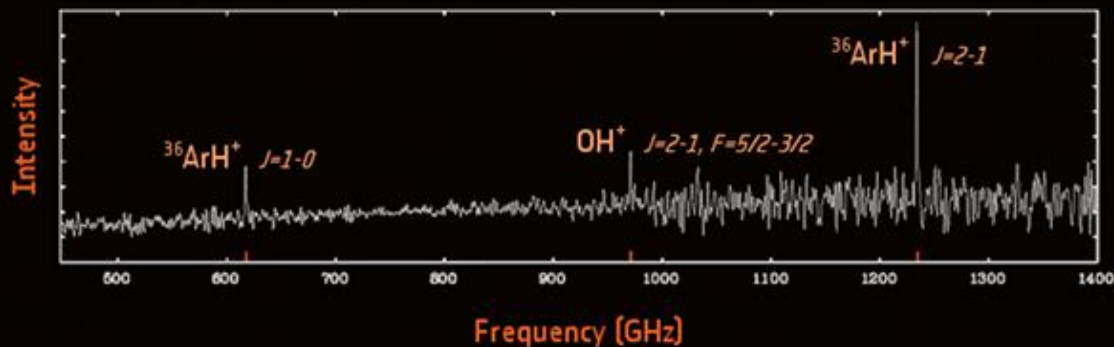
The results described in this article are reported in "*Detection of a Noble Gas Molecular Ion, ³⁶ArH⁺, in the Crab Nebula*", by M. J. Barlow et al., published in Science, 342, 6163, 1343-1345, 13 December 2013. DOI: 10.1126/science.124358213.

12 December 2013



$^{36}\text{ArH}^+$

$^{36}\text{ArH}^+$



^{40}Ar

The argon isotope found in the Crab Nebula is different from the one that dominates in Earth's atmosphere, ^{40}Ar , which derives from the decay of a radioactive isotope of potassium (^{40}K) present in our planet's rocks.

^{36}Ar

The Herschel data indicate that the argon hydride found in the Crab Nebula is made up of the argon isotope ^{36}Ar . This is the first time that astronomers could identify the isotopic nature of an element in a supernova remnant.

"Finding that argon in the Crab Nebula consists of ^{36}Ar was not surprising because this is the dominant isotope of argon across the Universe.

"And it's also the main argon isotope to be synthesised in the nuclear reactions during supernova explosions, so its detection in the Crab Nebula confirms that this iconic nebula was created by the explosive death of a massive star," explains Barlow.

On Earth, radioactive potassium-40 decays to argon-40 as the most common isotope. In stars, nucleosynthesis mostly creates the lighter argon-36 and argon-38.

Astrophysical detection of the helium hydride ion HeH^+

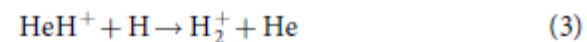
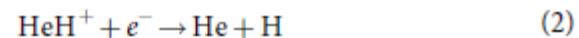
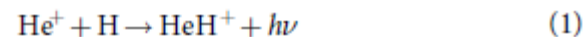
Rolf Güsten^{1*}, Helmut Wiesemeyer¹, David Neufeld², Karl M. Menten¹, Urs U. Graf³, Karl Jacobs³, Bernd Klein^{1,4}, Oliver Ricken¹, Christophe Risacher^{1,5} & Jürgen Stutzki³

During the dawn of chemistry^{1,2}, when the temperature of the young Universe had fallen below some 4,000 kelvin, the ions of the light elements produced in Big Bang nucleosynthesis recombined in reverse order of their ionization potential. With their higher ionization potentials, the helium ions He^{2+} and He^+ were the first to combine with free electrons, forming the first neutral atoms; the recombination of hydrogen followed. In this metal-free and low-density environment, neutral helium atoms formed the Universe's first molecular bond in the helium hydride ion HeH^+ through radiative association with protons. As recombination progressed, the destruction of HeH^+ created a path to the formation of molecular hydrogen. Despite its unquestioned importance in the evolution of the early Universe, the HeH^+ ion has so far eluded unequivocal detection in interstellar space. In the laboratory the ion was discovered³ as long ago as 1925, but only in the late 1970s was the possibility that HeH^+ might exist in local astrophysical plasmas discussed⁴⁻⁷. In particular, the conditions in planetary nebulae were shown to be suitable for producing potentially detectable column densities of HeH^+ . Here we report observations, based on advances in terahertz spectroscopy^{8,9} and a high-altitude observatory¹⁰, of the rotational ground-state transition of HeH^+ at a wavelength of 149.1 micrometres in the planetary nebula NGC 7027. This confirmation of the existence of HeH^+ in nearby interstellar space constrains our understanding of the chemical networks that control the formation of this molecular ion, in particular the rates of radiative association and dissociative recombination.

The deployment of the German Receiver for Astronomy at Terahertz Frequencies (GREAT)⁹ heterodyne spectrometer on board the Stratospheric Observatory for Infrared Astronomy (SOFIA)¹⁰ has now opened up new opportunities. Although the HeH^+ $J = 1-0$ transition at 149.137 μm (2010.183873 GHz; ref. 2¹) cannot be observed from ground-based observatories, skies become transparent during high-altitude flights with SOFIA. The latest advances in terahertz technologies have



We then computed the equilibrium abundance of HeH^+ , including the three reactions identified as being important in the layers in which HeH^+ is most abundant^{7,13}:



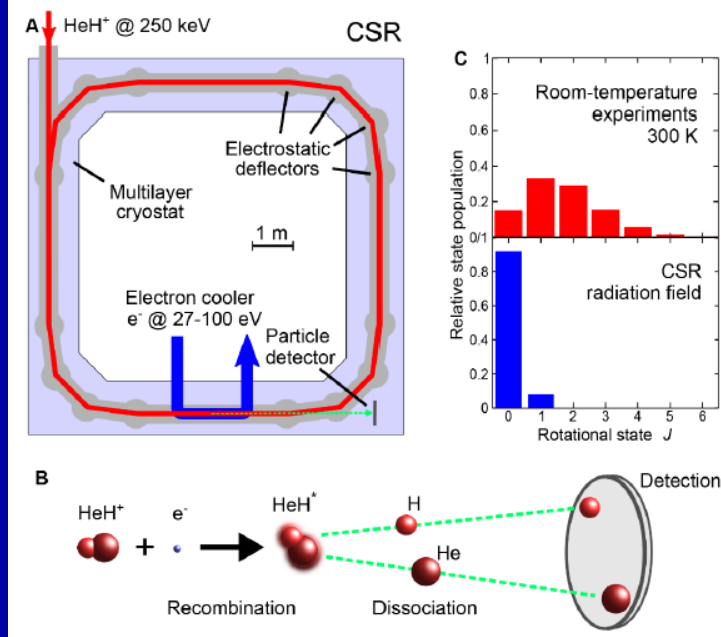
Cite as: O. Novotný *et al.*, *Science*
10.1126/science.aax5921 (2019).

Quantum-state-selective electron recombination studies suggest enhanced abundance of primordial HeH⁺

Oldřich Novotný^{1*}, Patrick Wilhelm¹, Daniel Paul¹, Ábel Kálosi^{1,2}, Sunny Saurabh¹, Arno Becker¹, Klaus Blaum¹, Sebastian George^{1,3}, Jürgen Göck¹, Manfred Grieser¹, Florian Grussie¹, Robert von Hahn¹, Claude Krantz¹, Holger Kreckel¹, Christian Meyer¹, Preeti M. Mishra¹, Damian Muell¹, Felix Nuesslein¹, Dmitry A. Orlov¹, Marius Rimpler¹, Viviane C. Schmidt¹, Andrey Shornikov¹, Aleksandr S. Terekhov⁴, Stephen Vogel¹, Daniel Zajfman⁵, Andreas Wolf⁶

¹Max-Planck-Institut für Kernphysik, Saupfercheckweg 1, 69117 Heidelberg, Germany. ²Charles University, 18000 Praha, Czech Republic. ³Universität Greifswald, Institut für Physik, 17487 Greifswald, Germany. ⁴Rzhanov Institute of Semiconductor Physics, Novosibirsk 630090, Russia. ⁵Weizmann Institute of Science, Rehovot 76100, Israel.

*Corresponding author. Email: oldrich.novotny@mpi-hd.mpg.de



PHYSICAL REVIEW LETTERS **124**, 043401 (2020)

Dissociative Recombination of Cold HeH⁺ Ions

Roman Čurík^{1*}

J. Heyrovský Institute of Physical Chemistry, ASCR, Dolejškova 3, 18223 Prague, Czech Republic

Dávid Hvizdoš

*J. Heyrovský Institute of Physical Chemistry, ASCR, Dolejškova 3, 18223 Prague, Czech Republic
and Institute of Theoretical Physics, Faculty of Mathematics and Physics, Charles University in Prague,
V Holešovičkách 2, 180 00 Prague, Czech Republic*

Chris H. Greene²

*Department of Physics and Astronomy, Purdue University, West Lafayette, Indiana 47907, USA
and Purdue Quantum Science and Engineering Institute, Purdue University, West Lafayette, Indiana 47907, USA*

(Received 7 October 2019; revised manuscript received 27 November 2019; published 28 January 2020)



2018 Census of Interstellar, Circumstellar, Extragalactic, Protoplanetary Disk, and Exoplanetary Molecules

Brett A. McGuire^{1,2,3} ¹ National Radio Astronomy Observatory, Charlottesville, VA 22903, USA² Harvard-Smithsonian Center for Astrophysics, Cambridge, MA 02138, USA

Table 1
Commonly Used Facility Abbreviations

Abbreviation	Description
ALMA	Atacama Large Millimeter/submillimeter Array
APEX	Atacama Pathfinder Experiment
ARO	Arizona Radio Observatory
ATCA	Australian Telescope Compact Array
BIMA	Berkeley-Illinois-Maryland Array
CSO	Caltech Submillimeter Observatory
FCRAO	Five College Radio Astronomy Observatory
FUSE	<i>Far Ultraviolet Spectroscopic Explorer</i>
GBT	Green Bank Telescope
IRAM	Institut de Radioastronomie Millimétrique
IRTF	Infrared Radio Telescope Facility
ISO	<i>Infrared Space Observatory</i>
KPNO	Kitt Peak National Observatory
MWO	Millimeter-wave Observatory
NRAO	National Radio Astronomy Observatory
OVRO	Owens Valley Radio Observatory
PdBI	Plateau de Bure Interferometer
SEST	Swedish-ESO Submillimeter Telescope
SMA	Sub-millimeter Array
SMT	Sub-millimeter Telescope
SOFIA	<i>Stratospheric Observatory for Infrared Astronomy</i>
UKIRT	United Kingdom Infrared Telescope

3. Known Interstellar Molecules

Two-atom Molecules

3.1. CH (Methyldiyne)

Swings & Rosenfeld (1937) suggested that an observed line at $\lambda = 4300 \text{ \AA}$ by Dunham (1937) using the Mount Wilson Observatory in diffuse gas toward a number of supergiant B stars might have been due to the ${}^2\Delta \leftarrow {}^2\Pi$ transition of CH, reported in the laboratory by Jevons (1932). McKellar (1940) later identified several additional transitions in observational data. The first radio identification was reported by Rydbeck et al. (1973) at 3335 MHz with the Onsala telescope toward more than a dozen sources using estimated fundamental rotational transition frequencies from Shklovskii (1953), Goss (1966), and Baird & Bredohl (1971). The first direct

measurement of the CH rotational spectrum was reported by Brazier & Brown (1983).

3.64. H_3^+

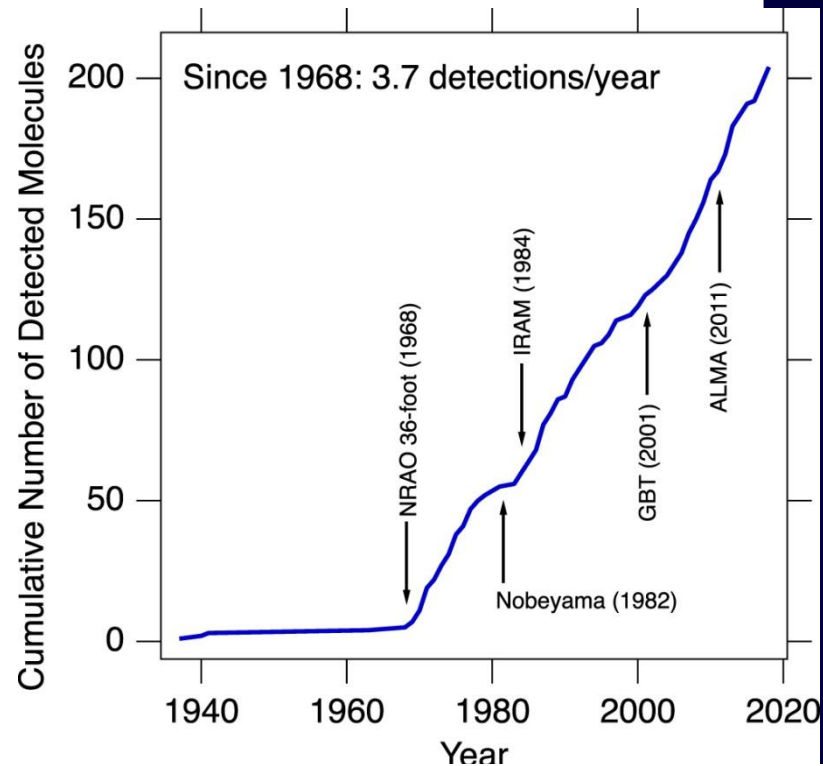
First suggested as a possible interstellar molecule in Martin et al. (1961), H_3^+ was detected 35 years later in absorption toward GL 2136 and W33A by Geballe & Oka (1996) using UKIRT to observe three transitions of the ν_2 fundamental band near $3.7 \mu\text{m}$. The laboratory work was performed by Oka (1980).

Molecules in interstellar space

Not actualized, approximation

	3	4	5	6	7	8	9	10	11	13
H ₂	C ₃	c-C ₃ H	C ₅	C ₃ H	C ₆ H	CH ₃ C ₃ N	CH ₃ C ₄ H	CH ₃ C ₅ N?	HC ₉ N	HC ₁₁ N
AlF	C ₂ H	l-C ₃ H	C ₄ H	l-H ₂ C ₄	CH ₂ CHCN	HCOOCH ₃	CH ₃ CH ₂ CN	(CH ₃) ₂ CO		
AlCl	C ₂ O	C ₃ N	C ₄ Si	C ₂ H ₄	CH ₃ C ₂ H	CH ₃ COOH?	(CH ₃) ₂ O	NH ₂ CH ₂ COOH?		
C ₂	C ₂ S	C ₃ O	l-C ₃ H ₂	CH ₃ CN	HC ₅ N	C ₇ H	CH ₃ CH ₂ OH			
CH	CH ₂	C ₃ S	c-C ₃ H ₂	CH ₃ NC	HCOCH ₃	H ₂ C ₆	HC ₇ N			
CH ⁺	HCN	C ₂ H ₂	CH ₂ CN	CH ₃ OH	NH ₂ CH ₃	CH ₂ OHCHO	C ₈ H			
CN	HCO	CH ₂ D ⁺ ?	CH ₄	CH ₃ SH	c-C ₂ H ₄ O					
CO	HCO ⁺	HCCN	HC ₃ N	HC ₃ NH ⁺	CH ₂ CHOH					
CO ⁺	HCS ⁺	HCNH ⁺	HC ₂ NC	HC ₂ CHO						
CP	HOC ⁺	HNCO	HCOOH	NH ₂ CHO						
CSi	H ₂ O	HNCS	H ₂ CHN	C ₃ N						
HCl	H ₂ S	HOCO ⁺	H ₂ C ₂ O							
KCl	HNC	H ₂ CO	H ₂ NCN							
NH	HNO	H ₂ CN	HNC ₃							
NO	MgCN	H ₂ CS	SiH ₄							
NS	MgNC	H ₃ O ⁺	H ₂ COH ⁺							
NaCl	N ₂ H ⁺	NH ₃								
OH	N ₂ O	SiC ₃								
PN	NaCN									
SO	OCS									
SO ⁺	SO ₂									
SiN	c-SiC ₂									
SiO	CO ₂									
SiS	NH ₂									
CS	H ₃ ⁺									
HF	SiCN									
SH	AlNC									
FeO?										

16 JULY 2015 | VOL 523 | NATURE | 323

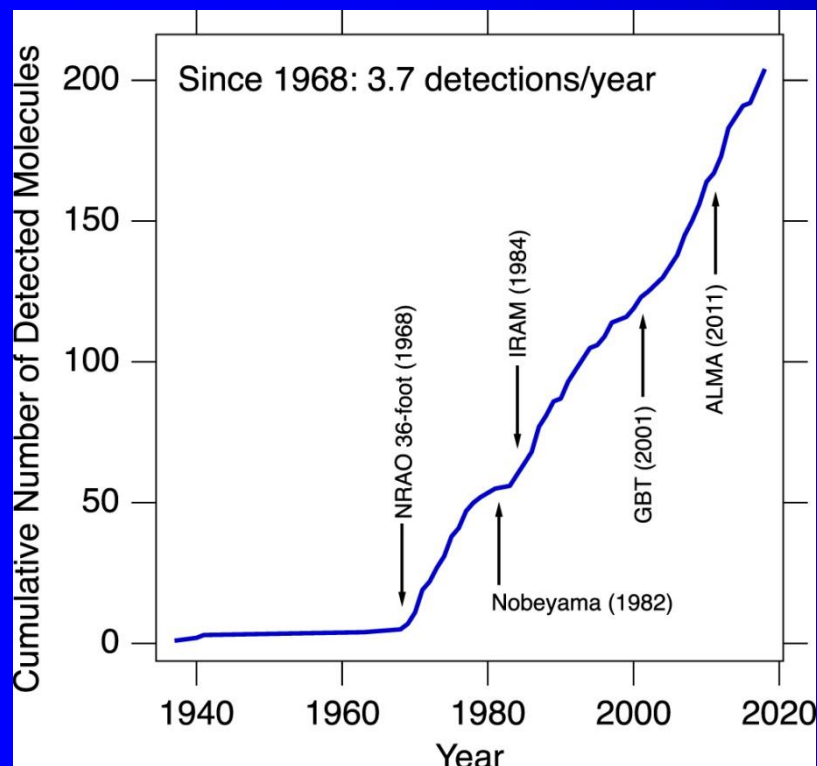


Cumulative number of known interstellar molecules over time. Commissioning dates of major contributing facilities are noted with arrows. [McGuire 2018]

Molecules in interstellar space

Not actualized, approximation

16 JULY 2015 | VOL 523 | NATURE | 323



Cumulative number of known interstellar molecules over time. Commissioning dates of major contributing facilities are noted with arrows. [McGuire 2018]

actualized, approximation 2021

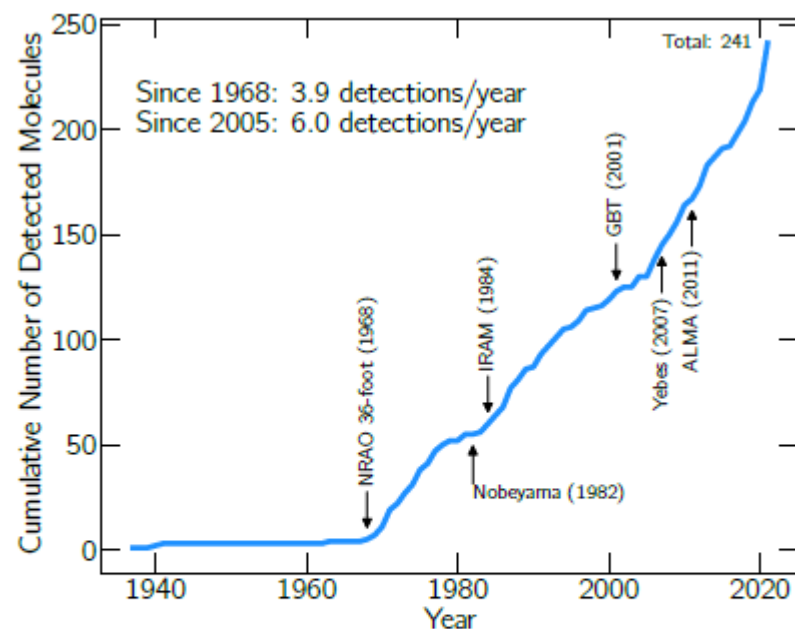


Figure 1. Cumulative number of known interstellar molecules over time. After the birth of molecular radio astronomy in the 1960s, there have been on average 3.9 new detections per year. The commissioning dates of several major contributing facilities are noted with arrows.

DRAFT VERSION OCTOBER 1, 2021
Typeset using L^AT_EX twocolumn style in AASTeX631

2021 Census of Interstellar, Circumstellar, Extragalactic, Protoplanetary Disk, and Exoplanetary Molecules

BRETT A. MCGUIRE^{1,2,3}

¹Department of Chemistry, Massachusetts Institute of Technology, Cambridge, MA 02139, USA

²National Radio Astronomy Observatory, Charlottesville, VA 22903, USA

³Harvard-Smithsonian Center for Astrophysics, Cambridge, MA 02138, USA

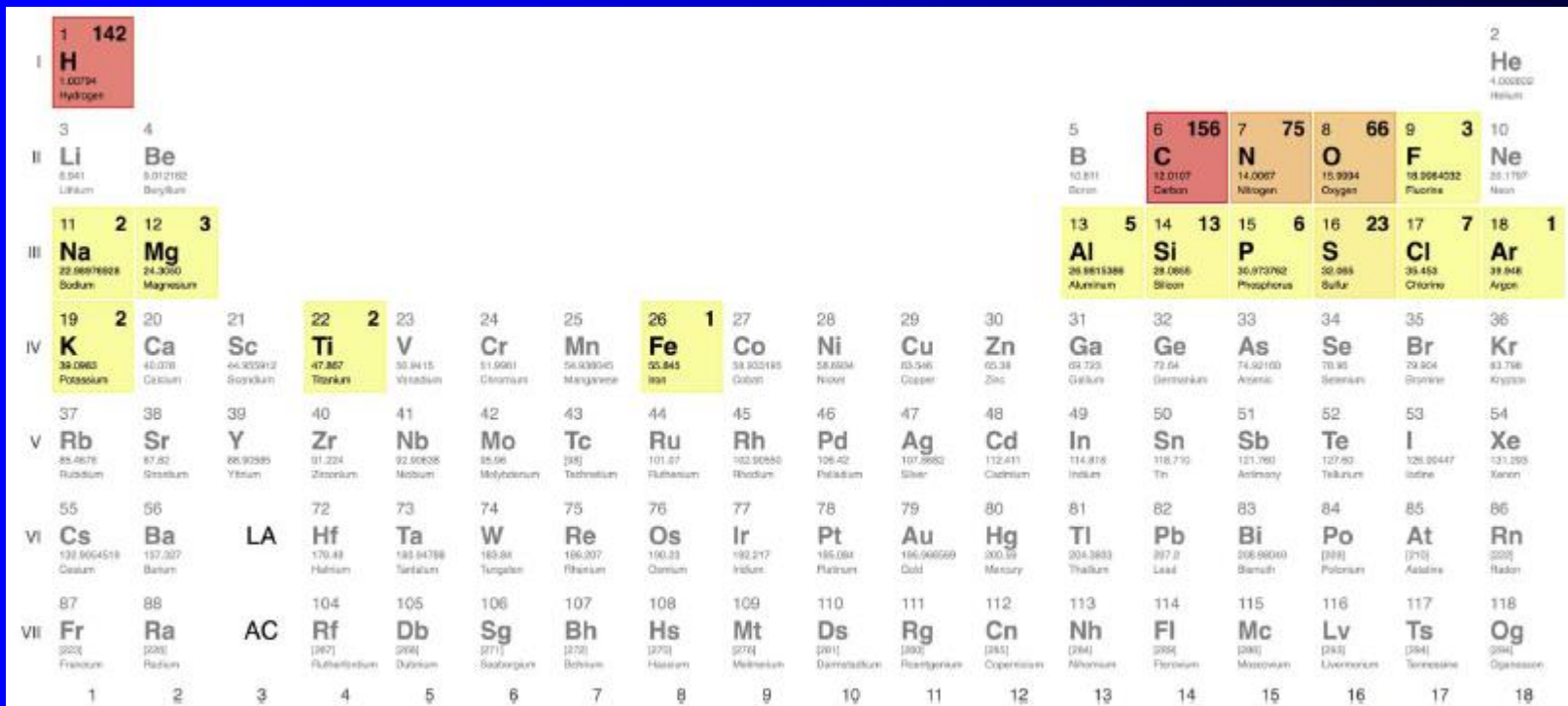


Figure 6. Periodic table of the elements, absent the lanthanide and actinide series, color-coded by number of detected species containing each element. For those elements with detected ISM molecules, that number is displayed in the upper right of each cell.



2018 Census of Interstellar, Circumstellar, Extragalactic, Protoplanetary Disk, and Exoplanetary Molecules

Brett A. McGuire^{1,2,3}

¹ National Radio Astronomy Observatory, Charlottesville, VA 22903, USA

² Harvard-Smithsonian Center for Astrophysics, Cambridge, MA 02138, USA

Received 2018 May 27; revised 2018 September 20; accepted 2018 September 20; published 2018 November 26

actualized, approximation (2021)

1 H 1.00794 1.008 g/mol																	2 He 4.002602 4.0026 g/mol															
3 Li 6.941 6.941 g/mol	4 Be 9.01224 9.0122 g/mol																	5 B 10.811 10.811 g/mol	6 C 12.011 12.011 g/mol	7 N 14.007 14.007 g/mol	8 O 15.999 15.999 g/mol	9 F 18.998 18.998 g/mol	10 Ne 20.180 20.180 g/mol									
11 Na 22.990 22.990 g/mol	12 Mg 24.305 24.305 g/mol																	13 Al 26.982 26.982 g/mol	14 Si 28.086 28.086 g/mol	15 P 30.974 30.974 g/mol	16 S 32.065 32.065 g/mol	17 Cl 35.453 35.453 g/mol	18 Ar 39.948 39.948 g/mol									
19 K 39.098 39.098 g/mol	20 Ca 40.078 40.078 g/mol	21 Sc 44.956 44.956 g/mol	22 Ti 47.883 47.883 g/mol	23 V 50.942 50.942 g/mol	24 Cr 51.996 51.996 g/mol	25 Mn 54.938 54.938 g/mol	26 Fe 55.845 55.845 g/mol	27 Co 58.933 58.933 g/mol	28 Ni 58.693 58.693 g/mol	29 Cu 63.546 63.546 g/mol	30 Zn 65.38 65.38 g/mol	31 Ga 69.723 69.723 g/mol	32 Ge 72.64 72.64 g/mol	33 As 74.922 74.922 g/mol	34 Se 78.96 78.96 g/mol	35 Br 79.904 79.904 g/mol	36 Kr 83.798 83.798 g/mol															
37 Rb 85.468 85.468 g/mol	38 Sr 87.62 87.62 g/mol	39 Y 88.906 88.906 g/mol	40 Zr 91.224 91.224 g/mol	41 Nb 92.906 92.906 g/mol	42 Mo 95.94 95.94 g/mol	43 Tc 98 98 g/mol	44 Ru 101.07 101.07 g/mol	45 Rh 101.07 101.07 g/mol	46 Pd 106.36 106.36 g/mol	47 Ag 107.868 107.868 g/mol	48 Cd 112.411 112.411 g/mol	49 In 114.818 114.818 g/mol	50 Sn 118.71 118.71 g/mol	51 Sb 121.76 121.76 g/mol	52 Te 127.6 127.6 g/mol	53 I 126.905 126.905 g/mol	54 Xe 131.29 131.29 g/mol															
55 Cs 132.905 132.905 g/mol	56 Ba 137.327 137.327 g/mol																	72 Hf 178.49 178.49 g/mol	73 Ta 180.948 180.948 g/mol	74 W 183.84 183.84 g/mol	75 Re 186.207 186.207 g/mol	76 Os 190.23 190.23 g/mol	77 Ir 192.225 192.225 g/mol	78 Pt 195.084 195.084 g/mol	79 Au 196.967 196.967 g/mol	80 Hg 200.59 200.59 g/mol	81 Tl 204.384 204.384 g/mol	82 Pb 207.2 207.2 g/mol	83 Bi 208.98 208.98 g/mol	84 Po 209 209 g/mol	85 At 210 210 g/mol	86 Rn 222 222 g/mol
87 Fr 223 223 g/mol	88 Ra 226 226 g/mol																	104 Rf 261 261 g/mol	105 Db 262 262 g/mol	106 Sg 263 263 g/mol	107 Bh 264 264 g/mol	108 Hs 277 277 g/mol	109 Mt 268 268 g/mol	110 Ds 271 271 g/mol	111 Rg 272 272 g/mol	112 Cn 285 285 g/mol	113 Nh 284 284 g/mol	114 Fl 289 289 g/mol	115 Mc 288 288 g/mol	116 Lv 293 293 g/mol	117 Ts 294 294 g/mol	118 Og 294 294 g/mol

Figure 6. Periodic table of the elements, absent the lanthanide and actinide series, colored by number of detected species containing each element. For those elements with detected ISM molecules, that number is displayed in the upper right of each cell.

DRAFT VERSION OCTOBER 1, 2021
Typeset using L^AT_EX twocolumn style in AASTeX631

2021 Census of Interstellar, Circumstellar, Extragalactic, Protoplanetary Disk, and Exoplanetary Molecules

BRETT A. MCGUIRE^{1,2,3}

- ¹Department of Chemistry, Massachusetts Institute of Technology, Cambridge, MA 02139, USA
- ²National Radio Astronomy Observatory, Charlottesville, VA 22903, USA
- ³Harvard-Smithsonian Center for Astrophysics, Cambridge, MA 02138, USA

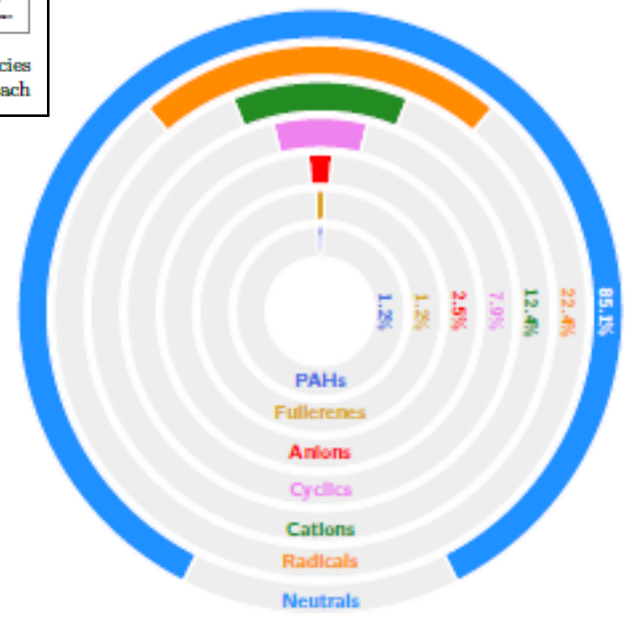


Figure 10. Percentage of known interstellar molecules that are neutral, cationic, anionic, radical species, or cyclic. Many molecules fall into more than one of these categories (e.g. most radical species have a net neutral charge).

Interstellar medium

92.1% of nucleons in the universe are protons

7.8% are helium nuclei !

0.1%.....C,N,O,S,Si....

Cosmic abundance

H

He

Mg

□ □ □ □
C N O Ne

Si S Ar

Fe

~0.005%.....D



Andromeda composite

1722



socha Atlanta



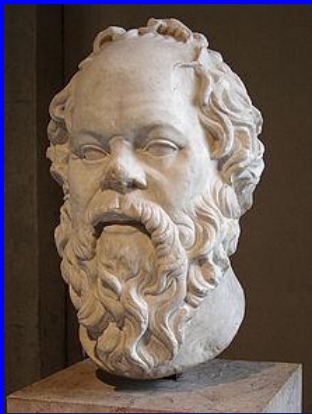
1722



Věž byla dokončena v roce 1722. Na vrcholu věže stojí socha Atlanta (olověná socha s železnou vnitřní konstrukcí, váha asi 600 kg, výška 2,4 m). Atlas nese nebeskou sféru (průměr asi 1,6 m, váha asi 150 kg) s korouhví.

(Pravděpodobně

Matyáš Braun)



Scio me nihil scire

The astrochemistry game plan

Laboratory astrophysics and related theory

Spectroscopy

Collisional excitation rate coefficients

Bimolecular reaction rate coefficients

Grain surface reactions

Photoionization and photodissociation cross-sections

Observations of astrophysical molecules

Emission line luminosities

Absorption line optical depths

Astrochemical modeling of ...

Diffuse IS cloud

Dense IS clouds

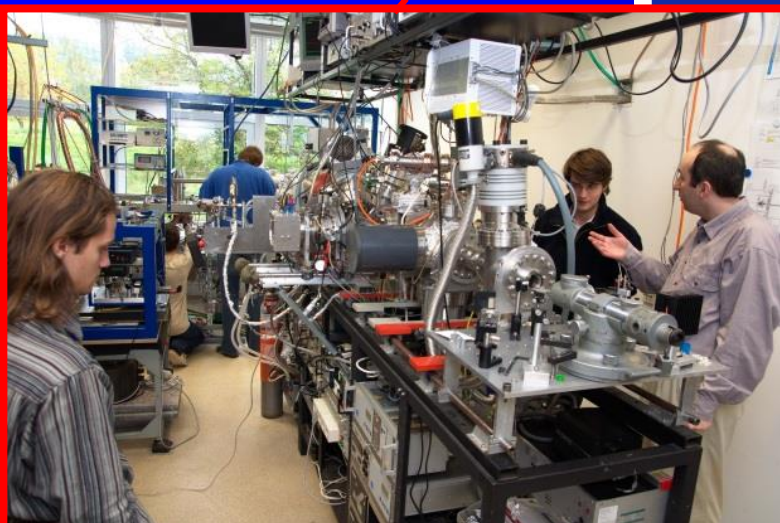
Photodissociation regions

Circumstellar outflows

X-irradiated regions

Excitation and radiative transfer

Information of general astrophysical interest



KFPP MFF UK

Načo chodiť do školy...

2014

FIRST TIME-DEPENDENT STUDY OF H_2 AND H_3^+ ORTHO-PARA CHEMISTRY IN THE DIFFUSE INTERSTELLAR MEDIUM: OBSERVATIONS MEET THEORETICAL PREDICTIONS*

T. ALBERTSSON¹, N. INDRIOLO², H. KRECKEL³, D. SEMENOV¹, K. N. CRABTREE⁴, AND TH. HENNING¹

¹Max-Planck-Institut für Astronomie, Königstuhl 17, D-69117 Heidelberg, Germany

²Department of Physics and Astronomy, Johns Hopkins University, Baltimore, MD 21218, USA

³Max-Planck-Institut für Kernphysik, D-69117 Heidelberg, Germany

⁴Harvard-Smithsonian Center for Astrophysics, 60 Garden Street, Cambridge, MA 02138, USA

Received 2013 December 4; accepted 2014 March 28; published 2014 May 2

The chemistry in the diffuse interstellar medium (ISM)

THE ASTROPHYSICAL JOURNAL, 787:44 (10pp), 2014 May 20

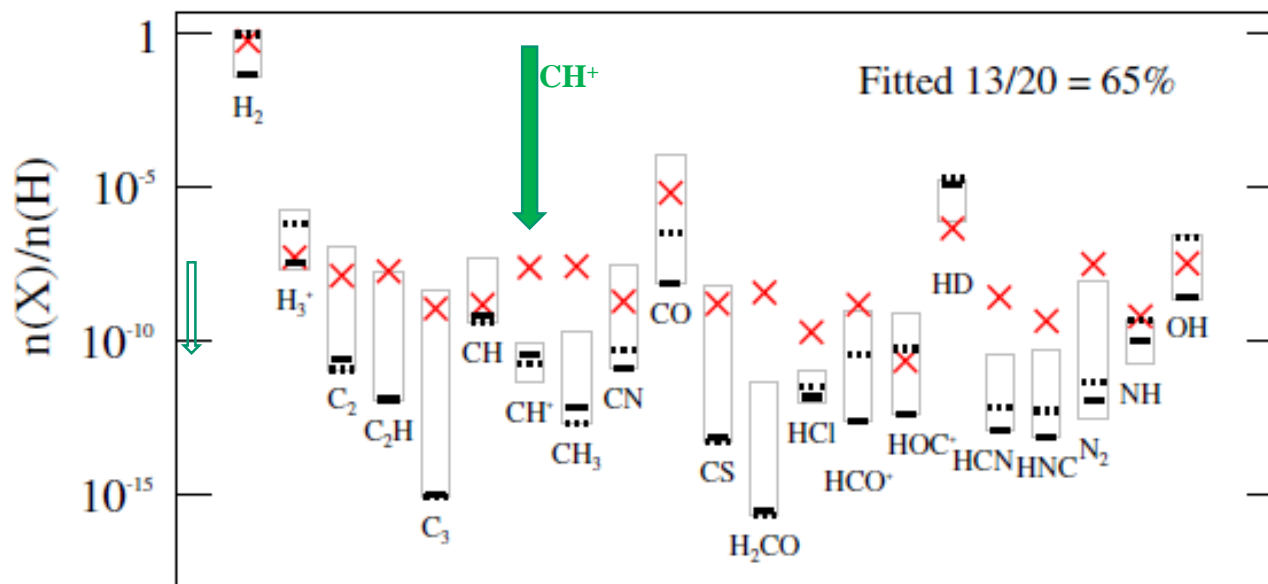


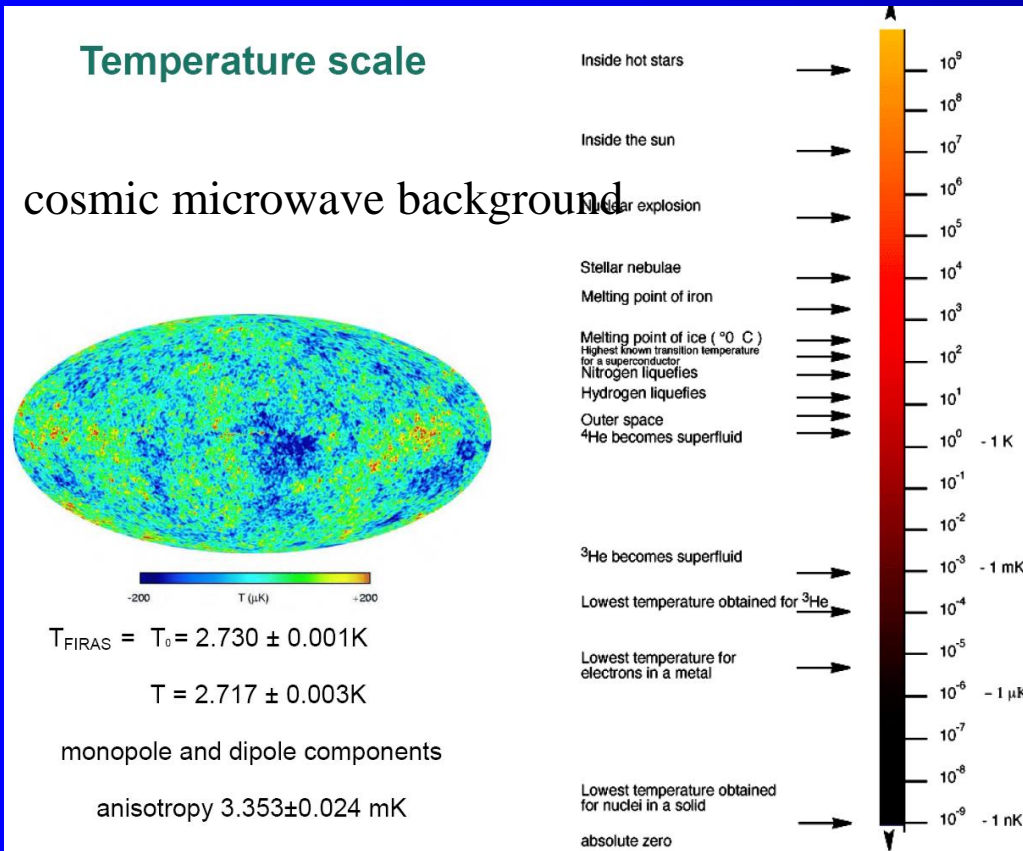
Figure 6. Comparison of observed abundances (red crosses) to modeled values of key species in diffuse clouds. Gray boxes show the range of abundances calculated from the considered models (Table 2) and black lines show abundances from the best-fit model “2X+C15” (30 K, solid line, and 90 K, dotted line).

(A color version of this figure is available in the online journal.)

Temperature scale should be logarithmic

Far Infrared Absolute Spectrophotometer (FIRAS)

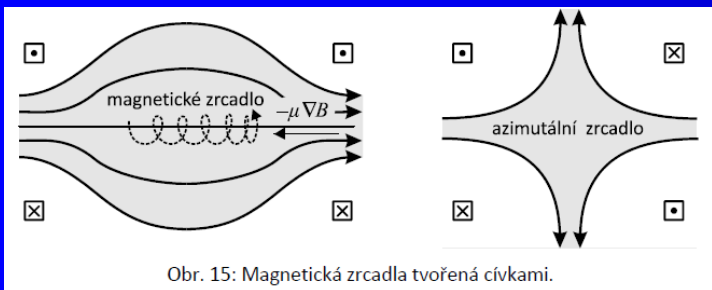
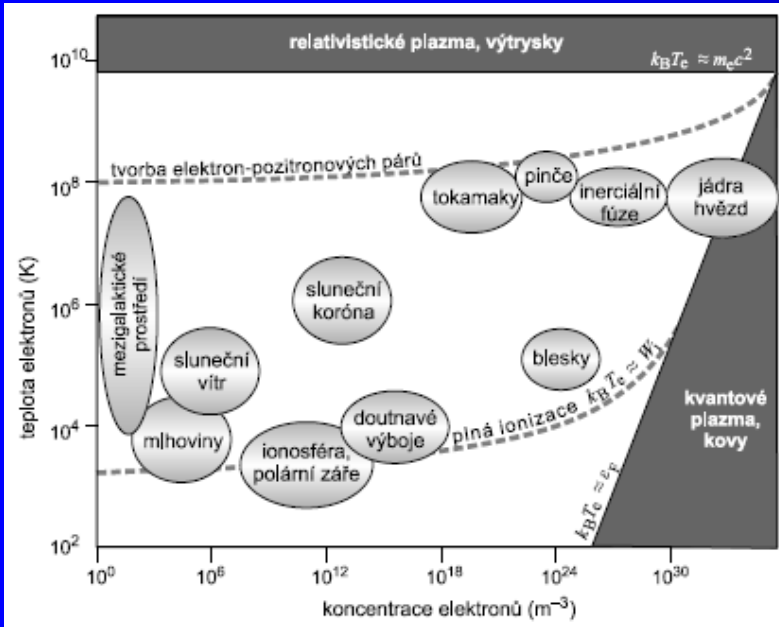
T



The **cosmic microwave background (CMB, CMBR)**, **Big Bang** cosmology, is **electromagnetic radiation** which is a remnant from an early stage of the universe, also known as "relic radiation". The CMB is faint **cosmic background radiation** filling all space. It is an important source of data on the early universe because it is the oldest electromagnetic radiation in the universe, dating to the **epoch of recombination**. With a traditional **optical telescope**, the space between stars and galaxies (the *background*) is completely dark. However, a sufficiently sensitive **radio telescope** shows a faint background noise, or glow, almost **isotropic**, that is not associated with any star, galaxy, or other object. This glow is strongest in the **microwave** region of the radio spectrum. The accidental **discovery of the CMB** in 1965 by American radio astronomers **Arno Penzias** and **Robert Wilson**^{[1][2]} was the culmination of work initiated in the 1940s, and earned the discoverers the 1978 **Nobel Prize in Physics**.

Úvod do teorie plazmatu

Petr Kulháněk



Obr. 15: Magnetická zrcadla tvořená cívkami.

Fermiho urychlování druhého druhu

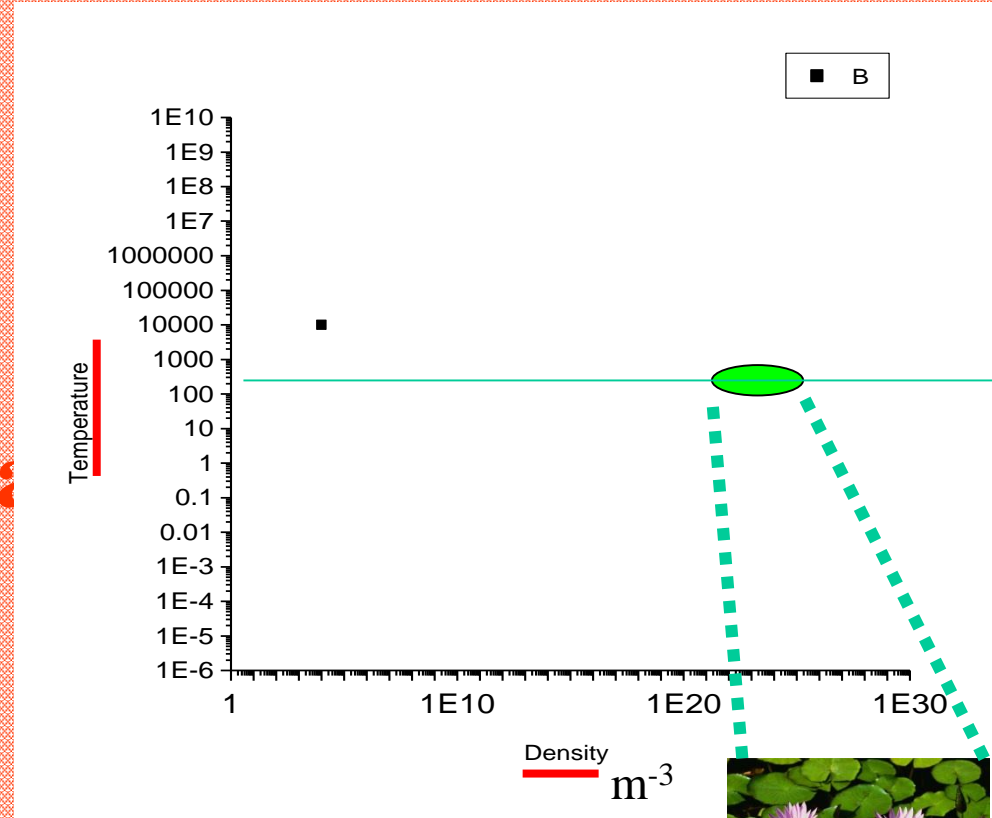
Představme si, že ve vesmíru se pohybují náhodně nabitě částice v prostředí různě se měnících magnetických polí. Nabitá částice bude tu a tam odražena od magnetických zrcadel polybujících se náhodným směrem. Díky Fermiho mechanismu bude statisticky někdy urychlena a někdy zpomalena. Rychlostní rozdíl se proto bude rozšiřovat a mezi částicemi se objeví určité procento velmi rychlých částic, které náhodně získaly energii z „příznivých“ odrazů od magnetických zrcadel. Tento mechanismus nazýváme *Fermiho urychlování druhého druhu* a italský fyzik Enrico Fermi se jím pokusil vysvětlit vysoké energie částic kosmického záření.



Obr. 17: Mlhovina Mravenec. Ve vnitřní části je pole dipólové, ve vnějších částech může v náhodných polích docházet k urychlování částic Fermiho mechanismem. HST.

Plasma

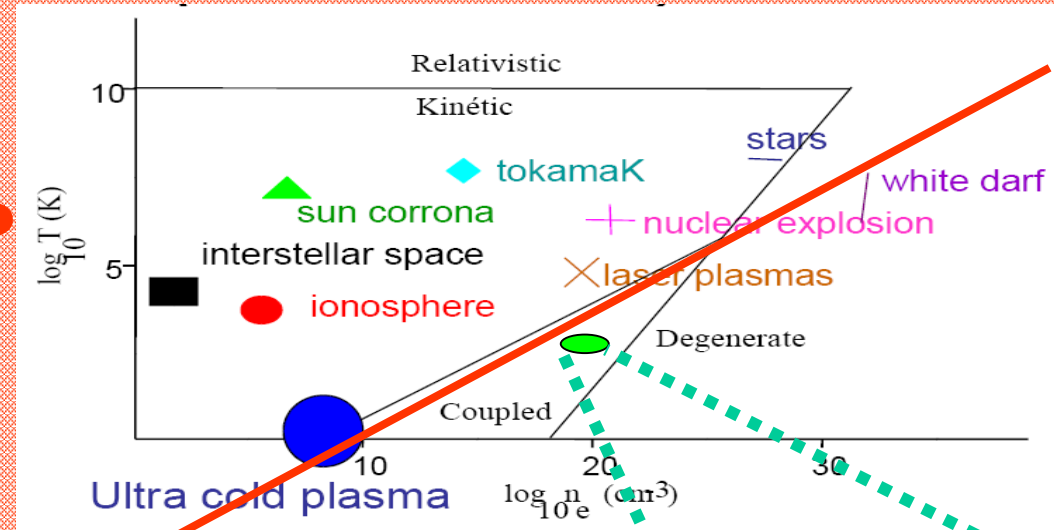
Pla



Not actualized, approximation

Plazma n_e ... T_e T

P



$$n_0 = 2,686\,781\,1(15) \times 10^{25} \text{ m}^{-3}$$



$$W_{kin} \sim W_{Pot..elektrost}$$

$$\frac{3}{2}kT \sim \frac{e^2}{\epsilon a} \sim \frac{e^2}{\epsilon N^{-1/3}}$$

$$T \sim \frac{10^{-38}}{k\epsilon} N^{1/3}$$

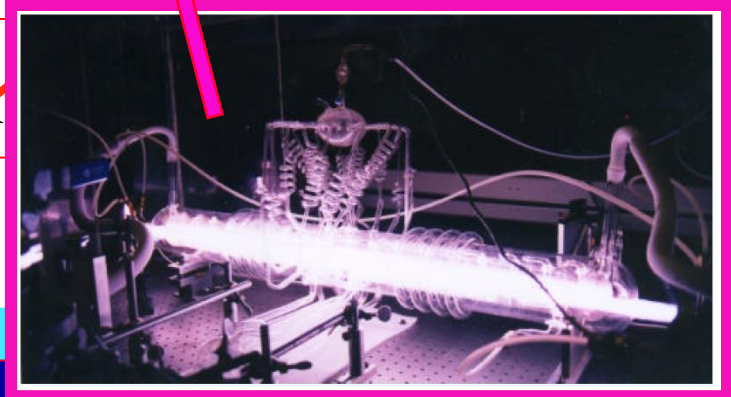
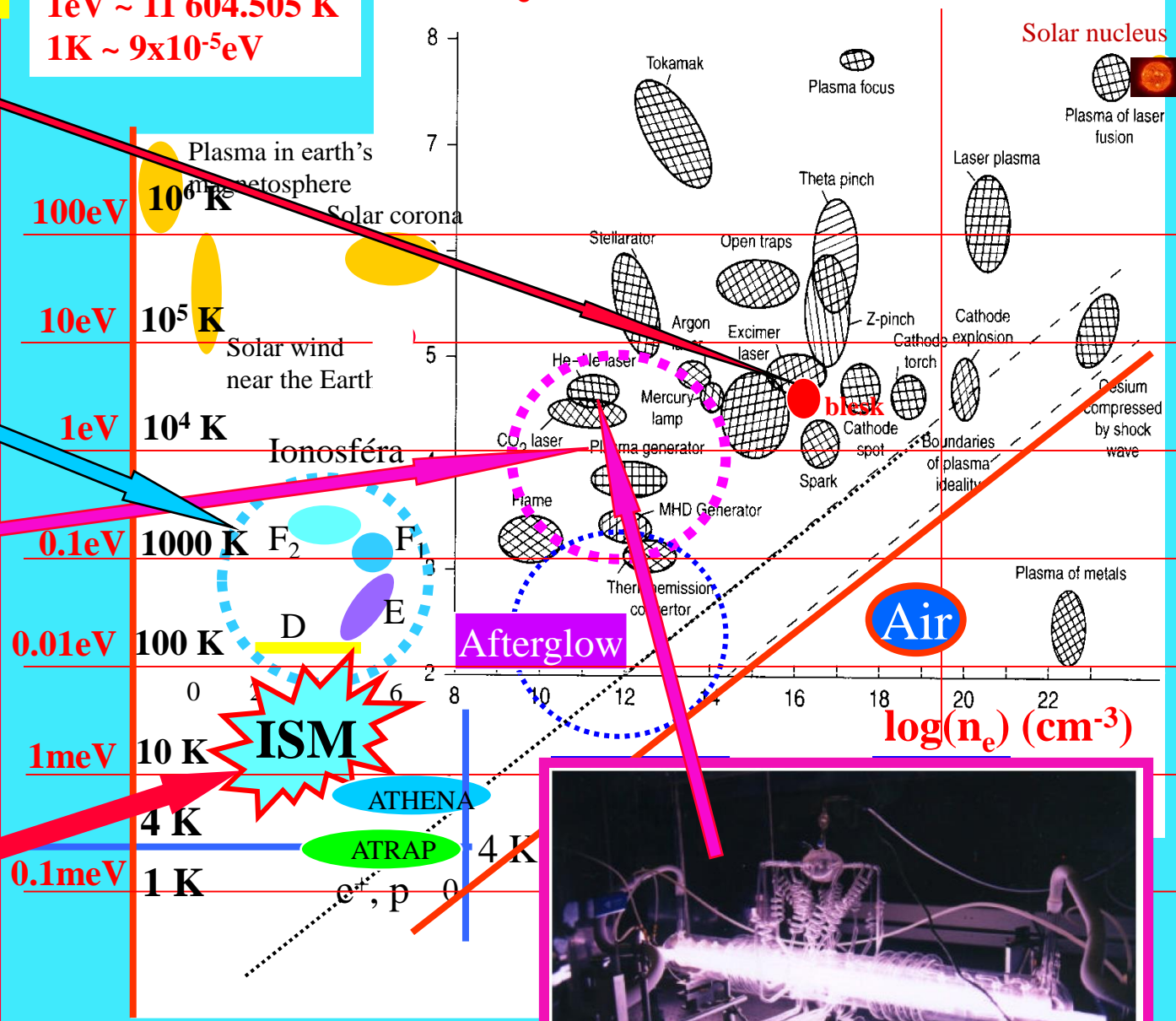
$$T_K = 1K \Rightarrow N_K = 10^9 \text{ m}^{-3}$$

Temperatures and energies

$E \leftrightarrow kT$
 $1\text{eV} \sim 11\,604.505\text{ K}$
 $1\text{K} \sim 9 \times 10^{-5}\text{eV}$

$\log T_e \text{ (K)}$

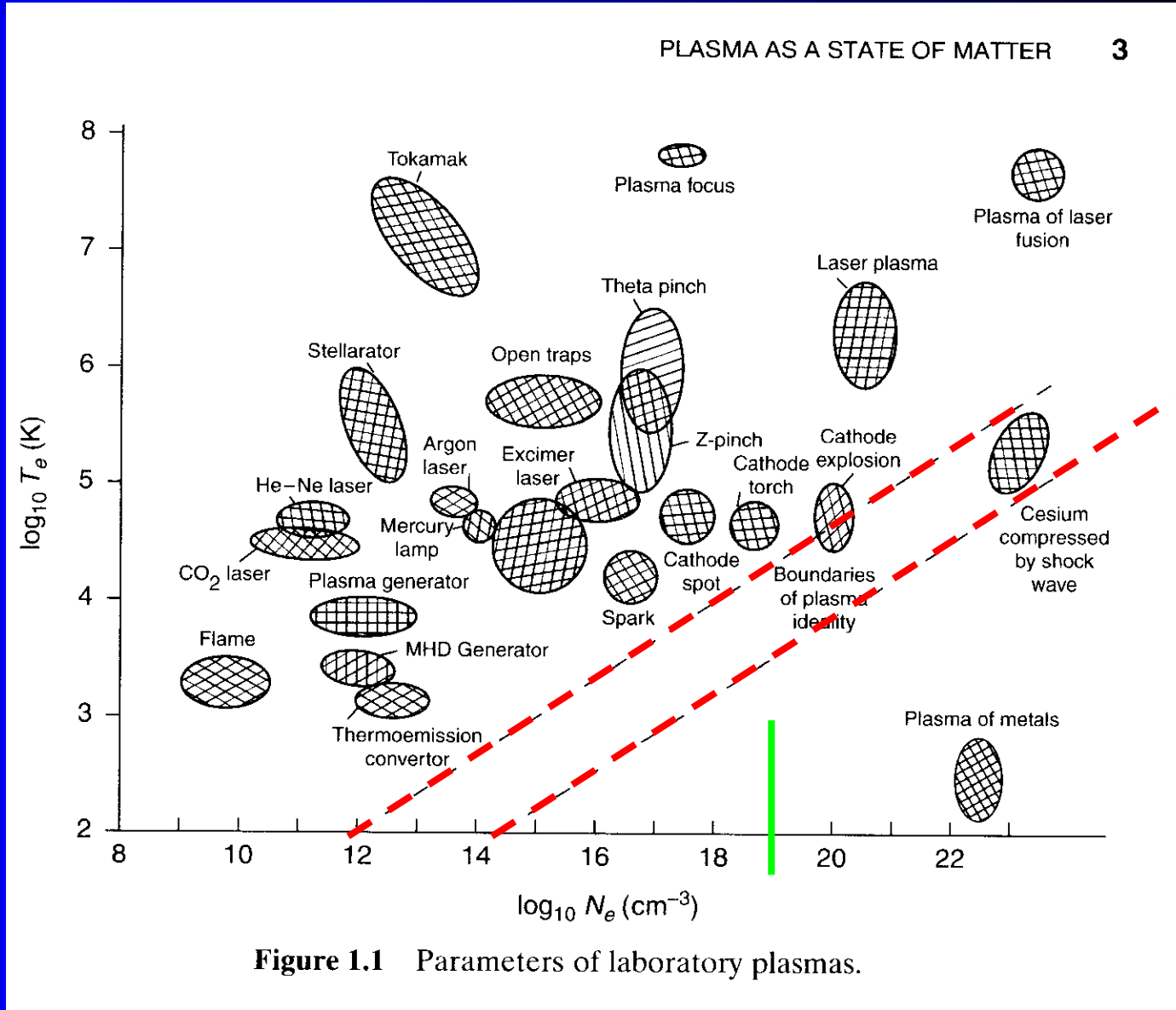
PLASMA AS A STATE OF MATTER



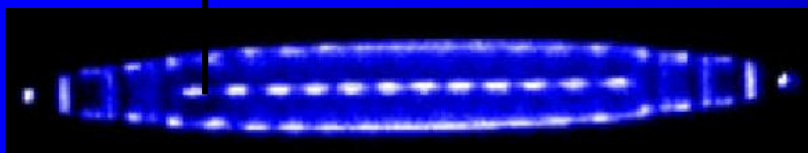
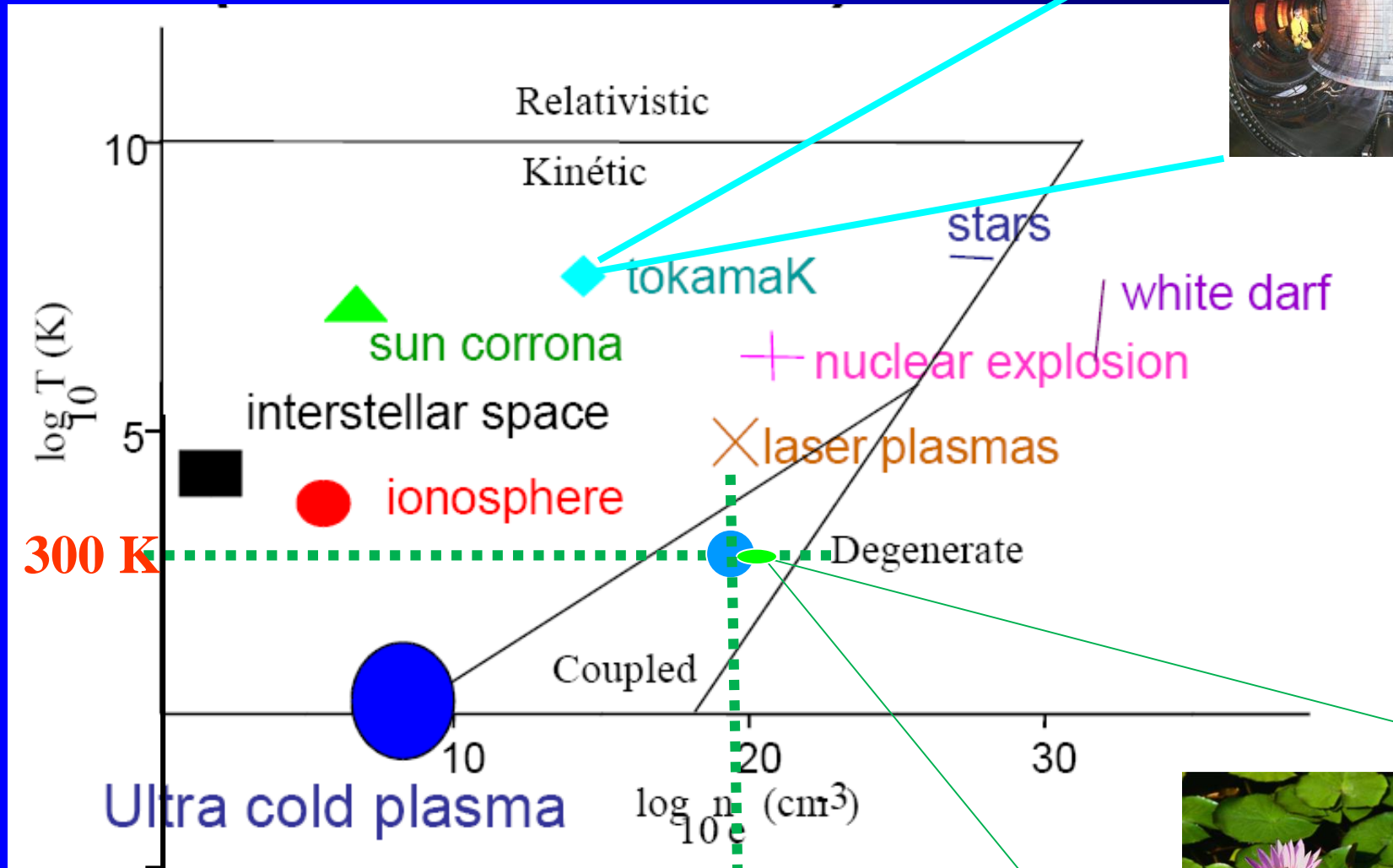
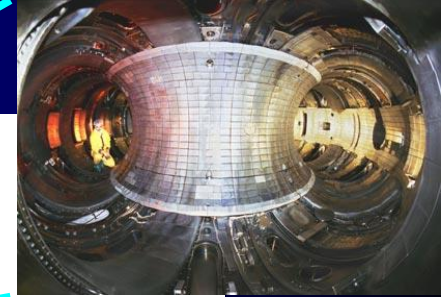
Not actualized, approximation

Parameters of laboratory plasmas

Not actualized, approximation



Electron temperature and electron number density - PLASMA



Experiment: $T \sim 6 \text{ mK}$

Neutral 1 atm



life

Parameters of plasmas found in nature

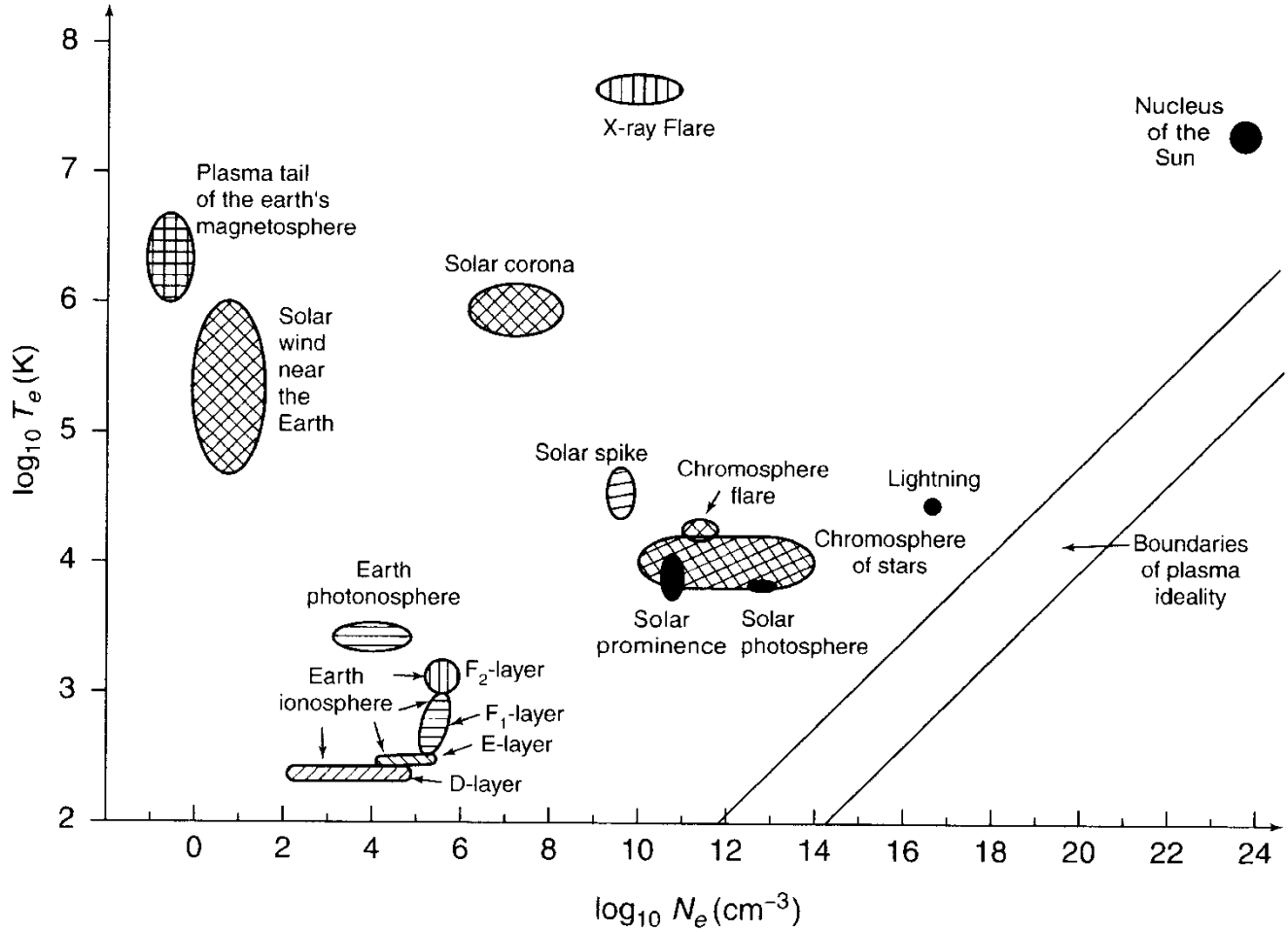


Figure 1.2 Parameters of plasmas found in nature.

Electron and gas temperatures in plasmas

4 PLASMA IN NATURE AND IN LABORATORY SYSTEMS

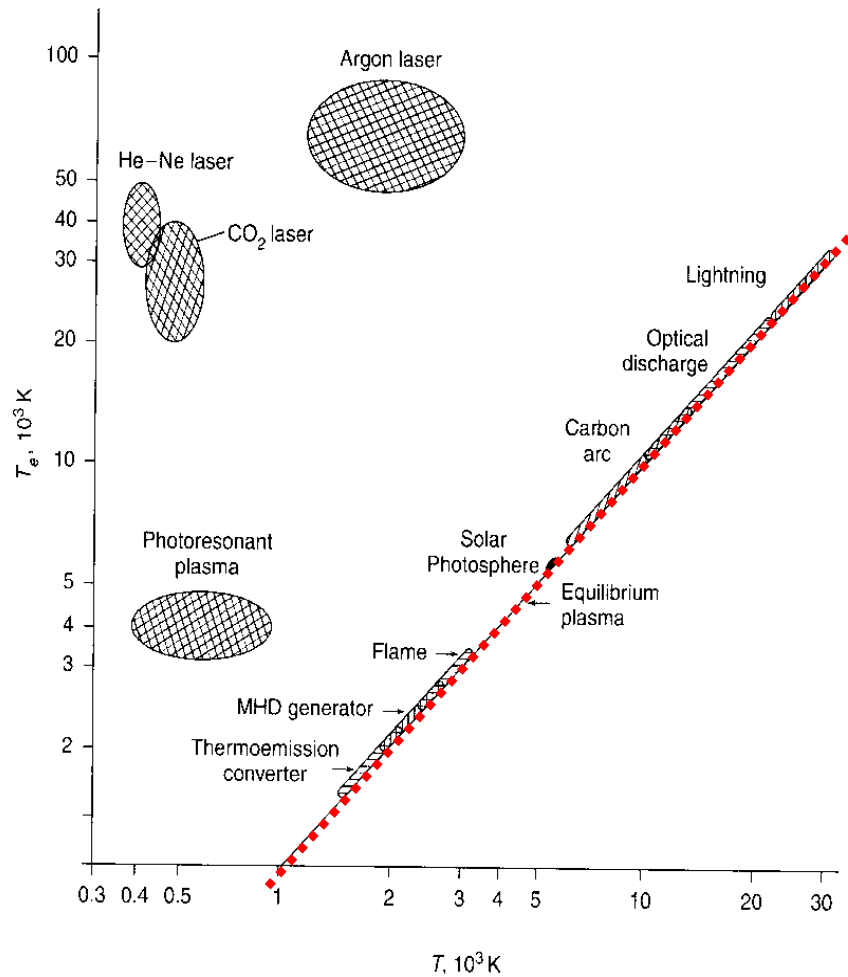


Figure 1.3 Electron and gas temperatures of laboratory plasmas. The straight line corresponds to the equilibrium plasma whose electron and gas temperatures are the same.

Difference in electron, ion and neutral gas temperature in plasma

Equilibrium; relaxation time,

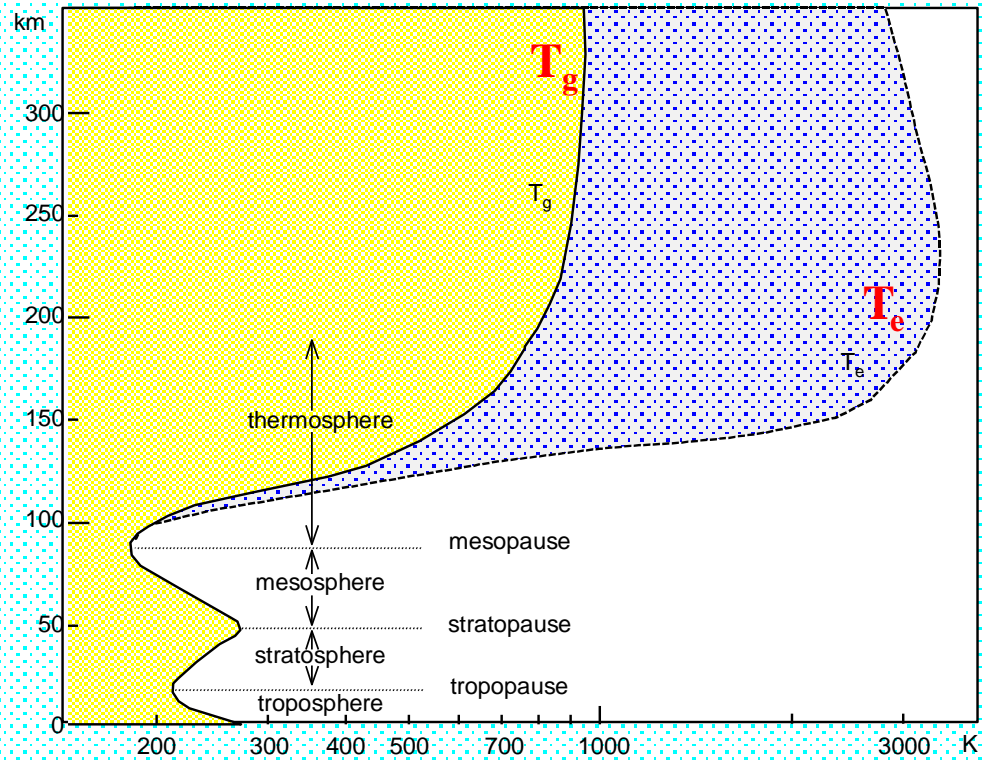
Probability of interactions...

Collisional frequency, Energy transfer

cross section

Temperature in the ionosphere

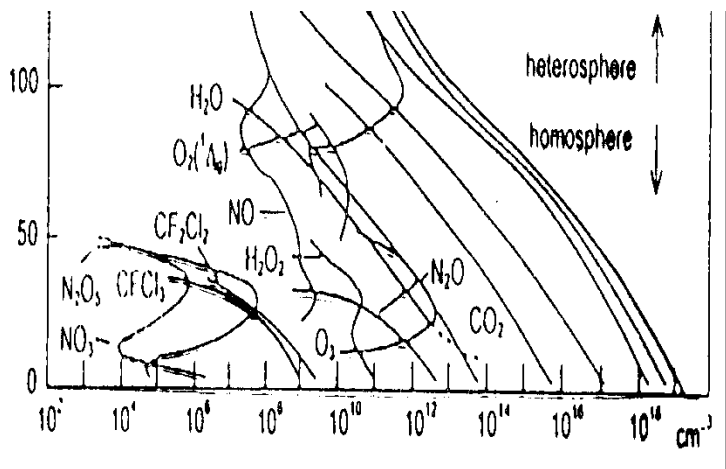
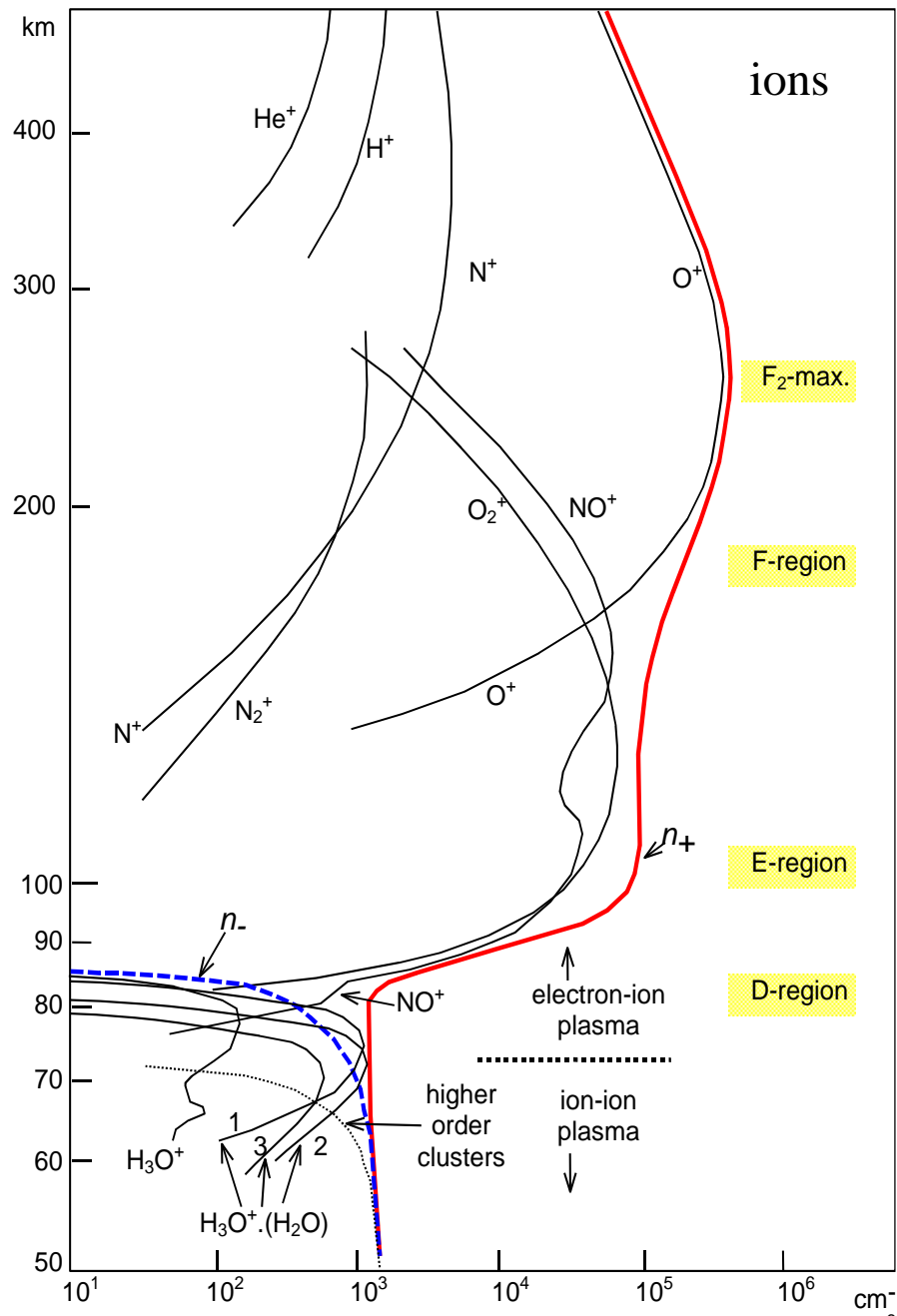
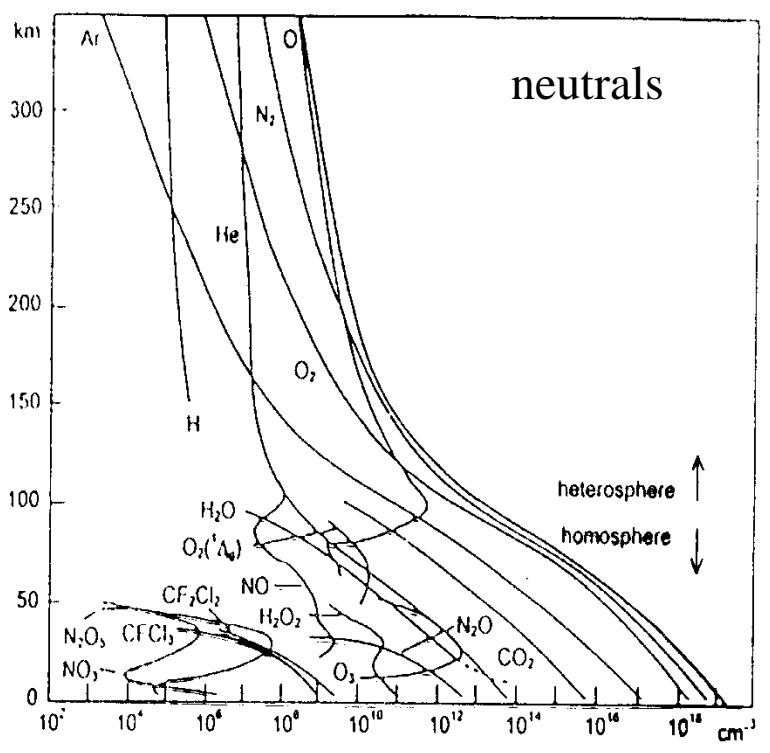
Temperatures in the ionosphere



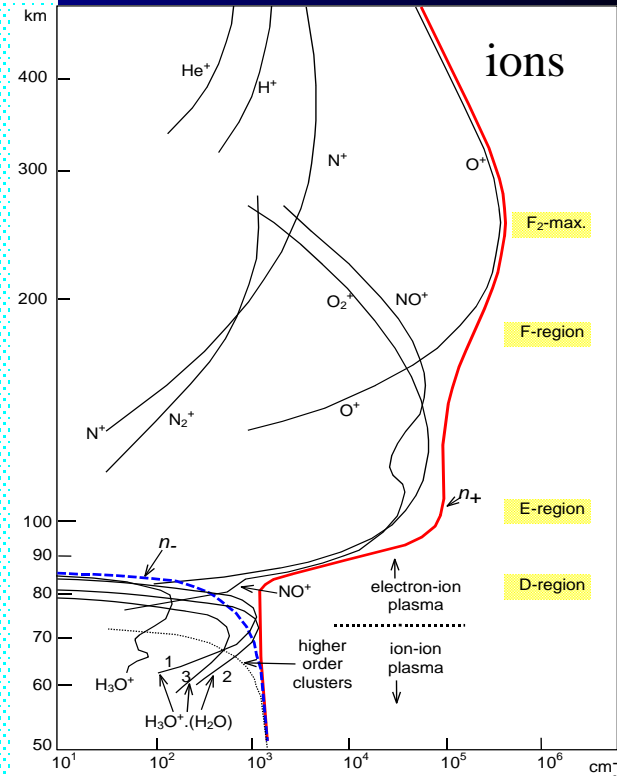
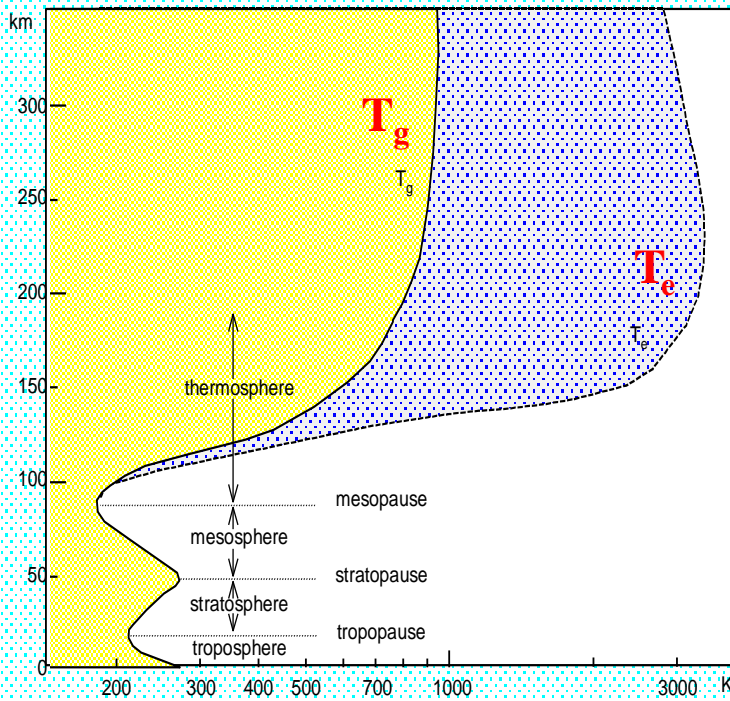
Ions chemistry

$$n_0 = 2,686\,781\,1(15) \times 10^{19} \text{ cm}^{-3}$$

Ions in the terrestrial atmosphere



Temperatures in the ionosphere



Recombination?? $\alpha(T)$

Crab Nebula

ISM

Hydrogen only??

Ions chemistry

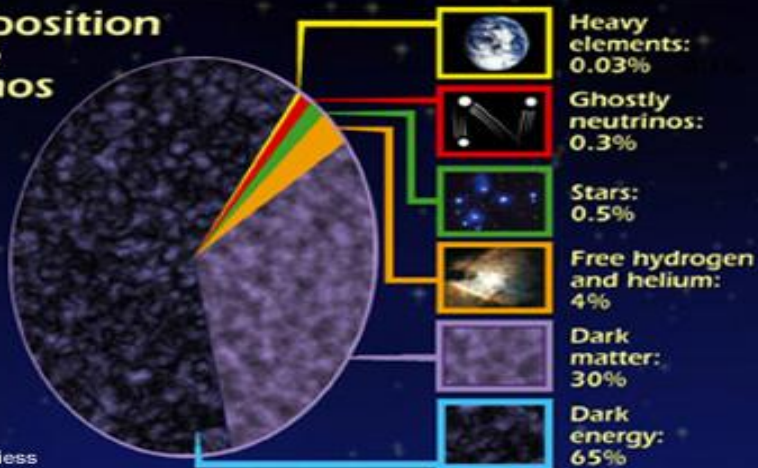
Electron – ion interactions

Negative ions ??

..... ??

Scio me nihil scire

Composition of the Cosmos



NASA/A. Riess

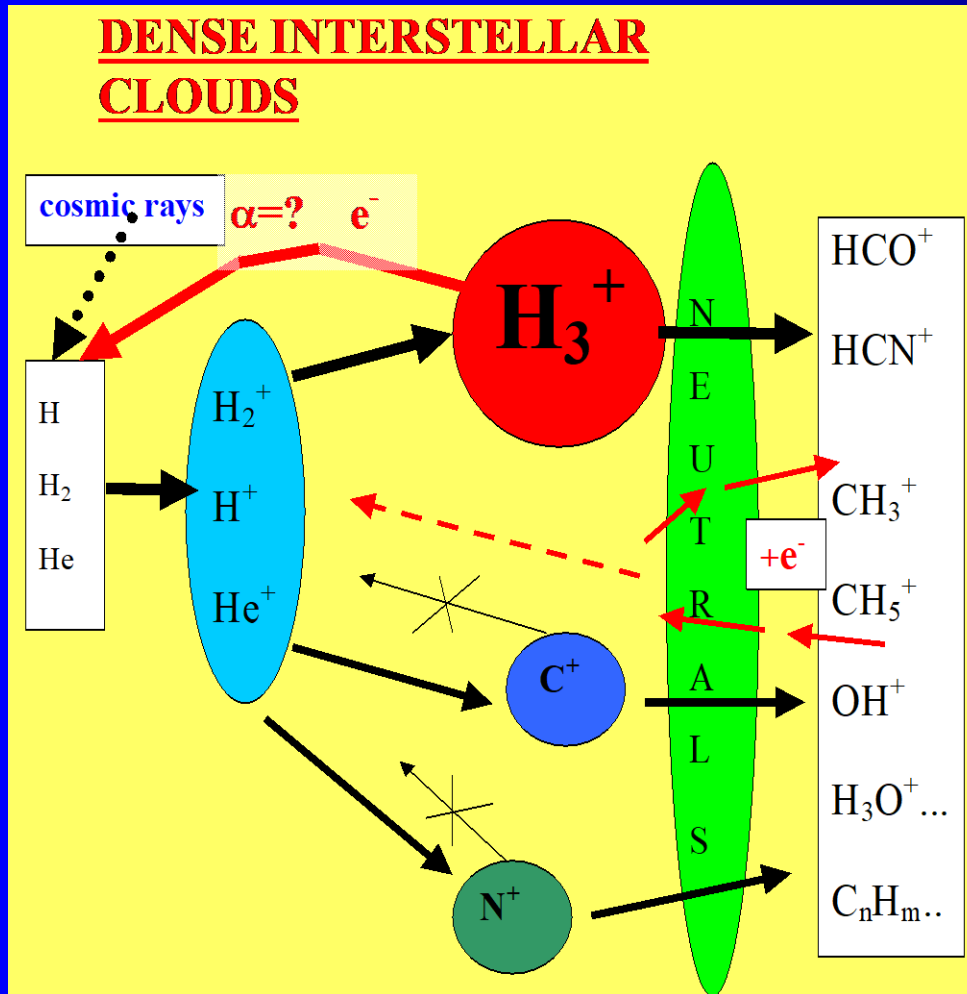
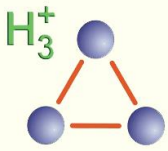
Hubble Heritage

NASA and The Hubble Heritage Team (STScI/AURA)

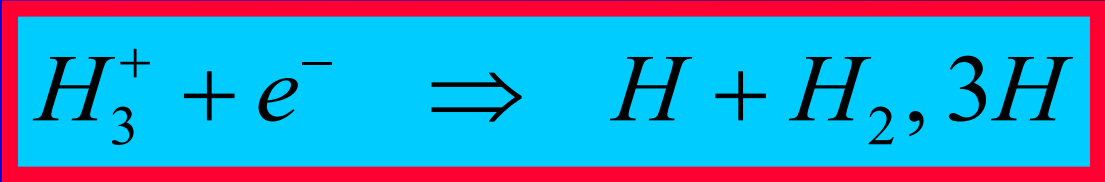
Interstellar medium

Hydrogen only??

92.1% of nucleons in the universe are protons
7.8% are helium nuclei !



$\alpha=?$
T ~ 10-50K

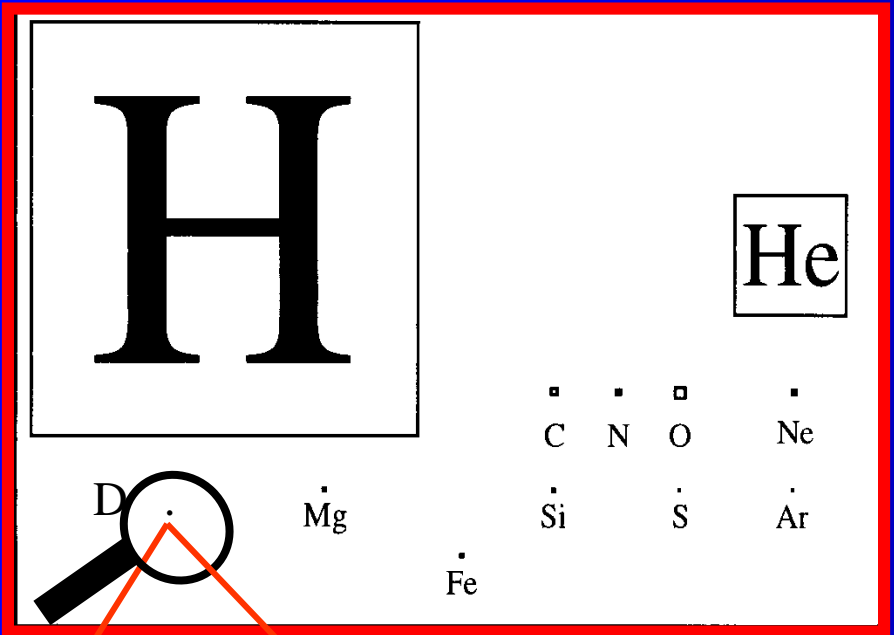


Interstellar medium, HD role

@ 10-50K

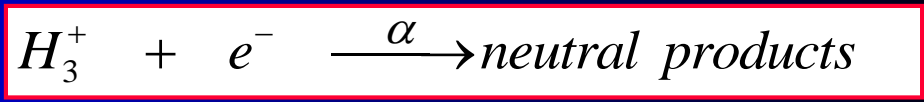
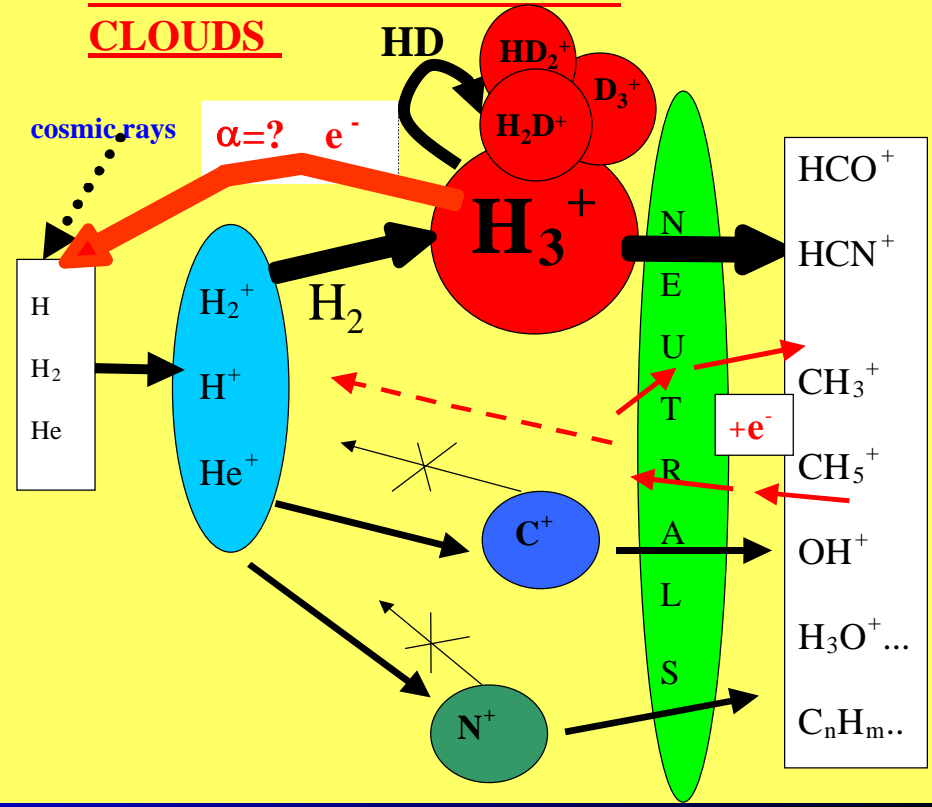
92.1% of nucleons in the universe are protons
 7.8% are helium nuclei !
 0.1%.....C,N,O,S,Si....

Cosmic abundance



D/H ratio ~ 10⁻⁵

DENSE INTERSTELLAR CLOUDS

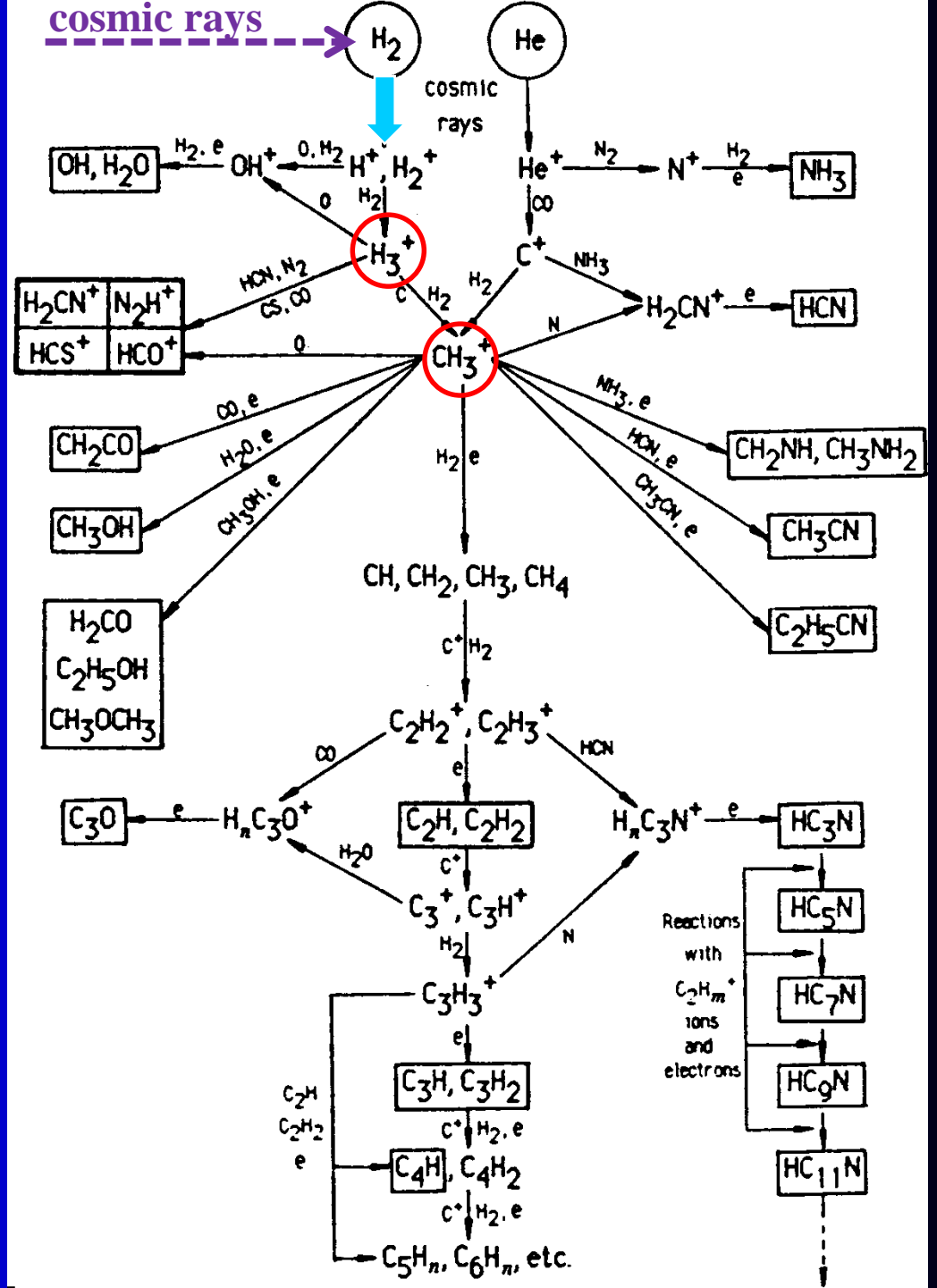
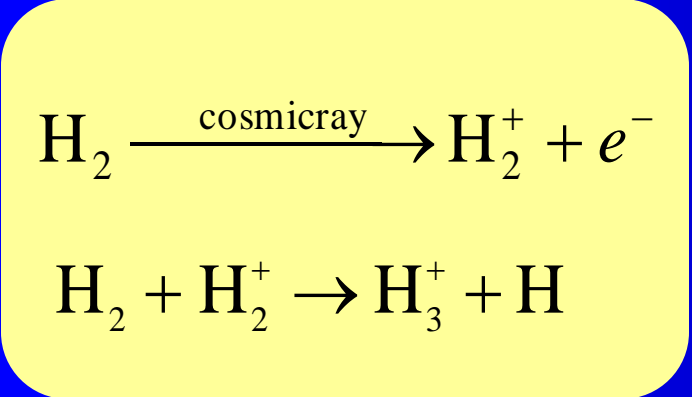


α (10 K) = ?????

k (10 K) = ?????



H₃⁺ in interstellar space

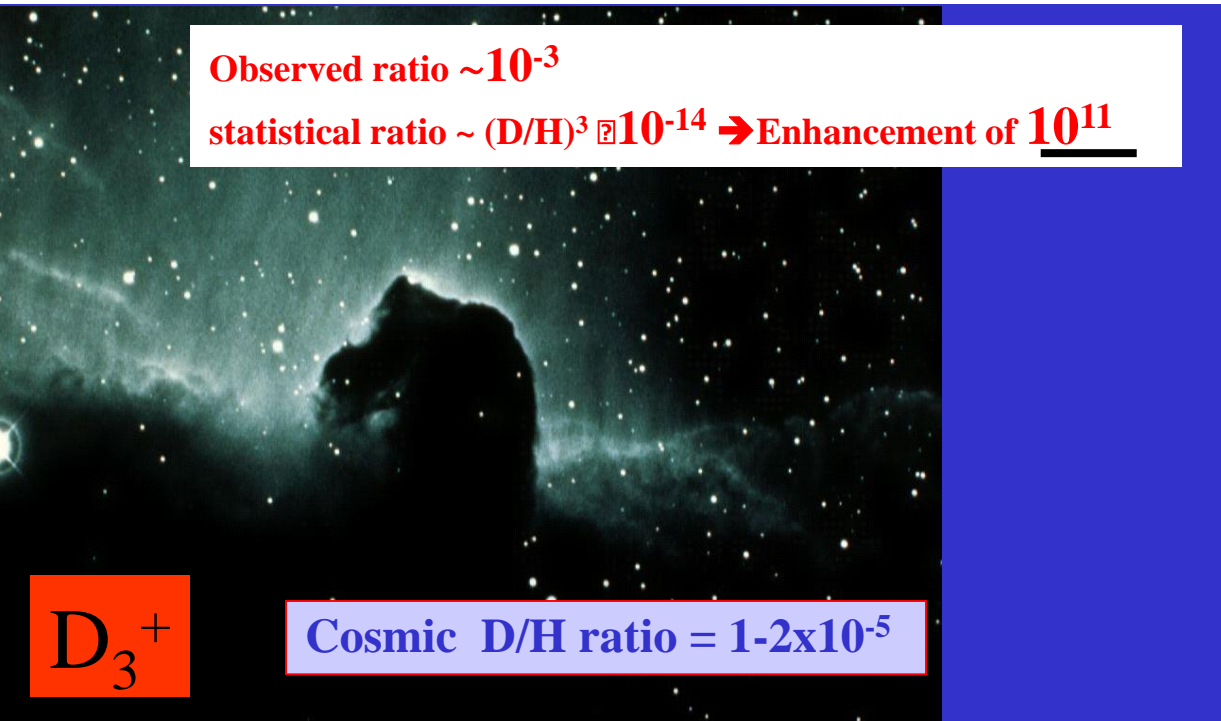


Observation of high population of deuterated molecules

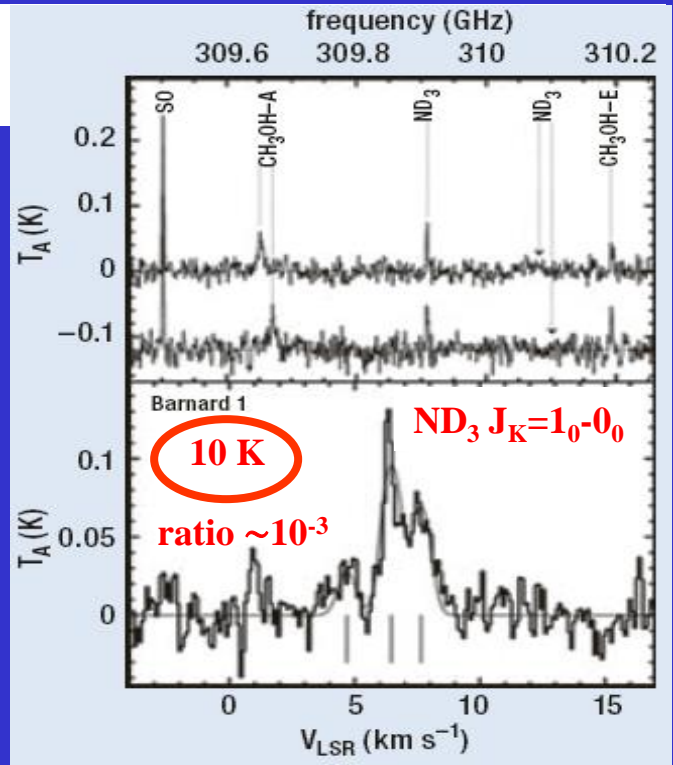
The first detection of deuterated molecules were made in the early 1970s..... **Observed enhancement of D in molecules**

H_2D	Stark	(1999)	$1_{10}-1_{11}$ transition of ortho- emission from young stellar object NGC 1333 IRAS4A.
H_2D^+	Caselli	(2003)	detected towards L1544.
HD_2^+	Vastel	(2004)	the first detection
$CH_2DOH...$	Parise	(2003, 2004)	have detected 4 isotopomers of deuterated methanol
NHD_2/NH_3	Roueff	(2000)	
	Loinard	(2001)	is 0.005 in the cold cloud L134N and 0.03 in the low-mass protostar 16293 E
D_2CO/H_2CO	Loinard	(2002)	
	Bacmann	(2003)	is between 0.01 and 0.4 in a low-mass protostars and prestellar cores
NH_2D/NH_3	J. Hatchell	(2003)	high ratios~4-33% in protostellar cores

ND_3/NH_3	Lis	(2002)	ratio $\sim 10^{-3}$ cold dense Barnard 1 cloud
	Tak	(2002)	Class 0 protostar NGC 1333 IRAS4A



Cosmic D/H ratio = $1-2 \times 10^{-5}$



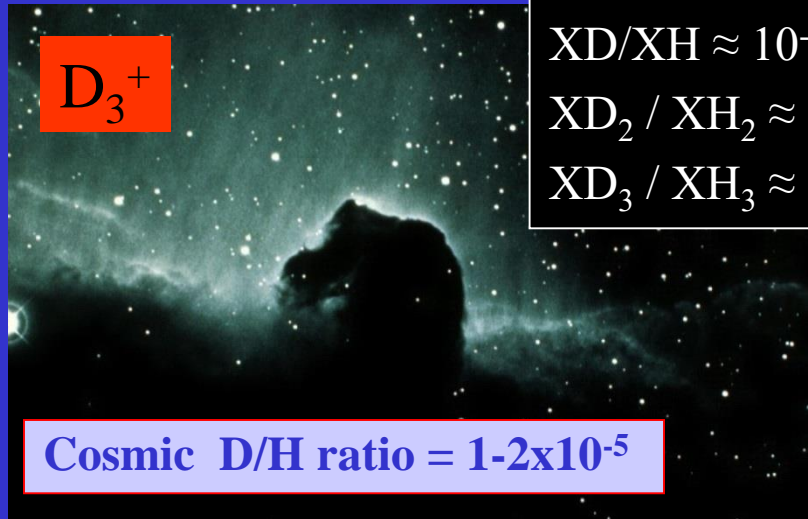
2: Spectrum of ND_3 towards the dark cloud B1. (Lis et al. 2002 ApJ 571 L55)

High population of deuterated molecules

D_3^+

Cosmic D/H $\approx 10^{-5}$
 XD/XH $\approx 10^{-1}$ - 10^{-3}
 XD₂ / XH₂ $\approx 10^{-2}$
 XD₃ / XH₃ $\approx 10^{-3}$

Cosmic D/H ratio = $1-2 \times 10^{-5}$



H_3^+

D_3^+

HD	H_2D^+	D_2H^+
N_2D^+	DCO ⁺	DCN
DNC	HDCS	D_2CS
HDO	DC ₃ N	DC ₅ N
C ₃ HD	HDCO	D_2CO
CH ₃ OD	CH ₂ DOH	CHD_2OH
CD ₃ OH	CH ₂ DCN	NH_2D
NHD_2	ND_3	CHD_2CCH
CH_3CCD	C ₂ D	C ₄ D
HDS	D_2S	

Deuterated molecules that have been detected in interstellar clouds as of February 2005.

Species	Observed ratio
NH_2D/NH_3	0.01
HDCO/H ₂ CO	0.005-0.11
DCN/HCN	0.023
DNC/HNC	0.015
C ₂ D/C ₂ H	0.01
DCO ⁺ /HCO ⁺	0.02
N_2D^+/N_2H^+	0.08
DC ₃ N/HC ₃ N	0.03-0.1
HDCS/H ₂ CS	0.02

Gas phase reactions,

ion-molecule reactions,
recombination

Grain surface reactions

Physics of condensation and evaporation from grain surface

Deuterated gas phase molecules in space

HD * #	HDCO	H₂D⁺ *	D₂CO
HDO *	HDCS	DCO⁺ *	ND₂H
DCN *	DC₃N	N₂D⁺	CHD₂OH
DNC	CH₂DOH		D₂S
HDS	CH₃OD		ND₃
C₂D	DC₅N		CD₃OH
C₄D	CH₂DCCH		D₂CS
C₃HD	CH₂DCN		
NH₂D	CH₃D		

Planets

Comets

CS disks

ISM

Extragalactic #

Cosmic D/H $\approx 10^{-5}$

XD/XH $\approx 10^{-1}$ - 10^{-3}

XD₂ / XH₂ $\approx 10^{-2}$

XD₃ / XH₃ $\approx 10^{-3}$

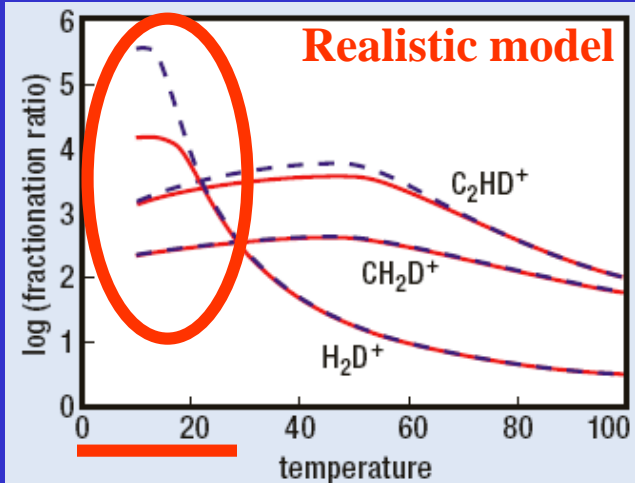
HD



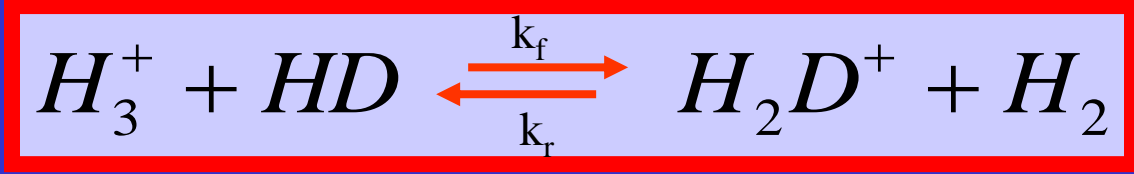
Energy

Small differences in zero point energies for deuterated molecules

$$\Delta H / k = -232 \text{ K}$$



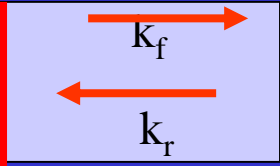
3: The enhancement in the fractionation of primary ions relative to the HD/H₂ ratio as a function of temperature in interstellar clouds



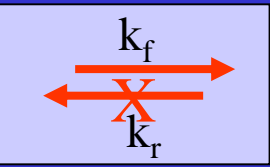
$$k_r/k_f \sim \exp(\Delta H / kT) \sim \exp(-232 / T)$$

In equilibrium $\frac{H_3^+}{H_2D^+} = \frac{H_2}{HD} \frac{k_r}{k_f}$

@ 300 K $k_r/k_f \sim \exp(-1) \sim 0.4$

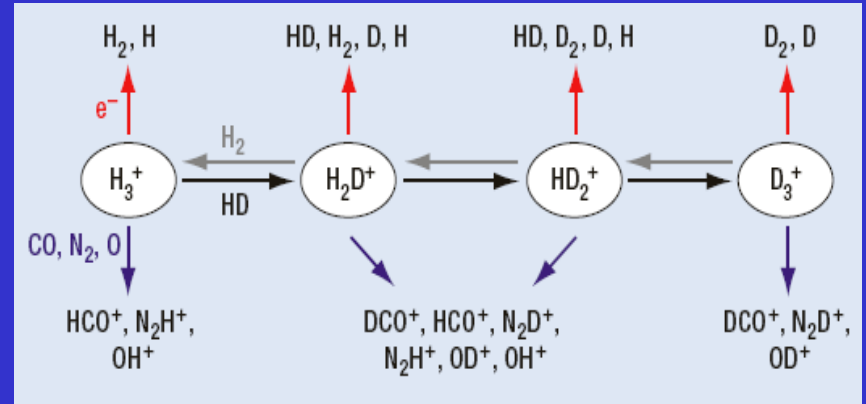
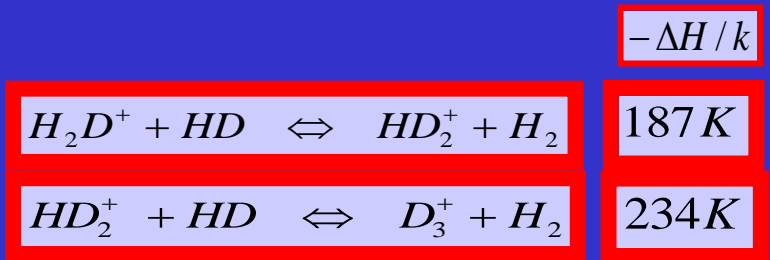


@ 10 K $k_r/k_f \sim \exp(-23) \sim 10^{-10}$



@ 10 K $\frac{H_3^+}{H_2D^+} = \frac{H_2}{HD} \frac{k_r}{k_f} \sim 10^5 \cdot 10^{-10} = 10^{-5}$

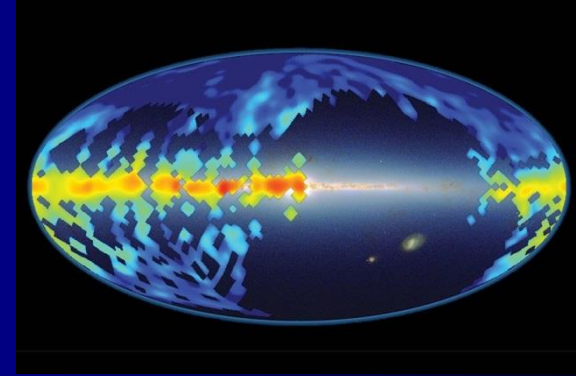
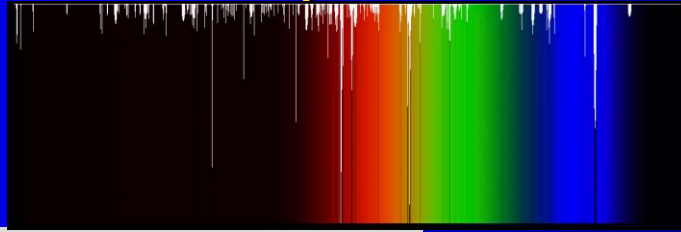
ONLY PARTLY !!!???



Molecules in interstellar space

DIBs - diffuse bands

1919-1922



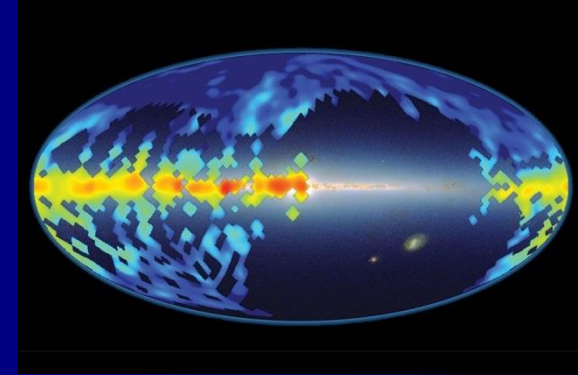
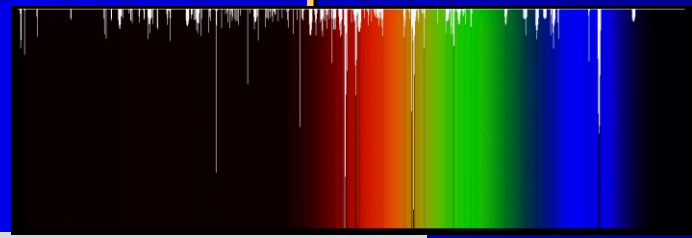
1919-1922 Heger discovers the DIBs

Nearly 100 years ago Mary Lea Heger discovered diffuse bands in the spectra of stars due to some sort of material maybe molecules in the space between stars and Earth. A map of the data from the Sloan Digital Sky Survey, by a team from Johns Hopkins produced this map. Red indicates areas with the most abundant DIB molecules, blue the least.

Molecules in interstellar space

DIBs - diffuse bands

1919-1922



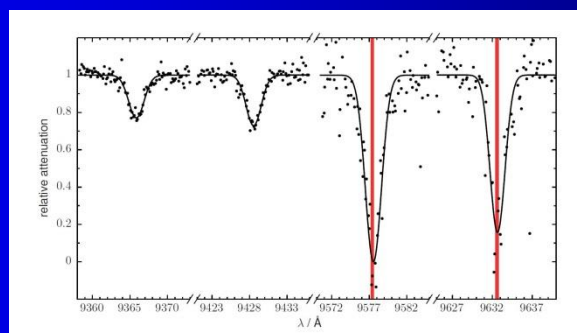
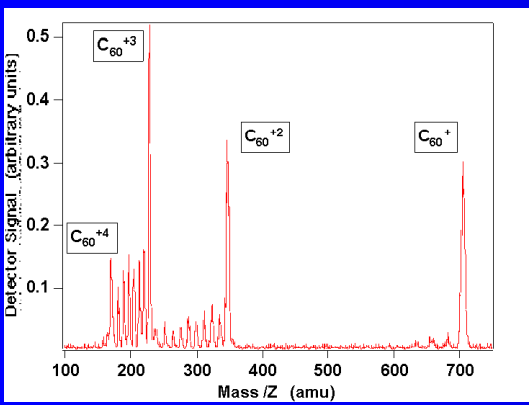
1919-1922 Heger discovers the DIBs
Nearly 100 years ago Mary Lea Heger discovered diffuse bands in the spectra of stars due to some sort of material maybe molecules in the space between stars and Earth. A map of the data from the Sloan Digital Sky Survey, by a team from Johns Hopkins produced this map. Red indicates areas with the most abundant DIB molecules, blue the least.

16 JULY 2015 | VOL 523 | NATURE | 323

LETTER **2015** doi:10.1038/nature14566

Laboratory confirmation of C_{60}^+ as the carrier of two diffuse interstellar bands

E. K. Campbell¹, M. Holz¹, D. Gerlich² & J. P. Maier¹

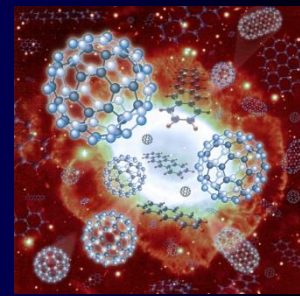
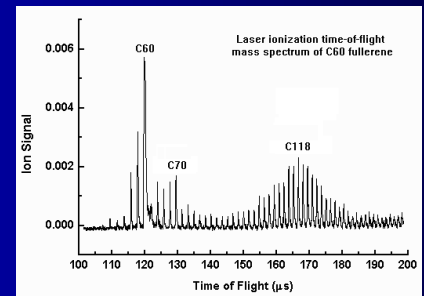
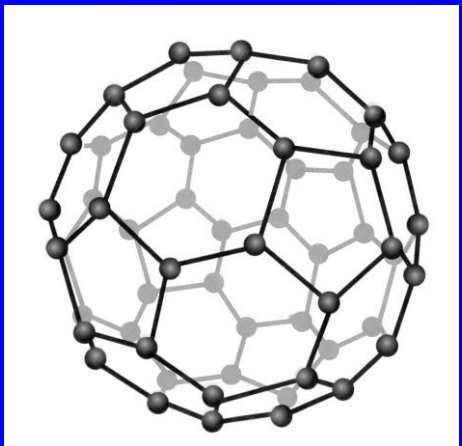


RESEARCH NEWS & VIEWS

ASTROCHEMISTRY

Fullerene solves an interstellar puzzle

Laboratory measurements confirm that a 'buckyball' ion is responsible for two near-infrared absorption features found in spectra of the interstellar medium, casting light on a century-old astrochemical mystery. **SEE LETTER P.322**



Observation of H_2O^+

A&A 550, A25 (2013)
DOI: 10.1051/0004-6361/201220466
© ESO 2013

2013

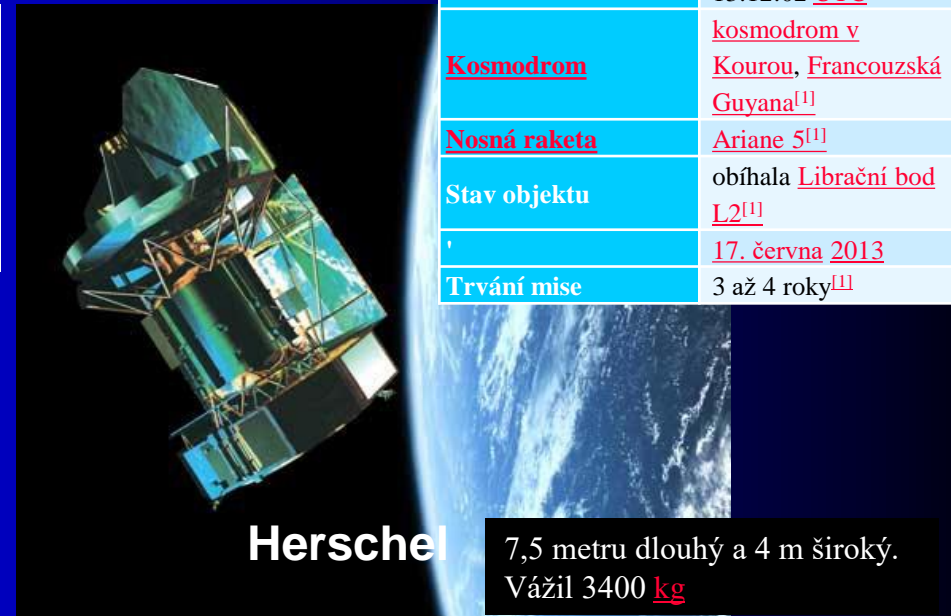
Astronomy
&
Astrophysics

Excited OH^+ , H_2O^+ , and H_3O^+ in NGC 4418 and Arp 220*

E. González-Alfonso¹, J. Fischer², S. Bruderer³, H. S. P. Müller⁴, J. Graciá-Carpio³, E. Sturm³, D. Lutz³,
A. Poglitsch³, H. Feuchtgruber³, S. Veilleux^{5,6}, A. Contursi³, A. Sternberg⁷, S. Hailey-Dunsheath⁸, A. Verma⁹,
N. Christopher⁹, R. Davies³, R. Genzel³, and L. Tacconi³

* *Herschel* is an ESA space observatory with science instruments provided by European-led Principal Investigator consortia and with important participation from NASA.

Mission duration Planned: 3 years (2009-2012)
Final, to 2013: 4 years, 1 month, 2 days



Herschel 7,5 metru dlouhý a 4 m široký.
Vážil 3400 kg

Start	14. května 2009 v 13:12:02 UTC
Kosmodrom	Kosmodrom v Kourou, Francouzská Guyana ^[1]
Nosná raketa	Ariane 5 ^[1]
Stav objektu	obíhala Librační bod L2 ^[1]
'	17. června 2013
Trvání mise	3 až 4 roky ^[1]

ABSTRACT

We report on *Herschel*/PACS observations of absorption lines of OH^+ , H_2O^+ and H_3O^+ in NGC 4418 and Arp 220. Excited lines of OH^+ and H_2O^+ with E_{lower} of at least 285 and ~ 200 K, respectively, are detected in both sources, indicating radiative pumping and location in the high radiation density environment of the nuclear regions. Abundance ratios $\text{OH}^+/\text{H}_2\text{O}^+$ of 1–2.5 are estimated in the nuclei of both sources. The inferred OH^+ column and abundance relative to H nuclei are $(0.5–1) \times 10^{16} \text{ cm}^{-2}$ and $\sim 2 \times 10^{-8}$, respectively. Additionally, in Arp 220, an extended low excitation component around the nuclear region is found to have $\text{OH}^+/\text{H}_2\text{O}^+ \sim 5–10$. H_3O^+ is detected in both sources with $N(\text{H}_3\text{O}^+) \sim (0.5–2) \times 10^{16} \text{ cm}^{-2}$, and in Arp 220 the pure inversion, metastable lines indicate a high rotational temperature of ~ 500 K, indicative of formation pumping and/or hot gas. Simple chemical models favor an ionization sequence dominated by $\text{H}^+ \rightarrow \text{O}^+ \rightarrow \text{OH}^+ \rightarrow \text{H}_2\text{O}^+ \rightarrow \text{H}_3\text{O}^+$, and we also argue that the H^+ production is most likely dominated by X-ray/cosmic ray ionization. The full set of observations and models leads us to propose that the molecular ions arise in a relatively low density ($\gtrsim 10^4 \text{ cm}^{-3}$) interclump medium, in which case the ionization rate per H nucleus (including secondary ionizations) is $\zeta > 10^{-13} \text{ s}^{-1}$, a lower limit that is several $\times 10^2$ times the highest current rate estimates for Galactic regions. In Arp 220, our lower limit for ζ is compatible with estimates for the cosmic ray energy density inferred previously from the supernova rate and synchrotron radio emission, and also with the expected ionization rate produced by X-rays. In NGC 4418, we argue that X-ray ionization due to an active galactic nucleus is responsible for the molecular ion production.

Modeling observations of the interstellar medium (ISM)

David Neufeld
Johns Hopkins University

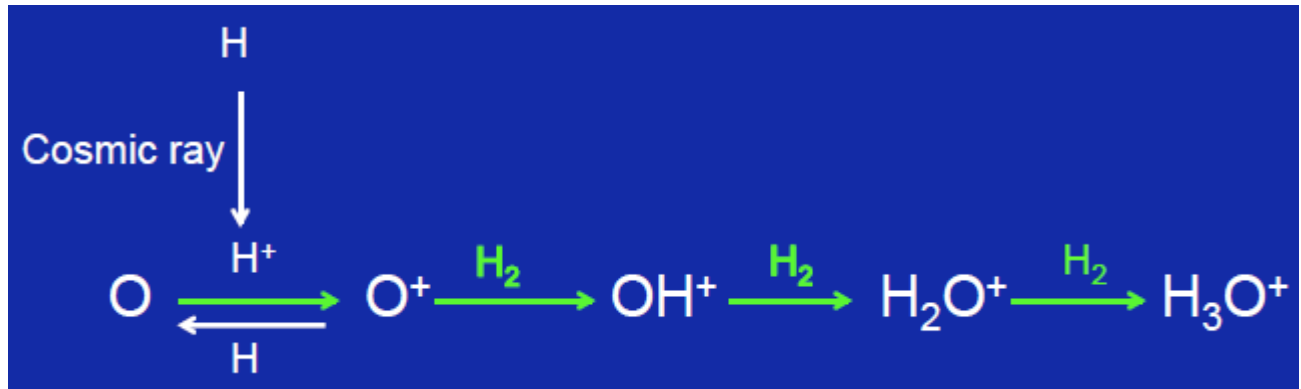
Measuring the cosmic-ray ionization rate with OH^+ and H_2O^+

Unlike C^+ and S^+ , O^+ does react with H_2 at low temperature. But O is not ionized by UV radiation longward of the Lyman limit, so OH^+ and H_2O^+ formation must be initiated by cosmic ray ionization

Recent discoveries of molecules in the diffuse ISM

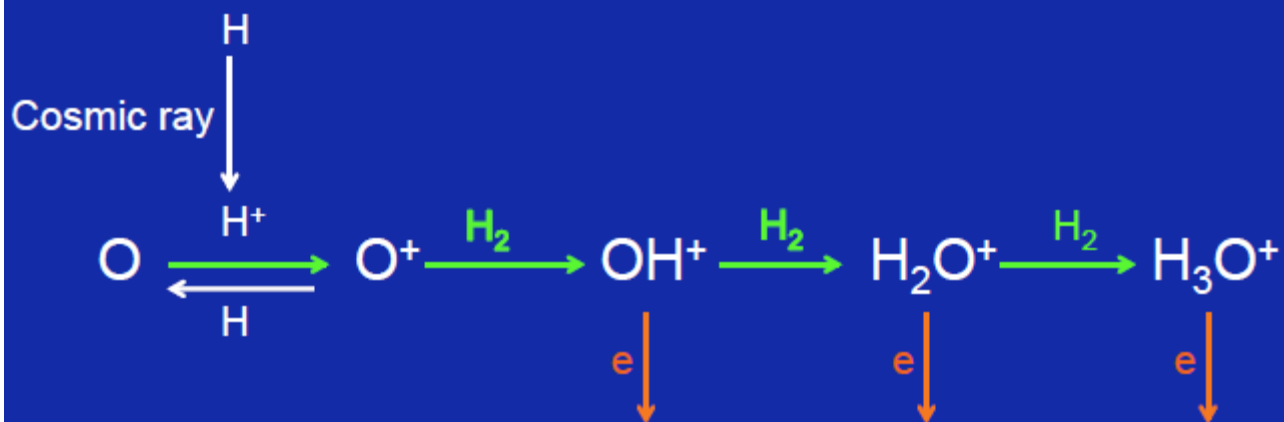
OH^+	Wyrowski et al. 2010	APEX
SH^+	Menten et al. 2011	APEX
H_2O^+	Gerin et al. 2010	Herschel
HF	Neufeld et al. 2010	Herschel
HCl^+	de Luca et al. 2013	Herschel
H_2Cl^+	Lis et al. 2010	Herschel
SH	Neufeld et al. 2012	SOFIA
ArH^+	Schilke et al. 2014	Herschel

All hydrides with high frequency rotational transitions that are unobservable from the ground or observable only from superb submillimeter sites



Determining the molecular fraction in the diffuse ISM

The $\text{OH}^+/\text{H}_2\text{O}^+$ ratio reflects a competition between reaction of OH^+ with H_2 and reaction with electrons



Observed $\text{OH}^+/\text{H}_2\text{O}^+$ ratios ~ 3 to 15 imply that only $2 - 10\%$ of the H is typically in H_2

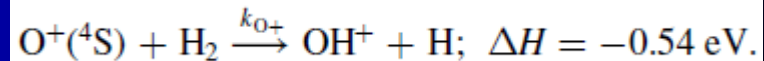


OH⁺ Formation in the Low-temperature O⁺(⁴S) + H₂ Reaction

Artem Kovalenko , Thuy Dung Tran , Serhiy Rednyk , Štěpán Roučka , Petr Dohnal , Radek Plašil ,
Dieter Gerlich , and Juraj Glosík

Department of Surface and Plasma Science, Faculty of Mathematics and Physics, Charles University, Prague, Czech Republic; radek.plasil@mff.cuni.cz

Received 2017 December 18; revised 2018 February 7; accepted 2018 February 18; published 2018 March 28

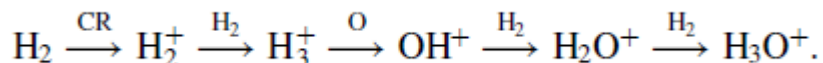
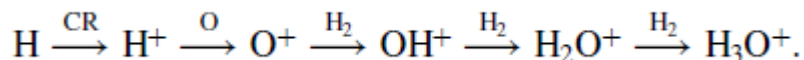
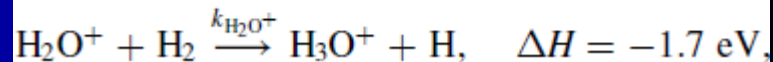
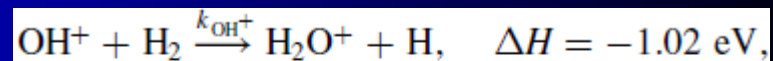


Formation of H₂O⁺ and H₃O⁺ Cations in Reactions of OH⁺ and H₂O⁺ with H₂: Experimental Studies of the Reaction Rate Coefficients from T = 15 to 300 K

Thuy Dung Tran , Serhiy Rednyk , Artem Kovalenko , Štěpán Roučka , Petr Dohnal , Radek Plašil ,
Dieter Gerlich , and Juraj Glosík

Department of Surface and Plasma Science, Faculty of Mathematics and Physics, Charles University, V Holešovičkách 2,
Prague, 180 00, Czech Republic; stepan.roucka@mff.cuni.cz

Received 2017 October 24; revised 2017 December 8; accepted 2017 December 8; published 2018 February 7



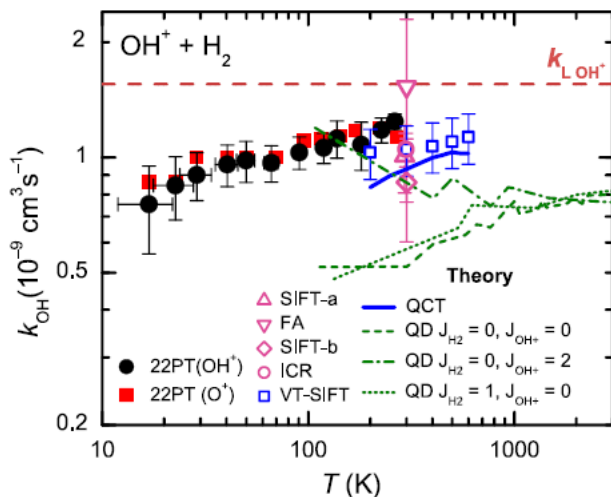


Figure 4. Temperature dependence of the rate coefficient k_{OH^+} of the reaction of OH^+ with normal hydrogen. The averaged data obtained in experiments with OH^+ and O^+ ions injected into the trap are indicated by full circles and squares, respectively. The systematic error due to pressure measurement is 20%. The dashed horizontal line ($k_{\text{L,OH}^+}$) indicates the Langevin collisional rate coefficient. The previous results at 300 K are FA (Fehsenfeld et al. 1967), ICR (Kim et al. 1975), SIFT-a (Jones et al. 1981), and SIFT-b (Shul et al. 1988). The temperature dependencies of k_{OH^+} calculated (QCT) and measured (VT-SIFT) by Martinez et al. (2015) are indicated by the full line and open squares, respectively. The dashed, dotted, and dash-dotted lines represent the phenomenological rate coefficients ($\nu\sigma$) derived from the theoretical QD cross-sections (Song et al. 2016a) corresponding to different rotational states of reactants as indicated in the legend.

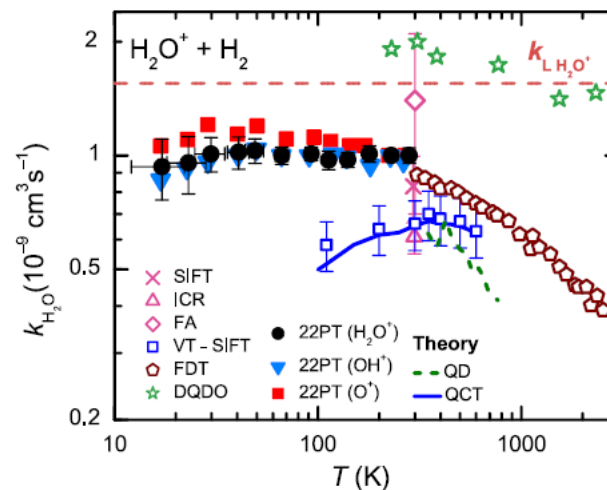


Figure 5. Temperature dependence of the reaction rate coefficient $k_{\text{H}_2\text{O}^+}$ of the reaction of H_2O^+ with normal hydrogen. The averaged data obtained in experiments with H_2O^+ , OH^+ , and O^+ ions injected into the trap are indicated by full circles, triangles, and squares, respectively. The systematic error due to pressure determination is 20%. The dashed horizontal line ($k_{\text{L,H}_2\text{O}^+}$) indicates the Langevin collisional rate coefficient. The previous results at 300 K are FA (Fehsenfeld et al. 1967), ICR (Kim et al. 1975), FDT (Dotan et al. 1980), and SIFT (Jones et al. 1981). The values measured (VT-SIFT) and calculated (QCT) by Ard et al. (2014) are indicated by the open squares and by the full line (QCT), respectively. The dashed line and stars represent the phenomenological rate coefficients ($\nu\sigma$) derived from the theoretical QD, and experimental DQDO cross-sections (Song et al. 2016b). The uncertainty of the DQDO results is 50%.

Interstellar Hydrides

Maryvonne Gerin,^{1,2} David A. Neufeld,^{3,4}
and Javier R. Goicoechea⁵

Annu. Rev. Astron. Astrophys. 2016. 54:181–225

First published online as a Review in Advance on
July 22, 2016

The *Annual Review of Astronomy and Astrophysics* is
online at astro.annualreviews.org

2016

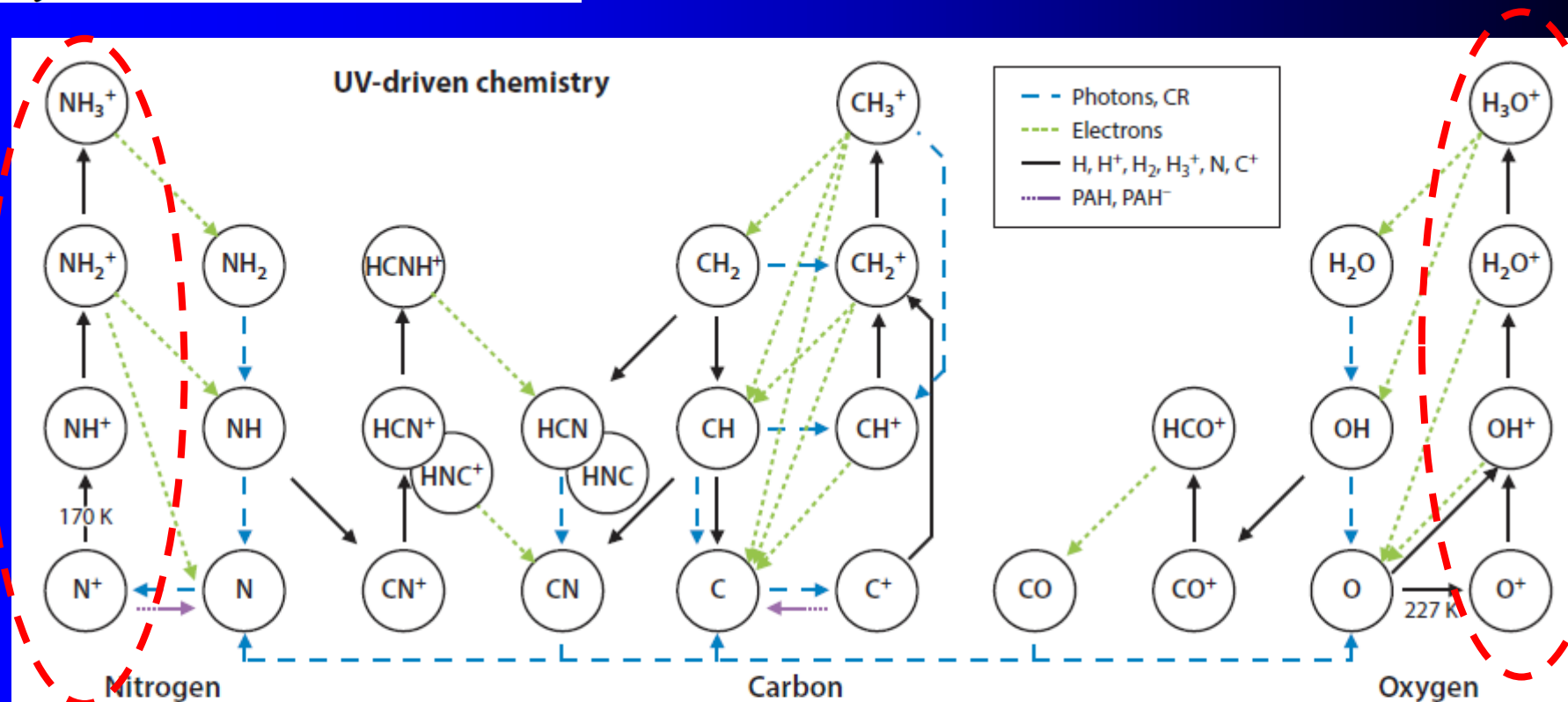


Figure 3

Illustration of the chemical network initiating the carbon, oxygen, and nitrogen chemistry in diffuse cloud conditions ($n_{\text{H}} = 50 \text{ cm}^{-3}$, $A_V = 0.4 \text{ mag}$, $\chi = 1$). The black arrows show the reactions with H, H⁺, H₂, H₃⁺, C⁺, and N, with values of the endothermicity for the reaction between N⁺ and H₂ and for the charge exchange reaction between O and H⁺. Note that CH₂⁺ is formed in the slow radiative association reaction between C⁺ and H₂. The dashed blue arrows indicate the reactions induced by FUV photons or cosmic rays (CR). Dissociative recombination reactions with electrons are shown with green dotted arrows. Purple arrows show the neutralization reactions on dust grains and polycyclic aromatic hydrocarbons (PAHs). Adapted from Godard et al. (2014) with permission.

Koniec skutočnej prednášky 1A 26. 10. 2023 ?